A STUDY OF SOLID-STEM EXPRESSION IN DURUM AND COMMON WHEAT

A Thesis Submitted to the College of

Graduate and Postdoctoral Studies

In Partial Fulfillment of the Requirements

For the Degree of Doctor of Philosophy

In the Department of Plant Sciences

University of Saskatchewan

Saskatoon

By

Kirby Todd Nilsen

PERMISSION TO USE

In presenting this thesis/dissertation in partial fulfillment of the requirements for a Postgraduate degree from the University of Saskatchewan, I agree that the Libraries of this University may make it freely available for inspection. I further agree that permission for copying of this thesis/dissertation in any manner, in whole or in part, for scholarly purposes may be granted by the professor or professors who supervised my thesis/dissertation work or, in their absence, by the Head of the Department or the Dean of the College in which my thesis work was done. It is understood that any copying or publication or use of this thesis/dissertation or parts thereof for financial gain shall not be allowed without my written permission. It is also understood that due recognition shall be given to me and to the University of Saskatchewan in any scholarly use which may be made of any material in my thesis/dissertation.

DISCLAIMER

This thesis was exclusively created to meet the thesis and/or exhibition requirements for the degree of Doctor of Philosophy at the University of Saskatchewan. Reference in this thesis/dissertation to any specific commercial products, process, or service by trade name, trademark, manufacturer, or otherwise, does not constitute or imply its endorsement, recommendation, or favoring by the University of Saskatchewan. The views and opinions of the author expressed herein do not state or reflect those of the University of Saskatchewan, and shall not be used for advertising or product endorsement purposes.

Requests for permission to copy or to make other uses of materials in this thesis/dissertation in whole or part should be addressed to:

Head of the Department of Plant Sciences
College of Agriculture and Bioresources
51 Campus Drive
University of Saskatchewan
Saskatoon, Saskatchewan S7N 5A8
Canada

OR

Dean
College of Graduate and Postdoctoral Studies
University of Saskatchewan
116 Thorvaldson Building, 110 Science Place
Saskatoon, Saskatchewan S7N 5C9
Canada

ABSTRACT

The wheat stem sawfly (WSS) is a damaging insect pest of wheat in North America. Resistance to WSS has primarily been achieved by introgressing the stem-solidness QTL *SSt1* into elite cultivars. This thesis comprehensively examined the expression of *SSt1* from both the phenotypic and genetic perspective. The first study investigated the influence of four sowing densities on pith expression for two newly released solid-stemmed durum cultivars, CDC Fortitude and AAC Raymore. Both cultivars had strong pith expression (average stem-solidness > 3.9) across all environments and sowing densities, in contrast to the common wheat cultivar Lillian (average stem-solidness = 2.2). Increasing sowing density had a positive effect on grain yield in all cultivars, but was negatively associated with stem-solidness. These findings suggest that, unlike with Lillian, altering sowing density is not required to achieve effective sawfly resistance with CDC Fortitude and AAC Raymore. For the second study, we improved the resolution of the *SSt1* interval in durum and common wheat by localizing coincident QTL near the telomere of 3BL (LOD = 94 - 127, R^2 = 78 - 92 %). The *SSt1* interval spanned a 1.6 Mb interval on chromosome 3B. Minor QTL were identified on chromosomes 2A, 2D, 4A, and 5A that synergistically enhanced the expression of *SSt1* to increase stem-solidness. These results suggest breeding for improved stem-solidness is possible by combining *SSt1* with favorable alleles at minor loci. Finally, we investigated gene expression and structural variation within the *SSt1* interval. This showed that in addition to structural variation between genome assemblies, the *SSt1* locus has also undergone a series of functional gene duplication/expansion events. One gene encoding a Dof transcription factor (*TraesCS3B01G60880*) was consistently up-regulated across solid-stemmed cultivars. Further investigation revealed that solid-stemmed cultivars carry multiple copies of *TraesCS3B01G60880*. Screening of a mutant population identified two mutant lines with a hollow-stemmed phenotype that either have a deletion, or reduced expression of *TraesCS3B01G60880*. Taken together, this research provides new insights into the phenotypic and genetic expression of *SSt1* in wheat, and will provide an important foundation for future experiments that will help breeders improve resistance to the WSS.

This thesis is dedicated to Erik and Josée.

ACKNOWLEDGEMENTS

I would like to give my special thanks to Dr. Curtis Pozniak for serving as my PhD supervisor, and for his guidance and friendship over the course of this project. I would also like to thank my advisory committee, Dr. Yuguang Bai (Head, Department of Plant Sciences), Dr. Tom Warkentin, (Defense Chair), Dr. Graham Scoles, Dr. Pierre Hucl, Dr. Art Davis (Department of Biology, University of Saskatchewan), and Dr. Christopher Burt (Rouergue Auvergne Gévaudan Tarnais, RAGT, United Kingdom) for serving as the external examiner

This work would not have been possible without many contributions from our outstanding research team at Durum Wheat Breeding program at the Crop Development Centre: Dr. Sean Walkowiak, Dr. P.R. MacLachlan, Dr. Aron Cory, Dr. Amidou N'Diaye, Dr. John Clarke, Krysta Wiebe, Jennifer Enns, Raelene Regier, Lexie Martin, Justin Coulson, Ryan Babonich, Russell Lawrie, Hillory Smith, Heidi Lazorko, Vinh Tang, Chanese Beierle, and Cory Howard. I would also like to acknowledge the support provided by Dr. Brian Beres, Dr. Yuefeng Ruan, Dr. Richard Cuthbert, Dr. Ron Knox, Dr. Fran Clarke, Dr. Steve Robinson and Mrs. Kyla Horner from Agriculture and Agri-Food Canada; Dr. Karen Tanino and Mr. Ian Willick at the University of Saskatchewan. Special thanks go out to Dr. Raju Datla, Dr. Prakash Venglat and Dr. Daoquan Xiang (NRC-CNRC Saskatoon). I would like to acknowledge the technical support provided by Ryan Dyck, Steven Simmill, Warren Taylor, Dan Yagos, Regan Nielson, Jordana Hudak, Kim Ziegler, Valerie Leithoff and Nicola Spencer, J. Powell, M. Steinley, H. Campbell, B. Neudorf, T. Greenwood (Technicians - DH/Biotech/Field Trials) and all members of the wheat breeding group at AAFC, Swift Current.

This research was carried out under the Canadian Triticum Applied Genomics (CTAG2) project. We are grateful for the funding provided by Genome Canada and project support provided by Genome Prairie. We also acknowledge financial support provided by the Saskatchewan Ministry of Agriculture, Western Grains Research Foundation, the Saskatchewan and Alberta Wheat Development Commissions, the AgriFlex Program of Agriculture and Agri-Food Canada, and Viterra. I would also like to personally acknowledge the funding providing by the Robert P. Knowles scholarship, the Earl David Mallough scholarship, the Paulden F. & Dorathea I. Knowles scholarship, the Gerhard Rakow Legacy Award, and the Seed of the Year scholarship.

TABLE OF CONTENTS

LIST OF TABLES

LIST OF FIGURES

LIST OF APPENDICES

LIST OF ABBREVIATIONS

ANK	Ankyrin repeat-containing domain proteins
ANN	Artificial neural network
BAC	Bacterial artificial chromosome
BAM	Binary alignment mapping
BSA	Bulked segregant analysis
CCOMT	Caffeoyl-CoA O-methyltransferase
CIM	Composite interval mapping
CNHR	Canada Northern Hard Red
CNV	Copy number variation
CPSR	Canada Prairie Spring Red
CPSW	Canada Prairie Spring White
CRD	Completely randomized design
CRISPR-Cas9	Clustered Regularly Interspaced Short Palindromic Repeats
CWAD	Canada Western Amber Durum
CWES	Canada Western Extra Strong
CWHWS	Canada Western Hard White Spring
CWRS	Canada Western Red Spring
CWRW	Canada Wester Red Winter
CWSWS	Canada Western Soft White Spring
DEG	Differentially expressed gene
DH	Doubled-haploid
DOF	DNA-binding with one zinc finger
EMS	Ethyl-methane sulfonate
FAO	Food and Agriculture Organization
FUT	Galactoside 2-alpha-L-fucosyltransferase
GO	Gene ontology
GTF	Gene transfer format
LD	Linkage disequilibrium
LG	Linkage group
LSD	Least significant difference
LS-means	Least square means
Mb	Megabase
MT	Metallothionein
MTP	Minimum tiling path
NGS	Next-generation sequencing
NIL	Near inbred line
OA	Osmotic activity
OMT	O-methyltransferase
ORF	Open reading frame

PAE	Pectin acetylesterase
PE	Paired-end
PEPC	Phosphoenolpyruvate carboxylase
qPCR	Quantitative PCR
QTL	Quantitative trait loci
RCBD	Randomized complete block design
RIL	Recombinant inbred line
RNAi	RNA interference
ROS	Reactive oxygen species
RP	Ribosomal protein
RPS28	Ribosomal protein S28
SED	Standard error of the difference
SNP	Single nucleotide polymorphism
SSCP	Single strand conformational polymorphism
SSt1	Solid-stem locus 1
TSS	Transcription start site
VIGS	Virus-induced gene silencing
VRN	Vernalization
WEW	Wild emmer wheat
WSC	Water soluble carbohydrate
WSS	Wheat stem sawfly
X^2	Chi-square
XEG	Xyloglucan endotransglucosylases /hydrolases

1. INTRODUCTION

Disclosure: Excerpts from this chapter have been published in:

Durum wheat: production, challenges and opportunities: J. M. Clarke, K. Nilsen, D. Kthiri, X. Lin and C. J. Pozniak, University of Saskatchewan, Canada; and K. Ammar, International Maize and Wheat Improvement Center (CIMMYT), Mexico

The wheat stem sawfly (WSS), *Cephus cinctus* Norton, can be a serious insect pest of durum wheat (*Triticum turgidum* L. var *durum*) and common wheat (*Triticum aestivum* L.) in North America. The WSS poses a major risk to wheat production in North America because much of its geographical range overlaps with the major wheat growing region which includes the southern parts of Alberta, Saskatchewan and Manitoba, Northern Montana, North Dakota and northern South Dakota (Beres et al., 2011b). In recent years, severe WSS damage has been reported in eastern Wyoming, Nebraska and Colorado (Bradshaw et al.; Spiegel, 2014). Although WSS was initially a pest of native grasses, cultivated wheat is now its preferred host (Wallace and McNeal, 1966), which was brought on by the rapid expansion of the wheat acreage over the last century (Beres et al., 2011b).

The name "sawfly" was given to *C. cinctus* because the adult female has a specialized "saw-like" ovipositor at the tip of its abdomen that it uses to cut into the host stem and deposit its eggs in the upper internodes of the wheat plant. Adult sawflies are short-lived insects that emerge from infested stubble from a previous year's crop, and are the only stage of the life-cycle to live outside of the host (Wallace and McNeal, 1966). The WSS spends most of its life-cycle inside the stem of the wheat plant in larval form. Damage to vascular tissue of the developing wheat plant occurs as the larva move upwards and downwards feeding on the inner stem tissue which can result in a loss of yield between 2.8 – 17% (Holmes, 1977). As the host plant approaches maturity, larvae move towards the base of the plant and chew a notch around the inner perimeter of the stem, weakening it to such a point where the plant will easily lodge, especially when exposed to wind (Beres et al., 2011b). Often, the lodging caused by WSS is the most obvious sign of an infestation. When the plant has lodged, the larva fills the opening in the stub with excrement (frass), and encases itself in a cocoon in preparation for winter. The following spring, the larva undergoes pupation, and eventually develops into a mature adult (Holmes and Peterson, 1960). Adult sawflies emerge from infested stubble by chewing their way out of the stub, either through the frass plug,

or the side of the stub (Holmes and Peterson, 1960). Yield losses more than 30% have been attributed to WSS infestation, from a combination of losses attributed to larval feeding activity, and lodging at maturity (Ainslie, 1920). Plants with the highest yield potential are the most likely to lodge from WSS damage, as these plants have the heaviest spikes (Beres et al., 2007).

Although no control strategy has been able to completely eradicate the WSS, the most effective way to minimize damage has been to grow solid-stemmed cultivars. The use of contact pesticides has been largely ineffective because larvae that feed within the wheat stem are shielded from chemical, and because the female WSS emerge over a 3-week period (Beres et al., 2012), rendering a single chemical application ineffective. Recently, the systemic insecticide Thimet 20-G (Phorate: 0,0-diethyl S-[(ethylthio) methyl] phosphorodithioate) was registered for use against the WSS in Montana. Despite reports of its effectiveness in killing WSS larvae, Thimet is highly toxic to humans, mammals, aquatic life and birds, and is therefore an environmental and safety risk. Delaying seeding until after May 20th can substantially reduce damage, but is not a practical strategy for Canadian wheat production where growing seasons are short, and seeding windows are tight (Beres et al., 2007). Solid-stemmed cultivars develop pith in the culm lumen (Clarke et al., 2002). Pith provides resistance to the WSS by deterring stem cutting, mechanically crushing eggs, and impeding larval development and growth inside the stem (Hayat et al., 1995). As a result, growing solid-stemmed wheat cultivars is an effective, low cost, and environmentally friendly method of managing WSS.

Stem-solidness is a trait that breeders can use to select for WSS resistance. To measure stem-solidness, plants are cut longitudinally from crown to spike and each internode is assigned a visual rating on a 1 to 5 scale (1 = hollow, 5 = solid) (Depauw and Read, 1982) (Appendix 1). The scores from each internode are averaged to obtain an overall stem-solidness rating for the plant. Wallace et al. (1973) suggest a minimum stem-solidness rating of 3.75 to achieve effective resistance to the WSS. Although phenotyping is straightforward, expression of stem-solidness involves complex interactions between genetic background and environment; and both should be considered in breeding.

Genetic background can impact expression of stem-solidness. There are multiple sources of stem-solidness in wheat and it remains unclear whether the underlying genetics are similar between sources. In durum wheat, the most well-known source is the South African cultivar Golden Ball (Clark et al., 1922). A second source was identified in the German cultivar Biodur,

which may be different from Golden Ball based on haplotype differences around the stem-solidness locus (K. Nilsen, unpublished data). The first three commercially registered solid-stemmed durum cultivars in Western Canada were CDC Fortitude (Pozniak et al., 2015), AAC Raymore (Singh et al., 2014), and AAC Cabri (Singh et al., 2016) and all derive their stem-solidness from the Biodur source. Under commercial sowing densities, all cultivars have comparable yield and protein content to the hollow-stemmed durum check Strongfield. In general, durum wheat has superior resistance to WSS than hexaploid wheat, and even hollow-stemmed durum wheat cultivars tend to be more resistant than hollow hexaploids (Eckroth and McNeal, 1953). Durum wheat cultivars typically have greater straw strength, which resists lodging. Durum cultivars often have thicker outer stem walls, which could resist WSS cutting, and the reduced culm lumen diameter may impede larval movement (Putnam, 1942). Eggs and larvae inside the hollow-stemmed durum cultivars suffer from higher mortality rates compared to common wheat, which include some mechanical resistance, increased node thickness, nutrient deficiency or higher oviposition on the stem.

In common wheat, the most commonly known source of stem-solidness is the Portuguese landrace S-615 (Beres et al., 2011b). The first commercially grown solid-stemmed cultivar in Canada was Rescue (Platt et al., 1948). A major problem with cultivars that are derived from S-615, including Rescue, is that differences in environment can cause inconsistent pith expression and plants usually fail to meet the minimum threshold score to ensure effective WSS resistance under field conditions. The reason for the expression difference is primarily due to light intensity, and rainfall. Platt (1941) found that stem-solidness in the S-615 source was positively correlated with hours of sunshine in June, and negatively correlated with rainfall in May and June. He found that wider row spacing produced plants that were more solid-stemmed due to a reduction in canopy shading. Platt also observed that the durum source Golden Ball, which expresses a solid-stem across environments, was not affected by row spacing or light intensity. Because of the inconsistent pith expression in the S-615 source, attempts were made to transfer the solid-stem source of Golden Ball into common wheat through interspecific crosses, but failed to recover any true hexaploid progeny with solid stems (Platt and Larson, 1944). One possible explanation is that genes carried by the D genome of common wheat work to epistatically suppress the expression of stem-solidness (Yamashita, 1937). Despite this, Holmes and Peterson (1957) observed WSS

populations decline to near zero in fields sown entirely to Rescue over a five-year study, demonstrating the importance of the solid-stem trait in managing WSS.

Even with the effectiveness of solid-stemmed common wheat cultivars, there has been a major reluctance on behalf of growers to adopt them, mainly because of a perceived yield drag associated with the solid-stem trait (McNeal et al., 1965; Weiss and Morrill, 1992). Other concerns regarding inferior agronomics and grain quality, including lower protein content, have also been noted. Contrasting studies have reported no significant association between stem-solidness and yield loss, although some did note grain protein content was negatively impacted in some genetic backgrounds (Hayat et al., 1995; McNeal and Berg, 1979). There is not sufficient evidence presented in the literature as to whether any potential yield penalty is due to the expression of pith itself, or a yield drag associated with the genetic background of S-615. In Western Canada, these issues were largely overcome through plant breeding efforts, which led to the development of the S-615 derived solid-stemmed common wheat cultivar Lillian in 2006 (DePauw et al., 2005). At the time of registration, Lillian had grain yield comparable to hollow-stemmed checks in the absence of WSS infestation, and was the first cultivar to carry the high protein gene GPC-B1 (DePauw et al., 2005). Lillian was sown to 32% of the total Canada Western Red Spring (CWRS) acreage in 2010, and remained the 6th most widely grown CWRS cultivar in 2015 (Grains Canada, 2017a).

The solid-stem trait is predominantly controlled by a major locus on the long arm of chromosome 3B, which is now referred to as *Qss.msub.3BL* (Cook et al., 2004) in common wheat, and *SSt1* (Houshmand et al., 2007) in durum wheat. It remains unclear whether both species share a common locus. McNeal (1961) examined progeny derived from a cross between Rescue and Golden Ball, but was unable to identify any line segregating for hollowness. This finding suggests the two sources either share a common locus, or have two different tightly linked loci conferring stem-solidness. Within each species, it is possible that additional sources also exist. For example, the durum cultivar Biodur appears to be different from Golden Ball based on haplotype patterns around the *SSt1* locus (unpublished data); stem-solidness in the durum cultivar Golden Ball and Biodur follow a mono-factorial pattern, suggesting a single gene or two tightly linked loci (Clarke et al., 2002; Putnam, 1942).

Altogether, control of WSS through stem-solidness is the most effective pest management strategy; however, our knowledge of how this trait is regulated is incomplete. The expression of

stem-solidness can be quite different between durum and common wheat, which can have a major impact on the level of WSS resistance obtained in the field. In durum wheat, the expression of stem-solidness is relatively stable across environments (Clarke et al., 2002), whereas expression in common wheat can show considerable variation, particularly in response to environmental conditions such as light intensity and moisture. At this point, it is not clear whether this difference in expression is related to different causal genetic factors on chromosome 3BL, or the interaction of other genes from elsewhere in the genome with the 3BL locus. Optimization of agronomic approaches may be required to maximize stem-solidness under field conditions, while also balancing agronomic performance. One strategy that has been investigated to improve the expression of stem-solidness in common wheat has been through manipulating light penetration through the canopy by reducing sowing densities. This approach has proven successful in some common wheat cultivars, but has yet to be investigated in durum wheat. Because altering sowing densities can come with penalties to yield, optimization is necessary in field experiments (Beres et al., 2012).

A single major QTL that controls the development of pith in the culm lumen, designated *SSt1*, has been identified on chromosome 3BL in durum wheat, but it remains unclear whether this QTL is coincident with a second QTL (*Qss.msub.3BL*) conferring stem-solidness in common wheat (Cook et al., 2004; Houshmand et al., 2007). This thesis focuses on improving our understanding of solid-stem expression in durum and spring wheat. This has been made possible by the recent availability of: 1) high yielding solid-stemmed wheat cultivars for both common and durum wheat, 2) mapping populations segregating for stem-solidness for both durum and common wheat, and 3) whole genome reference sequences for common and durum wheat. The genome sequences provide the unprecedented opportunity to investigate the genetic basis for stem-solidness and other important traits in wheat by presenting a tool for the rapid dissection of physical QTL intervals and their associated genes.

1.1. Questions addressed in this thesis

- How is the expression of stem-solidness affected by altering sowing density, how does it differ between durum and common wheat, and at what sowing density is optimal agronomic performance achieved?
- What are the physical intervals of the major stem-solidness locus on chromosome 3BL in durum and common wheat, and are they coincident?
- What are the candidate genes that could be responsible for conferring stem-solidness and how are these genes interacting with the global transcriptome?
- Does structural variation account for some of the discrepancies observed between genetic mapping data and physical position of marker sequences along reference sequences?

2. LITERATURE REVIEW

Disclosure: Excerpts from this chapter have been published in:

Durum wheat: production, challenges and opportunities**:** J. M. Clarke, K. Nilsen, D. Kthiri, X. Lin and C. J. Pozniak, University of Saskatchewan, Canada; and K. Ammar, International Maize and Wheat Improvement Center (CIMMYT), Mexico

2.1. Wheat origin and taxonomy

Wheat belongs to the genus *Triticum* within the family *Poaceae* and the tribe *Triticeae*. Cultivated wheat emerged approximately 10,000 years ago, as part of the Neolithic Revolution, when early human civilizations began to transition from nomadic hunter and gatherers to settled agriculturalists (Shewry, 2009). The expected geographical origin of wheat is thought to be in the fertile crescent somewhere near the South-East region of Turkey (Heun et al., 1997). Cultivated wheat was first domesticated by early farmers, probably through indirect selection, which resulted in a loss of shattering of the spike at maturity, and a change from glumes that were tightly attached to the seed (hulled) to free threshing forms (Shewry, 2009). The earliest cultivated wheats were *Triticum monococcum* (AA genome, 2n=2x=14) which was domesticated from natural populations of einkorn (*Triticum boeoticum*), and *Triticum turgidum* ssp. *dicoccon* (AABB genome) which was domesticated from wild populations of emmer (*Triticum turgidum* ssp. *dicoccoides* (AABB genome). Modern cultivated wheat is allopolyploid, containing genomes obtained through interspecific hybridization events with progenitor species. Modern durum wheat (*Triticum turgidum* ssp. *durum,* AABB genome, 2n=4x=24) arose from the hybridization of *Triticum urartu* (AA genome) and an *Aegilops speltoides* related species (S genome related to B genome) around 500,000 years ago. Modern bread wheat (AABBDD genomes, 2n=6x=42) arose under cultivation within the last 10,000 years from the interspecific hybridization between cultivated emmer (*Triticum turgidum)* and *Aegilops tauschi* (DD genome). Because of the recent polyploidization of durum and common wheat, the genomes they contain share greater than 97% sequence identity, and each gene is usually present in 2, or 3 homoeologous copies (Uauy, 2017).

2.1.1. Global wheat production and current challenges

Wheat is the world's most widely grown food crop providing an estimated 20% of the daily protein and food calories for the global population. Around 95% of the wheat produced globally

is hexaploid bread wheat, whereas the remaining 5% is tetraploid durum wheat used in the production of semolina and couscous. A small proportion of global wheat production also consists of ancient wheat species such as einkorn, emmer and spelt (Shewry, 2009). Wheat is grown on 18% of the global agricultural land in production, anywhere between 45°S in Argentina, to 67°N in Norway Finland and Russia (Peng et al., 2011). Current land used for wheat production globally was 220.32 million hectares in 2017, estimated to produce 739.9 million metric tonnes, with an average yield in 3.34 tonnes per hectare (FAO, 2017). Improving agronomic and plant breeding practices is a worldwide priority to prevent a global food security crisis. The Food and Agriculture Organization (FAO) has projected that global food production will need to increase as much as 70 % over current levels by 2050 to feed a projected global population of over 9.1 billion people. That means that the rate of yield increase in cereals will need to rise a staggering 38% over current levels (Tester and Langridge, 2010). The greatest chance to achieve these targets will be from advances made in the developing world (Ray et al., 2013).

As the global population rises, we will see a corresponding decline of land in production per capita. To ensure global food security for future generations, wheat breeding targets will need to focus on: nitrogen use efficiency and resistance to abiotic stress including a major focus on salinity, drought and heat stress.

Climate change is also expected to have a major impact on global agricultural production. In Canada and other high latitude countries, warming might benefit agriculture by extending the growing season allowing for increased productivity and diversity of crops that can be grown. The global increase of CO_2 in the atmosphere is also expected to benefit C3 crops (Tester and Langridge, 2010). However, several negative consequences of global warming are expected, including a greater frequency of severe weather events, extended heatwaves and prolonged drought. The warming of the tropical Indian Ocean and the Pacific Ocean are likely to contribute to extensive drought in many countries, particularly in Eastern Africa (Funk and Brown, 2009). As agricultural production intensifies, there will need to be a focus on resistance to biotic stress, including: insect pests, such as the wheat stem sawfly and wheat midge; and fungal diseases, including the current threat imposed by the devastating stem-rust race Ug99 (Singh et al., 2011), stripe rust, and fusarium head blight.

2.1.2. Wheat production in Canada

Historically, wheat has been Canada's most important crop. However, in 2017, the number of canola hectares in production (9.23 Ha) exceeded wheat for the first time. The majority of wheat is produced in Saskatchewan, Manitoba and Alberta (McCallum and DePauw, 2008). In 2017, wheat was grown on 9.06 million hectares in Canada, expected to produce 27.1 million metric tonnes of grain (Statistics Canada, 2017). Spring-planted hexaploid common wheat (*Triticum aestivum* L.) accounts for approximately 70% of the harvested area, while 23% of the wheat that is grown in Canada is tetraploid durum wheat (*Triticum turgidum* L var *durum*) and the remaining 6% was sown to hexaploid winter wheat. The average wheat yield in Canada is 3.29 tonnes per hectare.

In Western Canada, wheat cultivars are currently differentiated into 10 different market classes based on functional characteristics, and end use quality (Table 2.1). Commanding premium prices in the global market, the Canada Western Red Spring (CWRS) and Canada Western Amber Durum (CWAD) are the two most widely grown market classes. The Canada Northern Hard Red (CNHR) market class was recently added in response to concerns about low gluten strength in several cultivars, which led to 25 CWRS cultivars and four Canada Prairie Spring (CPS) being re-classified as CNHR as of August 1, 2018 (Grains Canada, 2017b).

Table 2.1. Western Canadian durum and common wheat market classes

T. aestivum	
CNHR	Canada Northern Hard Red
CPSR	Canada Prairie Spring Red
CPSW	Canada Prairie Spring White
CWES	Canada Western Extra Strong
CWHWS	Canada Western Hard White Spring
CWRS	Canada Western Red Spring
CWRW	Canada Western Red Winter
CWSWS	Canada Western Soft White Spring
T. turgidum	
CWAD	Canada Western Amber Durum

2.1.3. Wheat genomic resources

To meet the increasing demand for wheat, the integration of genomics and breeding will be required to overcome challenges such as climate change and other abiotic and biotic constraints

(Mayer et al., 2014). The development of wheat genomic resources has been slower than other cultivated crop species largely because its genome is the largest of the cultivated crop species (at 17 Gb), and the highly repetitive (> 80%) nature of its genome (Mayer et al., 2014; Uauy, 2017). The wheat genome contains a high level of transposable elements relative to other crop species, which has hindered the accurate assembly and ordering of sequences (Mayer et al., 2014; Uauy, 2017). In addition, wheat is an allopolyploid and contains two, or three, complete sets of highly related (> 97% sequence identify) genomes, in durum, and common wheat, respectively, with low coding sequence divergence between them. Because of the genetic bottleneck which occurred during the hybridization leading to the emergence of cultivated hexaploid wheat, the polymorphism on the D genome is markedly lower than on the A or B genomes (Brenchley et al., 2012). Despite these challenges, the advances in wheat genomics have been rapid over the past several years, facilitated by improvements in wet chemistry, genotyping technologies, sequencing and sequence assembly and high-powered computing.

2.1.3.1. High-throughput genotyping

The development of high-throughput and high-density marker screening tools are essential for a wide variety of applications, including the construction of high quality linkage maps, characterizing genetic variation, performing diversity analysis, marker trait association studies and QTL experiments. Over the past decade, there has been a major shift towards the use of single nucleotide polymorphism (SNP) as molecular markers in plant and animal systems because SNPs have a high call frequency, low cost and error rate, and are amenable to high-throughput screening. One of the major breakthroughs in wheat genomics was the recent development of the wheat iSelect 9K SNP array (Cavanagh et al., 2013) and the now widely adopted wheat iSelect 90K SNP array (Wang et al., 2014). The wheat iSelect 90K SNP array was developed by aligning RNAseq reads from 19 accessions of bread wheat and 18 accessions of durum wheat to the Chinese Spring survey sequence. A total of 81,579 high quality functional SNPs were used for the assay, and were used to develop oligonucleotide probes. One of the issues with probe-based arrays in wheat is that cross-mapping can occur to homoeologous and paralogous loci. In fact, in-silico mapping of the 90K probes suggested a total of 518,537 binding sites in the CS survey sequence.

The iSelect assay works by hybridizing 50 base pair (50-mer) probes to custom Illumina Infinium BeadChips. Each probe is designed to hybridize to a locus one base before the target

SNP. An enzymatic single base pair extension of dual colored fluorescently labelled nucleotides specific to the two variants of the target SNP enables the detection of fluorescent signal on the iScan optical array scanner.

Perhaps the greatest benefit of the 90K SNP array is that it provides wheat researchers with a globally standardized genotyping system. Comparison between studies is now possible whereas in the past has otherwise proven challenging due to research groups using different genotyping platforms or different markers.

2.1.3.2. Consensus maps

A common application of genotypic data is the construction of genetic maps using genetic linkage information from mapping populations, usually derived from a cross between two diverging parental lines (Jackson et al., 2005). Often these bi-parental mapping populations have varying levels of polymorphism ranging from 20 - 40%, thus may be limited in their usefulness outside of the context of the initial cross (Somers et al., 2004). Consensus maps overcome this limitation by ordering all markers from several different genetic maps to create a consensus order of markers and recombination distances. In addition, they provide a large number of markers that can aid genome-wide association studies, and they can identify structural rearrangements between populations (Maccaferri et al., 2015). The first consensus map available in wheat was constructed using 1,235 microsatellite loci mapped to four different populations of hexaploid wheat (Somers et al., 2004). This consensus map served as a tremendous resource for wheat researchers working on map-based gene cloning projects and other areas of genomics research for many years. Recently, with the advent of the iSelect 90K SNP array, high density SNP consensus maps have been constructed in both wheat species. In common wheat, 46,977 SNPs were mapped from eight different hexaploid mapping populations (Wang et al., 2014); whereas in durum wheat, 30,144 markers (26,626 SNPS and 761 SSRs) were mapped using 13 different tetraploid mapping populations providing the first consensus map built exclusively for durum wheat (Maccaferri et al., 2015).

2.1.3.3. Wheat reference sequences and annotations

One of the major factors holding back advances in wheat genomics has been the lack of a high quality, complete and properly annotated reference sequence. Draft sequences for *T. urartu* and *Ae. tauschii* were recently completed (Jia et al., 2013), but were not of high quality and many genes

were unable to be assigned to chromosomes (Choulet et al., 2014). Early approaches to sequence the common wheat genome were centered around the landrace Chinese Spring. Advances in next generation (NGS) sequencing technology facilitated the first whole genome shotgun sequence assemblies, that were assembled into hundreds of thousands of short scaffolds (N50 < 10 kb) (Brenchley et al., 2012; Mayer et al., 2014). Mayer et al. (2014) used ditelosomic stocks of Chinese Spring to isolate each chromosome arm which were subsequently purified using flow-cytometric sorting, and sequenced using the Illumina NGS platform at very high depth (31 – 241x sequence coverage). These early resources were important for gene discovery and were used in the development of molecular markers; however, the assemblies were too fragmented to be useful in exploring the genes contained within QTL intervals highlighting the need for assembled full length pseudomolecules.

An alternative sequencing strategy using the minimum tiling path (MTP) of overlapping bacterial artificial chromosome (BAC) long insert libraries led to the release of the first assembled 774 Mb pseudomolecule for chromosome 3B (Choulet et al., 2014). Recently BAC sequence assemblies have been abandoned in favour of more efficient short read assembly algorithms such as the proprietary NRGene DeNovoMAGIC pipeline (http://www.nrgene.com) that has been successfully used to assemble more than 300 genomes thus far. The NRGene pipeline uses a combination of high coverage (200x) paired-end (PE), mate-pair reads, and most recently incorporates 10x sequence data to accurately assemble complex plant genomes (Yuan et al., 2017). This pipeline was successfully used to assemble the first genomes for wild emmer wheat (*T. turgidum* ssp. *dicoccoides*) cv. Zavitan (Avni et al., 2017), durum wheat cv. Svevo, and common wheat cv. Chinese Spring (Refseq v.1.0) (Curtis Pozniak, personal communication). Each assembly was released with accompanying high-confidence gene annotations, containing a predicted 65,012, 66,559 and 110,790 high confidence genes in Zavitan, Svevo, and Refseq v.1.0, respectively. The next step for wheat genomics is the pangenome, with projects such as the 10 Wheat Genomes Project that aims to study the core and dispensable genome, and characterize large scale structural variation among globally diverse cultivars (Wheat Initiative, 2016). The growing number of genome sequences currently available paves the way for functional genomics and genome editing (Kassa et al., 2016).

2.2. The wheat stem sawfly

The WSS belongs to the order Hymenoptera, suborder Symphyta, comprising one of the largest insect orders that also includes bees, wasps and ants. Almost all members of Symphyta feed on plants at the larval stage (Wallace and McNeal, 1966). The WSS is a member of the family Cephidae which is further divided into tribes, with the WSS being a member of the tribe Cephini. There are over 8000 species of sawfly (Taegar et al., 2010); those which are considered pests of grasses include *Cephus pygmeus, C. tabidus,* and *C. cinctus.* Of these, *Cephus pygmeus* and *C. tabidus* originated from Europe and Asia, and were introduced into North America accidentally (Wallace and McNeal, 1966), whereas *C. cinctus* is thought to be native to North America. This thought has been recently challenged; therefore, *C. cinctus* may instead be an introduced species from Europe and Asia (Ivie, 2001).

Economic losses associated with the WSS in North America have the potential to reach an estimated US $350-400 million annually (Beres et al., 2011b; Beres et al., 2017). The WSS has been recognized as an insect pest of wheat in North America since the late 1800s, and the first appearance of the WSS in Western Canada occurred near Souris MB and Indian Head SK in 1905 (Beres et al., 2011b). Early reports suggested the WSS exhibited a preference for native grasses, which served as a source of the pest in neighboring wheat crops (Holmes, 1979). In Western Canada, the WSS did not cause significant damage until 1922 when an estimated 5 million dollars (Holmes, 1979) of losses were incurred (Criddle, 1923). The spread of the WSS is thought to have followed the rapid expansion of wheat throughout the Northern Great plains and western prairie provinces during the early 1900s (Ainslie, 1920).

2.2.1. Life cycle and biology of the WSS

The WSS spends up to 10 months of the year in its larval form nested inside the host plant stem. Sex determination of the WSS follows a haplodiploid system where males are haploid (n = 9) and develop from unfertilized eggs, whereas females are diploid (2n = 18) and develop from fertilized eggs. Adults are long and slender with two pairs of wings and have a body length of 0.6 to 1.8 cm (Wallace and McNeal, 1966). Females are notably larger than the males (Ainslie, 1920). Males emerge earlier than females as part of a mechanism that ensures the earliest females to emerge can mate. Thus, the proportion of males becomes less as the season progresses and new females emerge (Holmes, 1979). Because of this, more female offspring hatch from fertilized eggs

deposited early in season when more males are present for mating, whereas more males emerge from unfertilized eggs deposited later in the season. Adult sawflies emerge in Western Canada anytime between June 10th - July 10th depending on temperature and live for approximately one week (Criddle, 1923). The adults are generally considered weak flyers; therefore, they tend to remain close to the site of emergence (Holmes, 1979). This factor contributes to the spatio-temporal patterns of infestation that occur near the edges of adjacent fields following a previous infestation. Producers that grow wheat in fields neighbouring native grass species will often experience similar patterns of infestation.

Mating occurs shortly after adult emergence, followed by oviposition within a few days thereafter. During the process of oviposition, the female WSS will land on the stem, walk up to the uppermost leaf, turn her head down and select a suitable site to deposit her eggs. The female WSS has a specialized saw-like ovipositor (hence "sawfly") that it uses to cut into the wheat stem during oviposition, which creates an opening so small that it is near impossible to find the scar once the plant has healed (Ainslie, 1920). The female will search for a suitable host plant in which to lay eggs, usually beginning at the upper internode of the developing wheat plant (Beres et al., 2011b). Females prefer succulent plants that are between the early boot and anthesis stage with a large enough stem diameter suitable for oviposition (Holmes and Peterson, 1960). A plant that has already produced a spike will never be selected for oviposition (Ainslie, 1920). As plant growth continues and the upper internodes begin to elongate, the WSS will lay eggs progressively higher on the plant (Holmes, 1979).

Each female may carry up to 50 eggs that are white in color and between 1-1.25 mm in length (Ainslie, 1920). Eggs are deposited in the culm of hollow-stemmed cultivars, or a hollowed-out portion in a solid-stemmed cultivar (Ainslie, 1920). Larvae will develop for six to seven days before breaking free of the egg sac to immediately begin feeding activity (Ainslie, 1920).

The WSS larva stage spans 60 days and has five instars. The total length of the larval stage is dependent upon temperature, and the phenological stage at which the host plant was at when the egg was deposited (Ainslie, 1920). If multiple eggs are present inside the same stem, the first larva to hatch will cannibalize the other eggs, and will also destroy any other larvae present, including the larvae and eggs of species known to parasitize the WSS. Larvae produce amylase and cellulase to aid in digestion of plant material for its diet, which consists of stem parenchyma and vascular tissue. Feeding continues until plant maturity. Light penetration through the stem stimulates

downward larval movement when the plant is nearing maturity; experiments have shown that in the absence of light, larvae do not move lower in the stem (Holmes, 1979). Similarly, as moisture content in the stem decreases later in the season, larvae will move downward to avoid desiccation.

The downward movement of WSS larvae is critical to the survival of the insect. Towards the end of the growing season, the larva will enter the area of the stem just below the ground and begin to cut a V shaped notch around the perimeter of the stem, a process which is called girdling. Eventually the stem is weakened to the point that it will cause the plant to lodge (Beres et al., 2011b). Stem-girdling is critical for the life cycle of the WSS, as most larvae that are incapable of achieving stem girdling will die during summer months (Cárcamo et al., 2011). Once stems have lodged exposing an open stem above, the larvae will fill the opening with frass which creates an ideal overwintering chamber. Finally, larvae will spin a silken cocoon around their body in preparation for winter entering a phase of obligatory diapause. Larvae are incredibly resilient, being highly cold hardy with a super cooling point between -20 and -28°C (Holmes, 1979), which allows them to withstand severe cold temperatures typical of prairie winters.

Larvae contained within exposed stubs can withstand periods of -20°C for at least 10 consecutive days without negatively affecting mortality (Beres et al., 2011b). The following spring, pupation will begin only after temperatures have reached above 10°C for 90 days, and the total pupation process is completed within 21 days. After pupation, the newly formed adult WSS will begin to chew through the frass plug, the final step before emergence (Beres et al., 2011b). Emergence is facilitated when the plug has been exposed to moisture (Holmes, 1979).

2.2.2. Geographical and host range of the WSS

The WSS poses a major risk to wheat production because almost the entire geographical range of the WSS overlaps with the major wheat growing region in North America. This region includes the southern parts of Alberta, Saskatchewan and Manitoba, Northern Montana, North Dakota and northern South Dakota (Beres et al., 2011b). In recent years, the insect has been expanding in geographical range into Iowa and the Nebraska panhandle causing widespread damage in some regions (Bradshaw et al., 2014).

The WSS can infest a wide range of hosts, although wheat is now considered its preferred host (Wallace and McNeal, 1966). Prior to the expansion of wheat production, the WSS was primarily a pest of native grasses in North America (Eckroth and McNeal, 1953), including certain

species of the genera *Elymus*, *Agropyron*, *Hordeum*, *Bromus*, *Phleum*, *Deschapsia*, *Calamagrostis*, and *Festuca* (Ainslie, 1920). The WSS will also infest many of the small grained cereals, including wheat, rye, spelt and barley. The spread of WSS was facilitated by the rapid expansion of the wheat acreage across the prairie provinces (Beres et al., 2011b).

2.2.3. Injury to the plant caused by the WSS and the effect on yield

The WSS causes extensive damage to the wheat plant because of larval feeding activity. Symptoms of sawfly infestation include stems that are cut and lodged on the ground, and shrivelled kernels with reduced weight and grade (Seamans, 1944). Female oviposition causes little to no measurable damage to the wheat plant; however, an entire wheat stem can be bored by a single larva in a period of only a few weeks as it winds upwards and downwards through the stem (Criddle, 1923). WSS larvae feed on parenchyma and vascular tissue which causes a reduction in the photosynthetic capacity of the infested wheat plant (Macedo et al., 2007). Experiments have shown a reduction in stomatal conductance, transpiration rates and CO_2 levels in WSS infested wheat grown in a growth cabinet (Macedo et al., 2005). Severe damage to vascular tissue can disrupt the flow of water and nutrients to the developing spike (Wallace et al., 1973). Larval feeding activity causes a reduction of kernel weight and mass, which can range from 2.8 - 17 %, but can be even more severe when the crop is under nutrient or water stress (Holmes, 1977; Morrill et al., 1992b; Seamans, 1944). Towards the end of the growing season, larvae chew their way to the base of the plant where they girdle the stem in preparation for overwintering. The most obvious sign of WSS infestation is when girdled wheat plants fall to the ground. Without the use of specialized equipment, lodged plants are often missed at harvest, greatly increasing the total yield loss. Under moderate infestation, a conservative estimate of yield loss attributed to the WSS cutting is around 30%, although much higher losses have been reported (Ainslie, 1920).

2.3. Controlling the WSS

Several environmental factors have been suggested by Seamans (1945) to influence WSS survival, and could be considered when forecasting severity of infestations. Precipitation received in the fall can cause even maturation of host plants resulting in eggs being better dispersed as opposed to multiple eggs being laid in the same plant. This can result in wider levels of infestation. Conversely, wet and cool conditions during early spring can negatively impact larval pupation. Excessive moisture received during peak larval feeding activity causes plants to uptake water

which can result in drowning of the larva. Recently environmental factors have been incorporated into an Artificial Neural Network (ANN) model capable of predicting stem cutting, which allows producers to change their harvest management strategy to reduce losses (Beres et al., 2017).

2.3.1. Parasitism of the WSS

Natural parasites of the WSS can be important for naturally reducing populations. There are nine species of insects known to parasitize the WSS, of which only two, *Bracon cephi* (Gahan) and *Bracon lissogaster* (Musesebeck), are currently effective in reducing WSS populations in wheat (Runyon et al., 2012); both *B. cephi* and *B. lissogaster* are ectoparasitic wasps of the Hymenoptera. Of the two, *B. cephi* is considered the most economically important towards reducing WSS losses. *Bracon cephi* is a solitary insect whereas *B. lissogaster* can be solitary or communal (Nelson and Farstad, 2012). Both species produce two generations per year in native grasses versus the single generation per year in the WSS. Rates of parasitism by *B. cephi* in wheat is highly variable, with parasitized WSS larvae ranging between 7 – 88 %.

The females of *B. cephi* and *B. lissogaster* can sense WSS larval movement inside the stem, periodically stopping to tap the stem with their antennae. Once located, the female will cut into the wheat stem and paralyze the WSS larva with her ovipositor by injecting it with toxins (Weaver et al., 2004). Next the female will deposit between one and four eggs, either on, or near, the paralyzed WSS larva. Paralyzed WSS larvae are more likely to be cannibalized by other WSS larvae present within the stem (Weaver et al., 2005). The oviposition of several eggs by female WSS within a single stem could be a mechanism to promote survival from parasitism (Weaver et al., 2005). After the parasitoid larva has hatched, it will feed on the WSS larva for six to eight days before spinning a cocoon close to the initial feeding site.

In contrast to the WSS larvae which overwinter below ground, larvae of both parasitoid species overwinter in the upper half of the stem located above ground. As such, excessive tilling and stubble management can negatively impact the parasitoid survival through to the subsequent growing season, while at the same time does little to reduce WSS survival. Therefore, minimal till, or chemical fallow are preferred over intensive tilling (Runyon et al., 2002). At harvest, cutting height should be raised to preserve *B. cephi* populations, especially in WSS prone areas. Parasitoid larvae can survive in solid-stemmed wheats and can therefore be used as part of an integrated crop management strategy.

2.3.2. Chemical control

Chemical control is generally not effective in managing WSS because much of the insect's life cycle is spent as larvae protected within the stem. Control of adult WSS through contact insecticides has not proven effective because insects emerge over a period of several weeks making multiple pesticide applications necessary. Thus, the primary target for WSS control is the larval or prepupal form. As such, the chemicals used must be systemic in their mode of action (Wallace and McNeal, 1966). Two chemicals have been used with varying levels of success. The organophosphorus insecticide phorate has been used as a seed treatment (Wallace and McNeal, 1966). Heptachlor and heptachlor epoxide are also used, although are not systemic in their mode of action but are up-taken into the plant in sufficient quantities to kill larvae (Holmes and Peterson, 1963). Recently the systemic insecticide Thimet 20-G (Phorate: 0,0-diethyl S-[(ethylthio) methyl] phosphorodithioate) was registered for use against the WSS in Montana (MSU, 2015), although the chemical is considered highly toxic to humans, earthworms, aquatic organisms, and birds, and poses the risk of contaminating groundwater.

2.3.3. Cultural control

Several cultural control strategies to reduce WSS populations have been investigated with varying levels of success. The insect overwinters in wheat stubble, thus early researchers intuitively hypothesized that burning of stubble would be effective in reducing larval populations in infested fields. However, it was later discovered that the burning of stubble does little to negatively impact larvae in stubs (Ainslie, 1920) because the heat of the fire does not penetrate deep enough into the ground to reach the insect (Criddle, 1923). Moreover, the burning of stubble is not a recommended practice in modern agriculture because of soil erosion issues and the removal of organic matter. Furthermore, because parasitoids overwinter higher in the stub, burning is likely to have a more of a negative impact on parasitoids and is therefore not recommended.

Tillage has sometimes proven effective in the control of WSS. The most effective tilling strategy is deep burial of infested residue at least 12 cm or more ideally with the stub landing face down into the soil (Wallace and McNeal, 1966). However, the WSS is a resilient insect and can chew its way though the soil to freedom if tilling depth is not achieved. In the cold winters experienced throughout Western Canada, larvae in stubs that are exposed above ground through fall tillage may not survive in years when snow cover is minimal (Holmes and Farstad, 1956).

Tilling or mowing of native grasses adjacent to wheat fields could harm natural parasitoids and is not advised.

Crop rotation to non-hosts such as flax, canola, or mustard is an effective control strategy when sown after a heavy WSS infestation. In addition, sowing to hosts that reduce survivability of the larvae, like barley, can effectively reduce an infestation from severe to mild (Wallace and McNeal, 1966). Some hollow-stemmed cultivars of wheat, including many durum cultivars, appear to be less prone to WSS infestation than others, or otherwise negatively impact larval growth and development (Sherman et al., 2010). The hollow-stemmed cultivars McKenzie, AC Intrepid, Katepwa, and AC Avonlea were shown to have a negative effect on WSS fitness when compared to other hollow-stemmed lines (Carcamo et al., 2005). Similarly, Beres et al. (2013a) found that McKenzie, AC Navigator and AC Avonlea all experience significantly less cutting damage than other hollow-stemmed cultivars.

Altering sowing density can influence susceptibility to the WSS. Increasing sowing density and decreasing row spacing can reduce stem cutting because this strategy reduces stem diameter, and the female WSS appears to preferentially select large diameter stems for oviposition (Luginbill and McNeal, 1959). On the other hand, decreasing sowing density may help maximize the expression of stem-solidness in some cultivars, thereby helping to improve resistance to the WSS. Agronomic experiments are essential to find the management practices that optimize WSS resistance and agronomics. For example, Beres et al. (2011a) found that the solid-stemmed cultivar Lillian showed optimized pith expression and grain yield at seeding rates between 250-350 seeds m^{-2}, whereas increasing seeding rates of hollow-stemmed cultivars to 400-450 seeds m^{-2} could also decrease the amount of stem cutting in areas prone to damage from WSS (Beres et al., 2011a). Similar experiments have not been conducted in durum wheat.

Because many of the early solid-stemmed cultivars had inferior agronomic performance when compared to hollow-stemmed controls, a strategy to use cultivar blends consisting of hollow and solid-stemmed cultivars has been investigated. However, these studies suggest that the strategy may only be effective under low to moderate infestation (Weiss et al., 1990). Beres et al. (2007) compared stem cutting in AC Eatonia (solid-stemmed) and AC Abbey (hollow-stemmed), to a 1:1 (hollow:solid) cultivar blend, and found that solid-stemmed cultivars always incurred the least stem-cutting of the three treatments.

The use of trap crops has been investigated as a strategy to control the WSS. This control strategy is centered around the observation that sawfly infestation is heaviest near the edge of fields bordering previous sites of infestation (Weaver et al., 2004). This is primarily because sawfly are weak flyers and will prefer to oviposit on the nearest suitable host. This causes greater damage under strip-cropping systems, implemented in some regions to reduce wind erosion and preserve soil moisture, where alternating strips of crop and fallow are sown thereby increasing the ratio of edge to interior (Weaver et al., 2004). Adoption of agricultural practices like strip-cropping promoted WSS population growth. To take advantage of the edge effect associated with WSS oviposition, trap crops have been used to reduce WSS population size. This approach uses WSS susceptible cultivars and species around the field perimeters and along ditches where native grasses harbouring WSS larvae exist (Beres et al., 2011b). Non-wheat trap crops include rye grass (*Lolium perenne* L. Poaceae) and brome grass (*Bromus inermis* Leyss. Poaeceae). After early infestation, trap crops are removed by mowing, or tillage, well before maturity thereby destroying any larvae present. The cutting of native grasses in neighbouring sites is not recommended due to the negative impact on parasitoids of the WSS (Beres et al., 2011b).

An alternative strategy to sowing susceptible cultivars along the field perimeters is to sow a resistant cultivar, such as a solid-stemmed durum or common wheat cultivar (Beres et al., 2009). The benefits of this strategy over conventional trap crops are numerous. In this system, the trap crop can be harvested, thus the pre-harvest removal of the trap crop is not required. Not only does this prevent issues associated with tillage, it also preserves natural parasitoid populations. However, use of the solid-stemmed cultivar AC Eatonia under heavy infestations was not effective in reducing WSS populations; this may have been attributed to environmental effects that can reduce stem-solidness in some cultivars (Beres et al., 2009).

2.3.4. Expression of solid-stem in common wheat

The expression of the solid-stem trait in hexaploid wheat is influenced by environment including the amount of light/rain received, photoperiod, plant density/spacing and temperature (McNeal et al., 1966; Platt, 1941; Weiss and Morrill, 1992). Light is clearly the most important environmental factor, as shading has been shown to completely inhibit the expression of pith in common wheat (Platt, 1941). In contrast, high intensity of sunlight results in maximal pith expression (Holmes, 1984; Roberts and Tyrrell, 1961). Solid-stem expression is also inversely

related to the amount of precipitation received and number days with measurable precipitation specifically between May 25-July 5 (Hayat et al., 1995).

Nitrogen (N) and phosphorus fertilizer rates can increase expression of pith in hexaploid wheat, however excessive application may inhibit pith expression (Beres et al., 2012). Micronutrient blends do not appear to influence pith expression. Moderate N application rates (30 to 60 kg N ha^{-1}) coupled with moderate seeding rates (250-300 seeds m^{-2}) of solid-stemmed cultivars may provide the best balance of pith expression and yield potential (Beres et al., 2012).

2.3.5. Host resistance to WSS

The solid-stem phenotype has been used as the primary means of minimizing damage caused by the WSS for almost a century. Beginning in the early 1930s, attempts to select for host resistance to the WSS were initiated (Beres et al., 2011b) after (Kemp, 1934) proposed that solid-stemmed cultivars could negatively impact feeding of the stem mining WSS larvae. Under WSS pressure, solid-stemmed cultivars can incur up to 50% less damage (DePauw et al., 1994), and modern spring sown cultivars have superior yield and quality when compared to susceptible cultivars (Beres et al., 2007; Beres et al., 2009). Solid-stemmed cultivars are not immune to WSS damage, but should be considered the starting point for an integrated pest management approach (Beres et al., 2013a). Some of the early solid-stemmed lines were agronomically inferior to their hollow-stemmed counterparts, thus performing poorly in years when WSS pressure was low. Recent Western Canadian breeding efforts have led to the release of the solid-stemmed spring wheat line AC Lillian and CDC Landmark, both of which have comparable yield and quality characteristics to hollow cultivars irrespective of WSS pressure (DePauw et al., 2005). Similarly, three solid-stemmed durum lines CDC Fortitude (C. Pozniak), AAC Cabri, and AAC Raymore (D. Singh) were recently registered in Western Canada, all of which have strong performance relative to check cultivars.

2.3.6. Development of the wheat stem

To understand how wheat phenological development relates to WSS infestation, it is important to consider how stem elongation occurs. The wheat stem is composed of two structures, the node and internode, with the final number of each depending on several genetic and environmental factors (Holmes, 1979). In general, the terminal four to seven nodes will elongate

to form the shoot, whereas additional basal nodes remain hidden below the basal leaf sheath and do not extend (McMaster, 1997). In fall-planted winter wheat, stem elongation will only begin after the vernalization requirement has been met the following spring, whereas in spring-planted wheat there is no such vernalization requirement. The timing of stem elongation in winter wheat is influenced by genetic factors including the vernalization (VRN) genes on chromosome 5A, 5B and 5D (Chen et al., 2009), which could influence when the stem is exposed during peak sawfly flight. During stem elongation, the basal internode elongates first, and is followed subsequently by the node above it, as growth continues towards the uppermost internode (peduncle) which elongates last. During stem elongation, there is a period of concurrent elongation between two neighboring internodes.

Internode growth originates from a meristematic tissue located at the base of each internode. The origin of pith in solid-stemmed cultivars has not been identified, although it likely originates from the same meristematic region that gives rise to internode growth. In some solid-stemmed wheats, there is a tendency for pith to collapse and leave pockets of air space, presumably because elongation of the stem wall occurs faster than the pith can expand to fill the space (Putnam 1941). Alternatively, pith parenchyma may cease growth and division early in stem-elongation, which might lead to minor tearing and small cavities within the culm. The higher incidence of pith breakdown in some plants that are heterozygous for *SSt1* suggests that gene dosage might be involved. The speed at which stem elongation occurs varies between cultivars (Whitechurch et al., 2007), thus could have a major influence on pith development.

2.4. Stem-solidness in wheat

2.4.1. Origin of solid-stemmed wheat

There are at least four known sources of solid-stemmed wheat from which most modern lines are thought to have originated (Beres et al., 2013b). Depending on the source there can be significant differences in the level of pith expression (Beres et al., 2011b). The known sources include:

1) S-615 (hexaploid landrace)
2) Golden Ball (durum)
3) Biodur (durum)
4) *Thinopyrum ponticum* (Podp.) Z.-W. Liu & R.-C Wang (tall wheatgrass)

S-615 is a landrace that originated from New Zealand from which most solid-stemmed hexaploid cultivars released prior to 2010 were derived (Beres et al., 2011b). In North America, the first commercially available solid stem variety derived from S-615 was 'Rescue' and was released in 1948 (Platt et al., 1948) followed by the release of 'Chinook' in 1952 (Grant and McKenzie, 1964). The WSS resistance in Rescue was inadequate due to a considerable variation in pith expression, which could range from semi-solid to practically hollow (Platt et al., 1948). Recently it was discovered that S-615 is heterogeneous for *SSt1* (Beres et al., 2013b). It is therefore possible that some of the variability in solid-stem expression derived from the S-615 source could be due to heterogeneity in some seed sources.

The second source of stem-solidness is Golden Ball, which is a durum (*Triticum turgidum* L. var *durum*) cultivar with a solid stem, particularly in the top internode where most WSS eggs are oviposited (Platt, 1941). The genetic control of stem-solidness in Golden Ball was originally classified as being monogenic and partially dominant (Putnam, 1942). A single gene in Golden Ball was localized to chromosome 3B and it is likely the same gene carried by S-615 (Larson and Macdonald, 1963). This gene can be crossed into other durum lines to achieve effective levels of stem-solidness. The same does not hold true when crossing the gene from Golden Ball into hexaploid wheat, which almost always results in progeny with inferior levels of stem solidness. Platt and Larson (1944) were unable to recover hexaploid progeny with solid stems in interspecific crosses between RL1097/Golden Ball and Regent/Golden Ball. Larson and Macdonald (1963) made crosses between S-615/Golden Ball and Rescue/Golden Ball, but were unable to obtain any hexaploid progeny in later generations that were as solid as Golden Ball. They did, however, obtain progeny that were similar in solidness to S-615. It was concluded that D-genome suppression was likely responsible for the lack of solidness in the top internode in all hybrids (Larson and Macdonald, 1963). More recently, Clarke et al. (2005a) successfully developed two WSS resistant hexaploid wheat germplasm lines (G9608B1-L12J11BF02, G9608B1-L12J13AU01) by crossing Golden Ball with *Aegilops taushii* L. (2n = 2x = 14, DD) and selecting solid-stemmed progeny. Both lines show considerable improvement in pith expression comparable to Golden Ball, and are an improvement over solid-stemmed lines derived from the S-615 source.

Biodur is a cultivar of German origin that has been used as the predominant source of stem solidness in Western Canadian durum wheat breeding programs. Currently registered CWAD

cultivars CDC Fortitude (Pozniak et al., 2015), AAC Raymore (Singh et al., 2014) and AAC Cabri (Singh et al., 2016).

Finally, *T. ponticum*, is a wild relative of modern wheat. Attempts to transfer the resistance from *T. ponticum* into hexaploid wheat are often unsuccessful, yielding offspring that are less solid than S-615. Nevertheless, the hexaploid line 'CAC' and the Australian cultivar 'Janz' both derive their stem-solidness from *T. ponticum* and have a high level of resistance to stem-cutting (Beres et al., 2013b).

2.4.2. Genetic control of stem-solidness

Pioneering work by Yamashita (1937) led to the proposal of several genetic factors located on each of the genomes in wheat. In tetraploid wheat, he postulated that the A genome carries a gene conferring stem-hollowness and a gene conferring stem solidness. He also suggested multiple alleles of a gene conferring stem-solidness on the B genome, and identified a gene which was name O_D on the D genome that epistatically inhibits the expression of stem-solidness genes located on the A and B genome. In an examination of monosomics of S-615, Larson and Macdonald (1959) found that genetic factors on several D genome chromosomes carry suppressors of stem-solidness, which supported the findings of Yamashita.

Putnam (1942) was the first to suggest durum wheat carries a major dominant gene conferring stem-solidness on the B genome. Bozzini and Avanzi (1962) were able to induce the expression of stem-solidness in the normally hollow-stemmed durum wheat 'Cappelli' by X-ray irradiation, which they hypothesized was due to the disruption of a gene conferring stem-hollowness, which again supports the observations of Yamashita (1937).

Unlike in durum, the expression of the solid stem trait in hexaploid wheat is variable. Depending on the study, its genetic control has been described as being dominant, partially dominant, recessive or complex (Clarke et al., 2002). There is also a large effect of environment and genetic background on trait expression which suggests stem-solidness is quantitatively inherited in hexaploid wheat (Hayat et al., 1995). For example, when studying the crosses Red Bobs/C.T.715, and Redman/S-615, McKenzie (1965) found that four genes were responsible for controlling stem-solidness, including one major gene, and several minor genes with epistatic effects. Additional crosses made between hollow-stemmed cultivars Thatcher and Renown with S-615 and S-633 suggested up to three genes were involved in stem-solidness, but solidness was

only expressed when all three genes were in the homozygous recessive condition (McKenzie, 1965; Platt et al., 1941).

Larson and Macdonald (1966) studied whole chromosome substitution lines where individual chromosomes of the hollow hexaploid line Apex were substituted into the solid cultivar S-615. They found that both lines carry loci important for stem solidness and hollowness. Chromosomes 2A, 2D, 4A, 6A and 6D of Apex caused the stem to be hollower whereas chromosome 5D caused increased pith expression in the upper part of the lower internodes. The 3B substitution line was hollower than S-615 at all internodes. Moreover, chromosome 3D of S-615 was shown to have a smaller but positive effect on pith development. Gene dosage may also be important for solid stem expression because under ideal environmental conditions disomic S-615 3B lines had more pith than monosomic 3B in Apex (Larson and Macdonald, 1966).

It is now well established that much of the genetic variance conferring the solid-stem trait in most genetic backgrounds is controlled by a single gene (*SSt1*) on chromosome 3B in both wheat species. Both S-615 and Golden Ball carry the "resistant" marker allele for *SSt1* on chromosome 3BL (Beres et al. 2013b), suggesting that they may contain the same genetic factor(s) conferring pith expression. In common wheat, Cook et al. (2004) were first to use QTL mapping to identify the major locus *Qss.msub.3BL* linked to the SSR markers *gwm247, gwm340* and *Xgwm547*. In durum wheat, a gene controlling stem-solidness was found to work in a dominant manner by examining the progeny of the crosses Trinakria/DT267, Hugenot G/DT369, Hugenot W/DT369 8678-1048A/Hugenot G Kamilaroi/Hugenot G, and W9262-260DS/Kofa (Clarke et al., 2002). Genetic studies later localized this major gene in durum wheat to chromosome 3BL (*SSt1*) between the flanking SSR markers *gwm114* and *gwm247* (Figure 2.1A) (Houshmand et al., 2007). Recent unpublished work has identified several additional markers contained within the map interval (Figure 2.1).

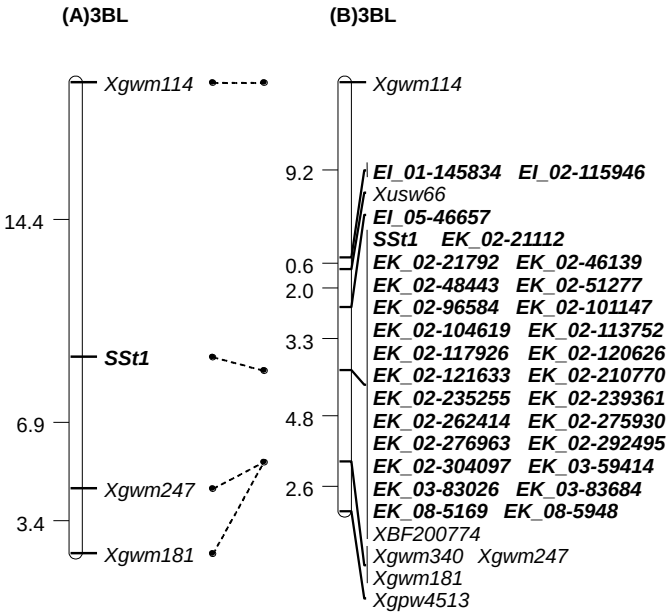

Figure 2.1. Mapping the *SSt1* locus (A) Original genetic map position of *SSt1* (Houshmand et al. 2007); (B) High density genetic map of *SSt1*. Markers in bold were developed from BAC sequences obtained from the current 3B physical map. Distance between markers is on left of genetics maps in cM. (unpublished data).

In addition to the locus on 3BL, Lanning et al. (2006) used bulked segregant SSR analysis to map stem-solidness in a cross between solid line Choteau, and semi-solid line MTHW9904. This study identified a secondary locus on chromosome 3DL (*Qss.msub-3DL*) carried by Choteau linked to the SSR primer *gwm645*. It is currently unknown whether *Qss.msub-3DL* corresponds to the homoeologous region of *Qss.msub-3BL*

Recent evidence suggests that multiple alleles could be present at the *Qss.msub-3BL* locus, that these alleles may influence whether the plant retains its stem-solidness at maturity, or undergoes pith breakdown leaving a hollow, or partially hollow stem. The first evidence for multiple alleles at *Qss.msub-3BL* was presented by Talbert et al. (2014) who found different banding patterns using the SSR marker *gwm340* in the lines 'Scholar' and 'Conan'. Both Scholar and Conan express similar levels of stem-solidness, however, the Conan allele conferred a higher level of resistance to stem cutting in field experiments. Varella et al. (2015) performed association mapping in a diverse panel of hexaploid lines and identified markers on chromosome 3B associated with early stem-solidness (*BS00065603_51*) and late stem-solidness (*BS00074345_51*).

Additional QTL conferring early stem-solidness were localized to 5D (*BobWhite_c8092_726*) and 1B (*RAC875_c8662_762*). The temporal pattern of stem-solidness expression was investigated in more detail by (Varella et al., 2016) by examining the solid-stemmed cultivars 'Conan' and 'Choteau'. Choteau, which derives its stem solidness from S-615, had strong dense pith that was present throughout stem elongation to maturity, whereas Conan had high levels of pith early in stem elongation, but became less solid at maturity. The Conan allele appears to have a unique haplotype around *SSt1* (Cook et al., 2017) differing from the S-615 source.

Most recently, Oiestad et al. (2017) looked at gene expression in two NILs from the entire uppermost internode of plants grown in the field at Feekes stage 7 prior to the appearance of the flag leaf; this study identified 260 genes within the *Qss.msub.3BL* interval, and suggested a putative candidate gene encoding an O-methyltransferase (OMT) based on differential expression between contrasting phenotypes.

2.4.3. Effect of solid-stem expression on yield

There are conflicting reports in the literature that suggest a possible negative correlation between the expression of the solid-stem trait and yield in the absence of WSS infestation (Hayat et al., 1995; McNeal et al., 1965; Weiss and Morrill, 1992). As a result, there has been some reluctance on behalf of growers to grow solid-stemmed cultivars, particularly when the risk of WSS activity is low (Beres et al., 2013a). One possible reason for the contradictory findings may be attributed to differences between spring and winter wheat. The authors of a study using near-isogenic lines (NILs) differing only by the presence or absence of the stem-solidness allele at *Qss.msub.3BL* concluded that a yield penalty was more related to genetic background, as opposed to negative pleotropic effects of *Qss.msub.3BL* on yield (Sherman et al., 2015). Therefore, selection for solid-stemmed cultivars with improved yield should be possible (Hayat et al., 1995). McNeal and Berg (1979) found that solid stemmed spring wheat cultivars yielded as much or better than hollow-stemmed cultivars. Ford et al. (1979) studied yield differences between hollow and solid-stemmed cultivars in 10 different crosses and observed no negative effect on yield associated with the solid stem trait. Moreover, solid-stemmed lines were more resistant to lodging compared to hollow-stemmed lines, preventing additional yield losses at harvest (Ford et al., 1979). The predominant source of the solid stem trait, S-615, is known to be agronomically inferior, and contributes few desirable traits outside of solid stem, which could explain some of the reported

negative correlations. Lebsock and Koch (1968) suggest the correlations between stem-solidness and yield are weak and can be overcome by parental selection and breeding.

2.4.4. Effect of solid-stem on the developing WSS

Pith acts as a physical barrier that restricts the movement of the WSS larva within the stem. Early investigation of WSS infestation using 18 solid-stemmed wheat lines showed larvae in solid-stemmed cultivars almost never succeeded in boring through the first node (Kemp, 1934), and never were successful in boring through two nodes (Morrill et al., 1994). Morrill et al. (1994) found that solid-stemmed cultivars had 89% lower infestation levels compared to hollow-stemmed counterparts, which may be attributed to the rapid desiccation that occurs in the pith that contributes to early larval desiccation and mortality (Holmes and Peterson, 1961; Holmes and Peterson, 1962). Because WSS larvae must reach the base of the plant before girdling the stem, Kemp (1934) also noted that solid-stemmed wheat cultivars infested by WSS larvae seldom experienced cutting. In addition to providing resistance to stem cutting, solid-stemmed cultivars can also have a negative effect on the insect's fitness and reproduction. Larvae that emerge from solid cultivars have significantly lower body weights (Beres et al. 2013b). Carcamo et al. (2005) found that solid stemmed cultivars AC Eatonia, AC Abbey, Lancer and Leader all had a negative impact on female WSS weight, size and fecundity. Thus, the reproductive potential of sawflies emerging from hollow stems is higher than those emerging from solid-stemmed cultivars attributable to increased insect biomass (Carcamo et al., 2005). Moreover, larvae emerging from some hollow cultivars carry significantly more eggs as adults than those emerging from solid cultivars. Solid-stemmed cultivars do not affect overwintering mortality (< 8 % of larvae die during winter) of *C. cinctus* (Cárcamo et al., 2011). It should be noted that stem-solidness may not be a perfect indicator of resistance to the WSS in both species of wheat, as differences in infestability, egg survival and larval survival exist among cultivars, and is influenced by environments (Roberts 1954).

2.5. The link between stem-solidness, drought resistance and remobilization of water soluble carbohydrates

New evidence suggests that the solid-stem phenotype could be an important contributor to the remobilization of water soluble carbohydrates (WSCs) such as the fructans, glucose, fructose, and sucrose from the stem under certain types of post-anthesis stress. In wheat, WSCs can make

up to 45% of the stem dry weight (Housley, 2000). Saint Pierre et al. (2010) found that stem-solidness was positively correlated with the WSC content in the upper internode, and that WSC content was positively correlated with grain yield under water limiting conditions. WSC content stored in the stem can be an important carbohydrate reserve that can be remobilized by the plant during grain filling under drought stress after anthesis, when photo assimilates are limiting (Ruuska et al., 2006; Sharbatkhari et al., 2016). Thus, the solid-stem trait may be of interest when breeding for resistance to drought, which is a major limiting factor for agriculture in many parts of the world (Saint Pierre et al., 2010). In addition, genotypes that accumulate greater amounts of stem WSCs have been linked to resistance to salinity by aiding in the osmotic adjustment (OA) and controlling the entrance of sodium into the root and uptake into the vacuoles to prevent damage to photosystems. Further research is required to better understand the complexities of carbon partitioning in modern solid-stemmed cultivars, but these findings suggest wheat breeders could target WSC content in new cultivars that are grown in regions under frequent drought stress.

3. SOWING DENSITY AND CULTIVAR EFFECTS ON PITH EXPRESSION IN SOLID-STEMMED DURUM AND COMMON WHEAT

ABSTRACT

The wheat stem sawfly (*Cephus cinctus*) is a destructive insect pest of spring, winter (*Triticum aestivum* L.) and durum wheat (*Triticum turgidum* L. var *durum*) throughout the Northern Great Plains of North America. Sawfly larvae hatch from eggs deposited inside the stem, and their subsequent feeding damages vascular tissue, reducing photosynthetic capacity and grain yields. Growing solid-stemmed wheat cultivars that develop pith in the culm lumen is the most effective method to minimize yield losses. Recent work has focused on optimizing sowing densities to achieve maximum levels of pith expression and grain yields in common wheat; however, little research has been conducted on durum wheat. We investigated the influence of four sowing densities (150, 250, 350, 450 seeds m^{-2}) on pith expression in two newly released solid-stemmed durum cultivars, CDC Fortitude and AAC Raymore, and compared them to the solid-stemmed common wheat cultivar, Lillian. CDC Fortitude and AAC Raymore displayed consistently high levels of pith expression across environments and sowing densities, in contrast to Lillian, which produced only slightly more pith than the hollow-stemmed durum check cultivar, Strongfield. A yield drag often associated with high pith expression was not evident as CDC Fortitude and AAC Raymore produced grain yield similar to Strongfield. When averaged over cultivars, increasing sowing density had a positive effect on grain yield in all cultivars, but was negatively associated with stem solidness. Our findings suggest that, unlike with CWRS solid-stemmed cultivars, altering sowing density is not required to achieve effective sawfly resistance with CDC Fortitude and AAC Raymore.

Disclosure:

This chapter has been published in Nilsen, K.T., J.M. Clarke, B.L. Beres, and C.J. Pozniak. 2016. Sowing Density and Cultivar Effects on Pith Expression in Solid-Stemmed Durum Wheat. Agronomy Journal 108:219-228.

3.1. INTRODUCTION

The wheat stem sawfly (WSS), *Cephus cinctus* Norton (Hymenoptera: Cephidae), has been one of the most damaging insect pests of common (*Triticum aestivum* L.) and durum wheat (*Triticum turgidum* L. var *durum*) across the Northern Great Plains of North America for more than a century (Beres et al., 2011b). Severe yield losses occur when WSS larval feeding activity damages the inner stem tissue, which reduces flag leaf photosynthetic ability (Delaney et al., 2010), and damages vascular bundles impairing the flow of water and nutrients to the developing grain (Morrill et al., 1992a). The greatest sawfly damage occurs in the southern parts of Alberta and Saskatchewan, southeastern Manitoba, and throughout Montana, North Dakota, South Dakota and western Minnesota (Beres et al., 2011b).

The life cycle of the WSS has been reviewed in depth by Beres et al. (2011b). Briefly, the insect spends up to 10 months of the year in its larval stage nested inside the wheat stem. In early spring, larvae will undergo pupation to reach the adult stage. Peak sawfly emergence generally occurs from June 10th - July 10th in western Canada (Beres et al., 2011a). Adult sawflies live for approximately one week and usually mate shortly after emergence followed by oviposition within a few days. The female sawfly has a specialized saw-like ovipositor (hence "sawfly") used to cut the wheat stem. During this process, the female will search for a suitable host plant in which to lay an egg, usually beginning at the upper internode of the developing wheat plant (Beres et al., 2011b). Females prefer succulent plants that are at early boot to anthesis stage with a large enough stem diameter suitable for oviposition (Holmes and Peterson, 1960). Eggs hatch approximately one week after deposition, and larvae immediately begin feeding on the inner stem wall (Holmes, 1954). As the growing season progresses, larvae tunnel down through the stem, damaging vascular tissue disrupting the flow of nutrients and water to the developing wheat kernels (Morill et al. 1992). At the end of the growing season, larvae will chew a notch around the inner perimeter of the stem at the base of the plant causing it to lodge. (Holmes, 1977). Due to the reduction in grain mass coupled with the fact that lodged stems are often not picked up during harvest, yield losses attributed to the WSS can be as high as 30 percent (Beres et al., 2007).

One strategy to prevent yield losses from the WSS is to grow solid-stemmed cultivars that develop pith within the culm lumen (Clarke et al., 2002). The development of pith increases egg mortality through mechanical crushing, and can act as a barrier impeding larval growth and development inside the stem (Holmes and Peterson, 1961; Holmes and Peterson, 1962). Solid

cultivars generally incur less damage from larval feeding, and have a lower proportion of stems cut at maturity (Sherman et al., 2015; Talbert et al., 2014). Surviving larvae collected from solid cultivars have lower body mass, size, and fecundity (Carcamo et al., 2005), although the presence of pith does not appear to significantly influence the overwintering mortality of the insect (Cárcamo et al., 2011). Solid-stemmed cultivars are not immune to sawfly damage, but should be considered the starting point for an integrated pest management approach (Beres et al., 2013a). There are currently no registered pesticides available to control WSS because the insect spends most of its life cycle inside the wheat stem shielded from insecticide contact (Wallace and McNeal, 1966). Adult sawflies emerge from infested stubble over a period of several weeks, making them difficult to control with a single chemical application, and multiple applications may be too costly to justify (Knodel et al., 2009). In western Canada, peak sawfly emergence has been shown to coincide with growing degree days (between 578-595 GDD), which could be used to predict the optimum time for chemical application (Beres et al., 2011c). Delaying seeding to avoid peak sawfly emergence time can substantially reduce damage, but this is not a practical strategy considering the short growing season on the Canadian prairies (Beres et al., 2007).

Attempts to select for host resistance to the wheat stem sawfly were initiated beginning in the early 1930s (Kemp, 1934). Most of the solid-stemmed common wheat cultivars are derived from the *Triticum aestivum* L. line S-615. The first S-615 derived cultivars were Rescue, Chinook and Cypress (Larson and Macdonald, 1966). Currently registered S-615 derived solid-stemmed Canada Western Red Spring (CWRS) cultivars include AC Eatonia (DePauw et al., 1994), AC Abbey (DePauw et al., 2000), and Lillian (DePauw et al., 2005). Pith expression in common wheat cultivars derived from S-615 can be quite variable and is heavily influenced by environmental factors. Sunlight intensity, the amount of precipitation, and days with measurable precipitation between the end of May to early July (Eckroth and McNeal, 1953; Holmes, 1984) all influence expression of pith under commercial sowing densities. Variable sowing densities have been investigated as one strategy to manipulate light penetration through the canopy to achieve maximum levels of pith expression. Because altering sowing densities can also influence other yield components, agronomic studies are essential to understand the best compromise for achieving maximum yield while maintaining adequate sawfly resistance. Similar studies have previously reported that pith expression in common wheat was inversely related to sowing density (Beres et al., 2011a; Beres et al., 2012), and was optimized at sowing densities of 250 to 350 seeds

m^{-2} (Beres et al., 2011a). In contrast, grain yield was positively related to sowing density, and was highest at sowing densities of 350 to 450 seeds m^{-2} (Beres et al., 2011a).

The entire durum wheat growing region of North America falls within the geographical range of the WSS (Beres et al., 2011a), but to date no research has investigated the effect of sowing density on pith expression and components of grain yield in solid-stemmed durum wheat. Durum wheat displays superior sawfly tolerance over common wheat; and through greater straw strength, hollow-stemmed durum wheat cultivars are less prone to lodging than hollow common wheat once girdled and cut by larvae (Eckroth and McNeal, 1953). There are at least two main sources for stem solidness in durum wheat: 1) Golden Ball and 2) Biodur. Recently, two new Biodur-derived solid-stemmed durum cultivars were registered in western Canada, AAC Raymore (Singh et al., 2014) and CDC Fortitude (Pozniak et al., 2015).

Pith expression in common wheat is controlled by the major QTL *Qss.msub-3BL*, located on the long arm of chromosome 3B (Cook et al., 2004). Additional minor QTL have been localized to chromosomes 3D (Lanning et al., 2006) and 5D (Varella et al., 2015). Stem-solidness in durum wheat is controlled by a single dominant gene '*SSt1'* on chromosome 3BL (Houshmand et al., 2007) and its expression is relatively stable across environments (Clarke et al., 2002). Despite the proximity of *SSt1* to *Qss.msub-3BL*, it remains unclear whether common wheat and durum wheat share the same gene for stem-solidness.

The goal of this research was to investigate the effect of sowing density on pith expression and other agronomic traits in durum wheat in order to maintain the highest possible level of sawfly resistance without sacrificing grain yield potential. The research presented here tests the following hypotheses: i) pith expression in durum wheat will decrease with increased sowing density, whereas grain yield will increase, ii) pith expression in durum wheat will be more stable across environments than in common wheat, and iii) solid-stemmed durum cultivars CDC Fortitude and AAC Raymore will be similar in grain yield to hollow check Strongfield.

3.2. MATERIALS AND METHODS

3.2.1. Experimental design

Experimental field trials were established near Coalhurst (AB, Canada), Lethbridge (AB, Canada), and Saskatoon (SK, Canada) during the 2012 to 2014 growing seasons. The 2012 site near Saskatoon was located at the Goodale research farm. The 2013 field site at Goodale was lost due to early season flooding, therefore the location was moved to a field site near Kenaston (SK, Canada) in 2014. Cropping systems at all sites were conducted in a wheat-fallow scheme, except for the Kenaston site which was seeded into lentil stubble from the previous year. The experimental design for each location was a randomized complete block design with four replications, wherein treatments were arranged in a 4 x 5 factorial design testing the interaction between sowing density x cultivar. Five cultivars (CDC Fortitude, AAC Raymore, Strongfield, Golden Ball, Lillian) and four sowing densities (150, 250, 350 and 450 seeds m^{-2}) were selected for this experiment. The cultivars were selected from the Canada Western Amber Durum (CWAD), and Canada Western Red Spring (CWRS) market classes, which included the hollow control Strongfield (Clarke et al., 2005b), the solid-stemmed CWAD cultivars AAC Raymore (Singh et al., 2014) and CDC Fortitude (Pozniak et al., 2015), the solid-stemmed CWRS cultivar Lillian (DePauw et al., 2005) and the solid-stemmed durum landrace Golden Ball (Clark et al., 1922). Seeds were treated with fungicide (Dividend XL RTA, Syngenta Crop Protection Canada) prior to sowing.

3.2.2. Experimental measurements

Temperature and photoperiod were measured at each location using Hobo Pendent temperature and light loggers (Onset Computer Corporation; part no. UA-002-XX). Sensors were attached to fiberglass stakes positioned above the level of the canopy and placed in each replication between two plots at the approximate center of each range. Supplemental long-term average monthly temperature and precipitation data were collected from Environment Canada (http://climate.weather.gc.ca/) for each location.

Plant density (plants m^{-2}) was assessed in May - June, depending on location, by staking a 1 m section of two randomly selected rows within each plot. Spike densities (spikes m^{-2}) were assessed between the end of July and early August using the same approach. The number of spikes per plant was calculated by dividing the total number of plants m^{-2} by the number of spikes per m^{-}

^{2}. Plant heights (cm) were measured by taking an average of the whole plot after grain filling. Lodging ratings were recorded on a per plot basis prior to harvest using a 1 (no lodging) to 9 (completely lodged) scale.

Stem solidness ratings were recorded at physiological maturity by taking the average rating from the main stem of 10 to 25 plants selected randomly from each plot. Because the upper internodes of the plant were previously shown to be the most important for sawfly oviposition, stem internodes were labelled sequentially, beginning with internode 1 located closest to the spike of the plant, down to internode 5, located closest to the crown. Each stem was split longitudinally and each internode was assigned a rating according to the following scale; 1: Hollow stem - no pith development, 2: Minimal signs of pith development, may appear 'cotton-like', 3: Large hollow tunnel in the stem, or, a huge cavity at a particular point in the internode, 4: Size of cavity equivalent to a pencil lead, or, some cavitation has occurred at a particular point in the internode, 5: Solid-stem filled entirely with pith (Beres et al., 2012; Depauw and Read, 1982; Pozniak et al., 2015). Analysis of the stem solidness data was performed separately by internode, in addition to using a combined rating averaged across the entire stem.

Plots were harvested at maturity using a small plot combine to measure grain yield from which sub-samples were collected to test for grain protein concentration (%), test weight (kg hL $^{-1}$) and seed mass (g 1000 $^{-1}$). Grain protein was assessed using near infrared reflectance spectroscopy technology (Foss Decater GrainSpec, Foss Food Technology Inc.).

3.2.3. Statistical analysis

Data were analyzed using the MIXED procedure of SAS 9.3 (Littell et al., 2006). Sowing density, cultivar and the sowing density x cultivar interaction were considered as fixed effects and determined significant if $p \leq 0.05$. Site-years and replications were considered as random effects. Final data analysis was performed as a combined analysis across eight testing environments to generate least square means (LS means) for all traits. Normality of model residuals was assessed using the UNIVARIATE procedure of SAS 9.3. All interactions with random factors were considered as random within the mixed model. In cases where significance was declared, further testing was performed using Fisher's least significant difference ($LSD_{0.05}$) test to characterize differences between treatment means using the PDMIX800 SAS macro (Saxton, 1998). Orthogonal contrasts were performed to test the relationship of sowing density with phenotypic

expression of each trait. LS means for each treatment combination combined across environments were used to create a Pearson correlation coefficient matrix using the CORR procedure of SAS.

3.3. RESULTS

Monthly trends in temperature and light intensity were generally similar across testing environments, except for Lethbridge 2013 which received the highest light intensity, particularly during June and July (Table 3.1). Lower monthly average light intensities were recorded at Coalhurst (2014), and Lethbridge (2012 and 2014) compared to the other environments. There were, however, large variations in average weekly light intensity between environments, particularly between 5 and 10 weeks after planting (Figure 3.1). Growing season precipitation ranged from 191 to 359 mm (Table 3.1).

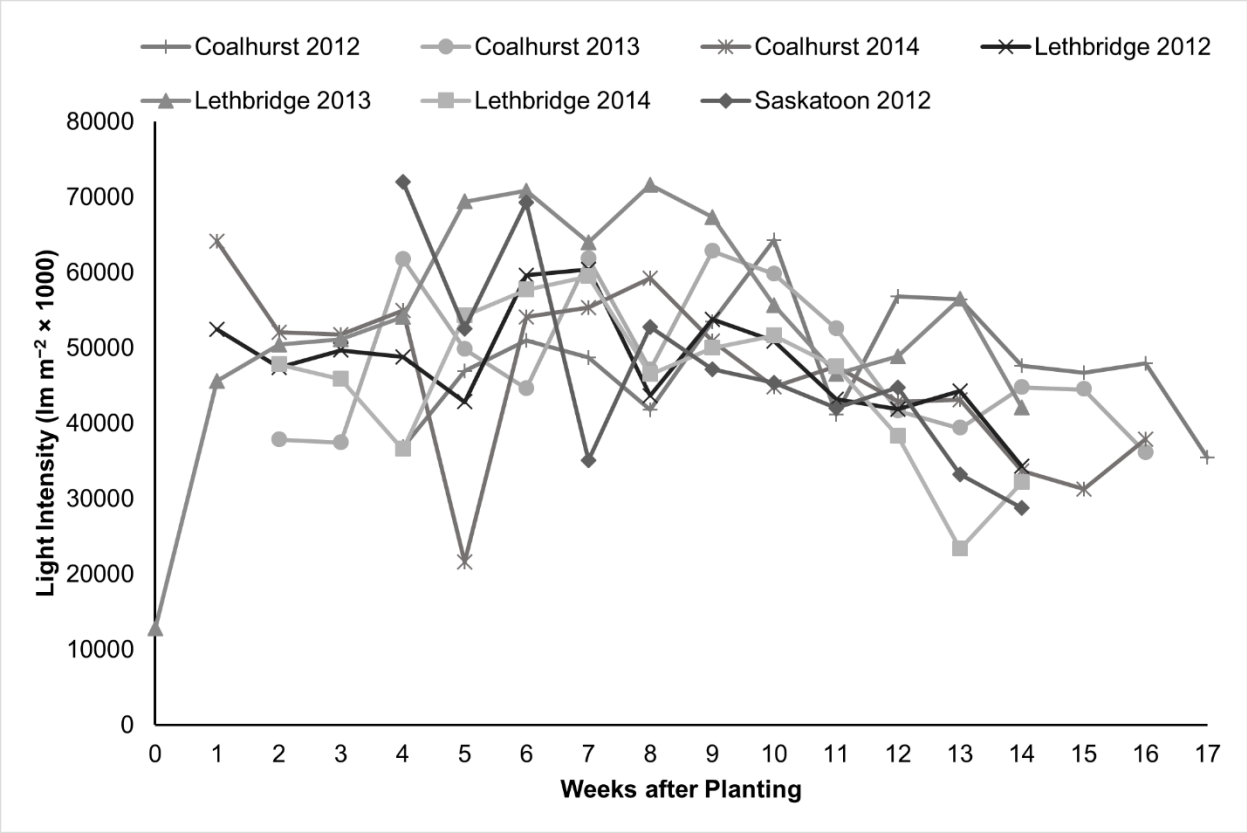

Figure 3.1. Average weekly light intensity (lm m^{-2} × 1000) recorded by Hobo sensors in field testing environments during 2012-2014. Data are presented based on the number of weeks after planting.

Table 3.1. Description of testing environments, soil type, sowing and harvest dates, average monthly temperature (°C), light intensity (lm m^{-2} x1000) and precipitation.

Location	Coalhurst, AB, Canada						Lethbridge, AB, Canada						Saskatoon, SK, Canada		Kenaston, SK, Canada	
Latitude and longitude	49° 44'N, 112° 57' W						49°69'N, 112°83'W						52° 02' N, 106° 34' W		51° 49' N, 105° 52' W	
Soil zone/series/texture	Dark Brown, Chernozemic Clay Loam						Dark Brown, Chernozemic Silty Clay Loam						Dark Brown, Chernozemic Loam		Dark Brown, Chernozemic Clay Loam	
Crop year	2012		2013		2014		2012		2013		2014		2012		2014	
Sowing date	25-Apr		7-May		9-May		17-May		17-May		18-May		23-May		28-May	
Harvest date	9-Sep		27-Sep		19-Sep		28-Aug		30-Sep		24-Sep		14-Sep		14-Sep	
Mean temperature and light intensity (Lm m^{-2}) × 1000	°C	Lux	°C	Lux	°C	Lux	°C	Lux	°C	Lux	°C	Lux	°C	Lux	°C‡	Lux
June	17.7	47885	18.2	52700	16.7	45698	17.4	48468	18.4	58851	16.7	46216	22.7†	63212	14.1	-
July	23.5	54894	21.9	55541	23.6	51322	22.6	53125	21.8	66232	23.5	53714	23.5	52161	18.3	-
August	21.2	43883	21.4	40912	20.6	37918	20.6	41629	21.3	47636	20.6	36315	20.5	40755	19.9	-
Precipitation (mm). 1 May to 15 Sept.	202.3		270.6		251.7		191.2		283.6		204.3		359.3		277.6	

†Sensor began recording data June 28

‡Sensor readings were not recorded, temperature data were taken from Environment Canada

Stem solidness varied among cultivars at each internode, and when averaged over all stem internodes (Table 3.2). Pith expression was greatest in the two commercially registered solid-stemmed durum cultivars, CDC Fortitude and AAC Raymore, lowest in the hollow-stemmed cultivar Strongfield, and intermediate in Golden Ball and Lillian. All three solid-stemmed durum cultivars displayed the same pattern of pith expression across internodes, which tended to be greater in the upper internodes becoming progressively less in internodes closer to the crown (Table 3.2). In contrast, pith expression in Lillian and Strongfield was greater in lower internodes becoming less solid towards the spike. CDC Fortitude, AAC Raymore and Golden Ball showed similar variation in pith expression between testing environments.

Table 3.2. Stem solidness (1-hollow to 5-solid) by internode and in response to sowing density across field testing environments during 2012-2014.

Factor	Treatment	Internode 1 (Spike)	Internode 2	Internode 3	Internode 4	Internode 5 (Crown)	Whole Stem Average
Cultivar	CDC Fortitude	4.38	4.28	4.01	3.73	3.47	4.00
	AAC Raymore	4.41	4.14	3.73	3.60	3.52	3.91
	Golden Ball	4.05	3.91	3.69	3.54	3.42	3.73
	Lillian	1.90	1.72	2.06	2.36	2.60	2.13
	Strongfield	1.41	1.46	1.70	2.22	2.73	1.89
	SED	0.081	0.071	0.072	0.072	0.097	0.063
	Pr > F	<.0001	<.0001	<.0001	<.0001	<.0001	<.0001
	LSD (0.05) †	0.158	0.139	0.142	0.142	0.19	0.124
Sowing density (seeds m^{-2})	150	3.32	3.21	3.15	3.20	3.17	3.22
	250	3.23	3.12	3.08	3.09	3.17	3.15
	350	3.23	3.10	3.03	3.07	3.14	3.13
	450	3.14	2.97	2.88	3.00	3.11	3.03
	SED	0.088	0.064	0.065	0.065	0.086	0.057
	Pr > F	0.0998	0.0015	0.0002	0.0219	0.8964	0.0077
	LSD (0.05)	ns	0.125	0.127	0.128	ns	0.112
Linear trend	Linear equation (*Y*)	ns	-0.0008x + 3.33	-0.0009x + 3.30	-0.0006x + 3.27	ns	-0.0006x + 3.31
	Regression value (R^2)	ns	0.94	0.94	0.92	ns	0.96
Contrasts (P*r* > F)	Linear	0.0194	0.0001	<.0001	0.0032	0.4643	0.0008
	Quadratic	0.9792	0.6738	0.3692	0.679	0.8423	0.8002
	Cubic	0.3977	0.4097	0.5489	0.4471	0.8435	0.5139
Cultivar × sowing density	Pr > F	0.3087	0.2164	0.354	0.2125	0.0889	0.1931

†SED: Standard error of the difference

‡LSD: Fisher's protected least significant difference

The relationship between sowing density and pith expression was linear and negative for each internode, and combined across internodes except for internodes one and five where no significant association was detected (Table 3.2). Maximum average stem pith expression was achieved with sowing densities below 450 seeds m^{-2} (Figure 3.2a). Pith expression in internodes 2 and 3 was most negatively affected by increased sowing density (Table 3.2).

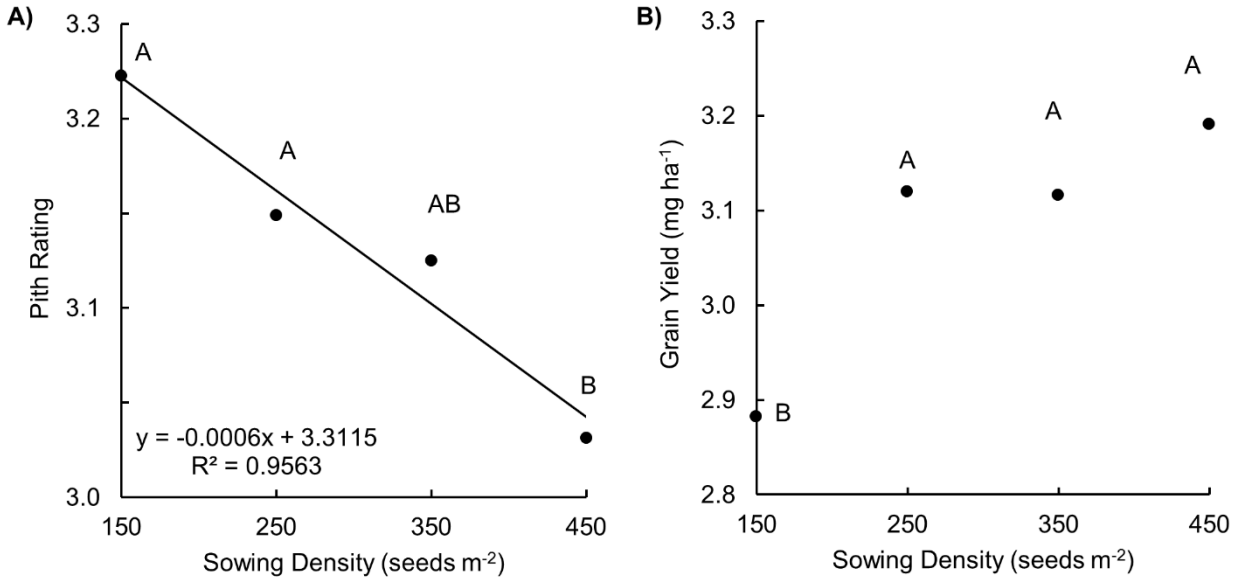

Figure 3.2. Influence of sowing density on a) pith expression and, b) grain yield. Data were averaged across cultivars and testing environments 2012-2014. Means with the same letter grouping were not significantly different using Fishers $LSD_{0.05}$.

Cultivar and sowing density influenced grain yield but the interaction between cultivar and sowing density was not significant (Table 3.3). Grain yield of CDC Fortitude and AAC Raymore were not significantly different from Strongfield, and all three cultivars yielded significantly higher than Lillian or Golden Ball. Contrast analysis revealed that increasing sowing density had a positive effect on grain yield in all lines. Maximum levels of grain yield were observed at sowing densities above 150 seeds m^{-2} (Table 3.3, Figure 3.2b).

Table 3.3. Components of grain yield by cultivar and in response to sowing density across field testing environments during 2012-2014.

Factor	Treatment	Grain Yield	Plant stand Density	Spike Density	Sed Mass	Test Weight	Grain Protein	Spikes per Plant
		Mg ha^{-1}	plants m^{-2}	heads m^{-2}	g 1000^{-1}	kg hL^{-1}	%	
Cultivar	CDC Fortitude	3.31	192	241	41.1	77.6	14.0	1.4
	AAC Raymore	3.24	187	248	43.8	77.5	14.4	1.5
	Golden Ball	2.59	181	219	46.3	77.3	13.3	1.4
	Lillian	2.86	182	278	36.4	76.2	15.9	1.7
	Strongfield	3.39	171	256	43.2	77.9	14.1	1.7
	SED†	0.149	5.7	17.5	0.95	0.55	0.24	0.06
	Pr > F	<0.0001	0.0215	0.0339	<.0001	0.0388	<.0001	<.0001
	LSD (0.05) ‡	0.30	12	35	2.0	1.1	0.43	0.25
Sowing density (seeds m^{-2})	150	2.88	119	218	42.9	77.0	14.7	2.1
	250	3.12	160	241	42.2	77.3	14.4	1.6
	350	3.12	203	254	41.9	77.4	14.2	1.3
	450	3.19	248	280	41.6	77.5	14.2	1.2
	SED	0.081	16.2	12.1	0.37	0.13	0.09	0.07
	Pr > F	0.0052	<.0001	0.0004	0.0193	0.0074	<.0001	<.0001
	LSD (0.05)	0.17	33	25	0.8	0.3	0.16	0.30
Linear trend	Linear equation (Y)	0.0009x + 2.80	0.4315x + 53.28	0.1996x + 188.54	-0.0039x + 43.34	0.0016x + 76.84	-0.0016x + 14.843	-0.0032x + 2.49
	Regression (R^2) value	0.78	0.9997	0.99	0.94	0.94	0.91	0.90
Contrasts (Pr > F)	Linear	0.0015	<.0001	<.0001	0.0029	0.001	<.0001	<.0001
	Quadratic	0.166	0.8925	0.8243	0.4683	0.3516	0.04	0.032
	Cubic	0.2258	0.996	0.5941	0.6398	0.9876	0.9367	0.758
Cultivar × sowing density	Pr > F	0.29	0.5474	0.5347	0.1031	0.8522	0.0697	0.1008

†SED: Standard error of the difference

‡LSD: Fisher's protected least significant difference

The main effects of cultivar and sowing density were significant for all components of grain yield (spike density, stand density, test weight, protein content, seed mass, spikes per plant), but the cultivar x sowing density interaction was not significant for any trait (Table 3.3). Spike density, test weight and protein concentrations of CDC Fortitude and AAC Raymore were not significantly different from Strongfield. There were significantly higher plant stand densities observed in CDC Fortitude, AAC Raymore, Golden Ball and Lillian than in Strongfield (Table 3.3). Strongfield, AAC Raymore, and Lillian had the highest spike densities, greater than in CDC Fortitude or Golden Ball. Similarly, Strongfield, Lillian and AAC Raymore had a greater number of spikes per plant than CDC Fortitude or Golden Ball. Seed mass was greatest in Golden Ball, lowest in Lillian and intermediate in Strongfield, AAC Raymore and CDC Fortitude. Test weights were not significantly different between the four durum cultivars, all of which were significantly higher than in Lillian. Grain protein content was greatest in Lillian, lowest in Golden Ball and intermediate in CDC Fortitude, AAC Raymore and Strongfield (Table 3.3).

Contrast analysis revealed significant linear relationships between sowing density and all components of grain yield. Quadratic relationships were also observed for grain protein concentration and spikes per plant (Table 3.3). Increasing sowing density had a positive effect on plant stand density, spike density and test weight, whereas the relationship was negative for seed mass, spikes per plant and protein concentration (Figure 3.3, a-f). Maximum test weights were observed at sowing densities above 150 seeds m^{-2}. As expected, the responses among sowing density, plant stand density, and spike density displayed a pronounced linear relationship. Increasing sowing densities from 150 to 450 seeds m^{-2} resulted in over twice as many plants, and 27% more spikes per square meter. Seed mass and protein concentration were inversely related to sowing density, and both were greatest at sowing densities of 150 seeds m^{-2} (Figure 3.3, d, f).

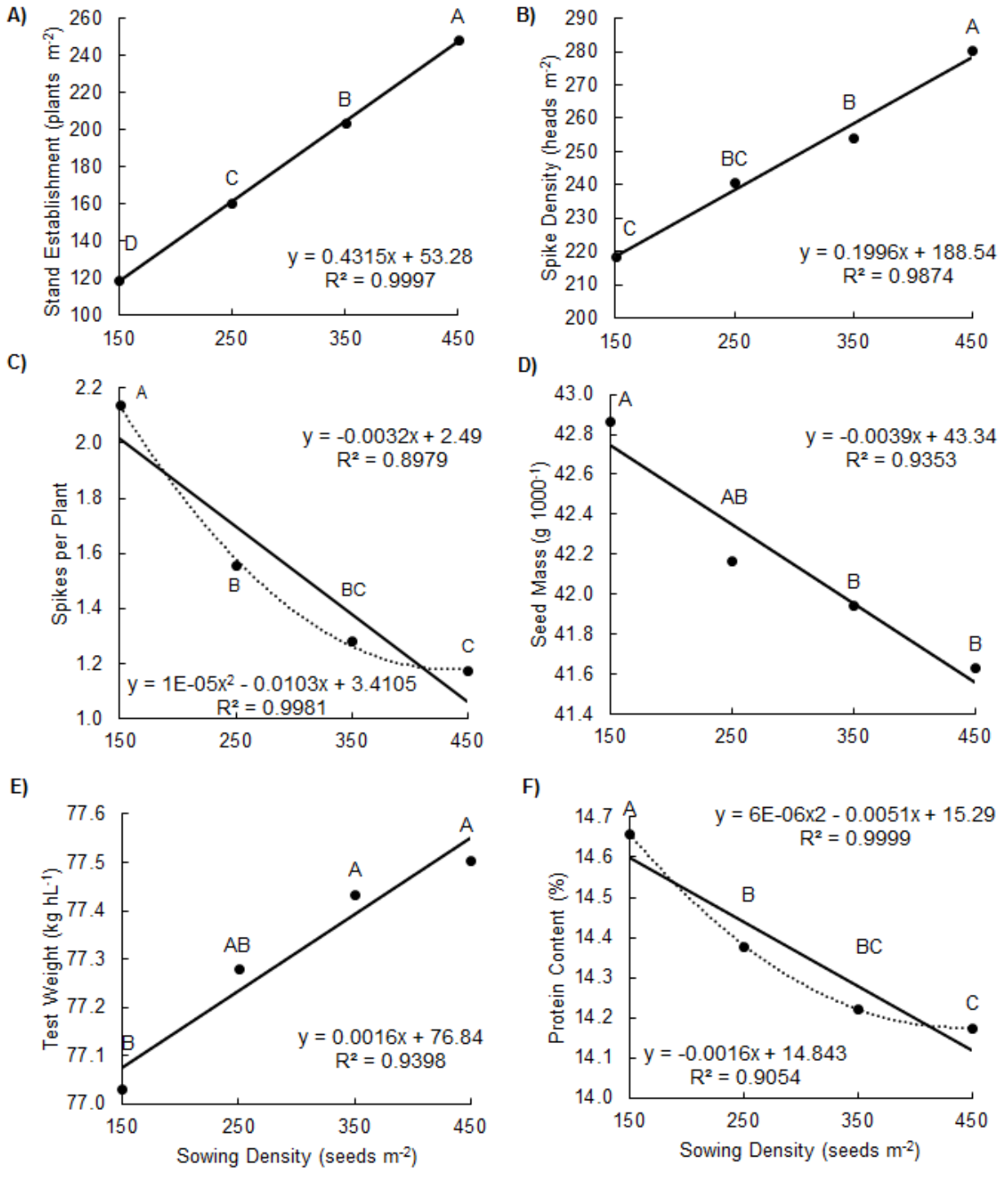

Figure 3.3. Influence of sowing density on components of grain yield: a) plant stand density, b) spike density, c) spikes per plant, d) seed mass, e) test weight, and f) protein content. Data were averaged across cultivars and testing environments 2012-2014. Means with the same letter groupings were not significantly different using Fishers $LSD_{0.05}$.

Results from correlation analysis of stem solidness and agronomic traits are presented in Table 3.4. Average stem solidness was positively correlated with seed mass (r = 0.48), and negatively correlated with spike density (r = -0.51) and protein content (r = -0.51). There was no significant correlation between stem solidness and grain yield, plant density, test weight, plant height, lodging or spikes per plant. Grain yield was strongly negatively correlated with lodging (r = -0.74) and plant height (r = -0.83), and positively correlated with test weight (r = 0.60). Plant density was strongly negatively correlated with the number of spikes per plant (r = -0.88) and positively correlated with spike density (r = 0.71). Seed mass was negatively correlated with protein content (r = -0.85) and spike density (r = 0.64), but positively correlated with lodging (r = 0.59) and test weight (r = 0.65). Test weight was negatively correlated with protein content (r = -0.79). Spike density was negatively correlated with lodging (r = -0.58), whereas lodging was negatively correlated with protein content (r = -0.58).

Table 3.4. Pearson's correlation coefficients testing the relationships between stem solidness, grain yield, and agronomic traits. All listed coefficients were significant at $p < 0.05$.

	Average Stem-Solidness	Spikes per Plant	Protein Content	Lodging	Height	Spike Density	Test Weight	Seed Mass	Plant Stand Density
Grain Yield	ns[†]	ns	ns	-0.74	-0.83	ns	0.60	ns	ns
Plant Stand Density	ns	-0.88	ns	ns	ns	0.71	ns	ns	
Seed Mass	0.48	ns	-0.85	0.59	ns	-0.64	0.65		
Test Weight	ns	ns	-0.79	ns	ns	ns			
Spike Density	-0.51	ns	ns	-0.45	ns				
Plant Height	ns	ns	ns	0.93					
Lodging	ns	ns	-0.58						
Protein Content	-0.51	0.44							
Spikes per Plant	ns								

[†]ns: No significant correlation

3.4. DISCUSSION

This study showed that sowing density and cultivar influenced stem solidness, yield and agronomic traits in durum and common wheat. Increasing sowing density negatively influenced pith expression and positively influenced grain yield in all cultivars. These results suggest sowing at densities of 350 seeds m^{-2} or less to maximize stem solidness. Female sawflies are known to preferentially select larger diameter stems for oviposition (Luginbill and McNeal, 1959). Because lower sowing densities are often associated with increased stem diameter, there may be an increased risk of stem cutting under extremely low sowing densities, which has been observed in some hollow-stemmed cultivars (Beres et al., 2011a). Therefore, sowing at densities closer to 350 seeds m^{-2} is recommended.

The solid-stemmed durum cultivars CDC Fortitude and AAC Raymore displayed superior stem solidness to Golden Ball and Lillian across all sowing densities. Both CDC Fortitude and AAC Raymore derive stem solidness from Biodur, which is a cultivar of German origin (Pozniak et al., 2015; Singh et al., 2014). A second source of stem solidness in durum wheat, Golden Ball, is also known to have pith expression superior to common wheat (McNeal, 1961). Golden Ball is of South African origin introduced to Canada but was later deregistered for its inferior pasta quality (Kemp, 1934; Knott, 1995). Although both sources were believed to carry the stem solidness gene *SSt1* (Houshmand et al., 2007), recent molecular evidence suggests the Biodur source may be different from Golden Ball based on differences in haplotype around the *SSt1* locus (Nilsen, unpublished data, 2015). Therefore, the improved stem-solidness of CDC Fortitude and AAC Raymore over Golden Ball might reflect genetic differences between sources, or could be a result of an accumulation of additional genetic factors conferring stem solidness throughout the breeding process.

The three solid durum cultivars had more pith development in the internodes closest to the spike, and became less solid towards the crown of the plant, in contrast to Lillian which had greater pith density in the lower internodes and became less solid towards the spike. This finding agrees with previous research, which found durum wheat to be more solid in the upper internode than common wheat cultivars derived from S-615. This difference was attributed to one or more genes on the D-genome suppressing stem solidness in common wheat (Larson, 1959b; McNeal and Wallace, 1967). The top internodes of the plant are the preferred location for sawfly oviposition

(Holmes and Peterson, 1960), therefore increased pith in this area of the stem could play an important role in conferring an extra level of resistance against stem cutting or early stage larval feeding in durum wheat. The lower two internodes of the plant were previously shown to be the region where larvae feed and accumulate the bulk of their body mass prior to winter (Delaney et al., 2010); therefore, Lillian could have a reduced level of resistance to early larval feeding in the upper internodes, but increased resistance against later stage larval feeding. Interestingly, the hollow-stemmed check Strongfield expressed some pith at the periphery of the inner stem walls, and tended to have a thicker outer stem wall than Lillian. Eckroth and McNeal (1953) found that hollow-stemmed durum wheat was more resistant to WSS than hollow-stemmed common wheat, but the reason for this increased resistance was unknown. The pith development coupled with the increased stem wall diameter in Strongfield may help to provide some resistance to stem cutting and could potentially slow larval movement inside the stem.

Grain yield was positively associated with increased sowing density in all cultivars, and stable yields were achieved at sowing densities above 150 seeds m^{-2}. Increasing sowing density reduced tillering capacity in all lines as evidenced by a decrease in the number of spikes per plant. Interestingly, we did not see a corresponding increase in seed mass that was previously reported in common wheat (Beres et al., 2011a), which may have been due to a differential response between durum and common wheat. We did, however, find a positive relationship between sowing density and test weight. Taken together, these findings suggest that most of the yield advantage at higher densities must have come from a reduction in the number of tillers produced per plant coupled with an increase in the number of seeds produced per spike.

Grain protein content was negatively associated with sowing density across all lines, which was previously reported in common wheat (Beres et al., 2011a). In the present study, Lillian had the highest grain protein content of all the lines tested. This finding was expected, because Lillian carries the high protein gene *Gpc-B1* and was the first solid-stemmed Canadian cultivar with yield and protein concentration similar to hollow-stemmed cultivars (DePauw et al., 2007)

CDC Fortitude and AAC Raymore yielded the same as the hollow-stemmed control Strongfield, which suggests that any yield penalty that may have been associated with the solid-stem trait has been overcome through the breeding process. This was also reflected in the phenotypic correlation which revealed no significant relationship between stem solidness and yield. We did find negative correlations with protein content and spike density, and a positive

correlation with seed mass, although these findings were probably more related to the differences between spring and durum wheat (lower protein, larger seed mass and reduced tillering), rather than due to stem solidness directly. Historically, some producers of common wheat were reluctant to grow solid-stemmed cultivars because of a perception of a negative association between stem solidness and yield potential in the absence of sawfly infestation (Weiss and Morrill, 1992). One study found a negative correlation between stem solidness and yield in progeny derived from the cross Thatcher/Rescue (Rescue is a derivative of S-615) (McNeal et al., 1965). Conflicting studies have found no negative correlation (Cook et al., 2004; Hayat et al., 1995; Lanning et al., 2006; McNeal and Berg, 1979; Sherman et al., 2015). In the present study, we did not see a negative correlation between stem-solidness and grain yield, which agrees with similar research performed in common wheat. However, further investigation to confirm this finding in durum wheat using near isogenic lines (NILs) is required. Taken together, these results demonstrate that producers should not be hesitant to seed solid-stemmed durum wheat regardless of sawfly pressure.

All lines showed variation in pith density across environments, however, pith expression in Lillian was more variable than the solid-stemmed durum cultivars tested**.** Wallace et al. (1973) suggest a minimum mean threshold stem solidness score of 3.75 to achieve effective resistance to the WSS. In this experiment, the solid-stemmed durum cultivars exceeded this level (average = 3.86) and thus should all have strong resistance across environments. In contrast, Lillian had only intermediate pith expression (average = 2.17), and in some environments, was practically hollow-stemmed. This finding was similar to results presented by Beres et al. (2011a), who suggest differences in response to environment or limited genetic potential as a possible cause of reduced stem solidness in Lillian. Inconsistent pith expression has been an issue in many of the registered CWRS cultivars that were derived from the S-615 source (Beres et al., 2013b). Previous research showed that with S-615 derived cultivars, low light intensity or shading for a period of seven days can negatively affect pith expression (Holmes, 1984). We performed further analysis to test for a correlation between average weekly light intensity between locations, and average stem solidness in Lillian (data not shown). Average light intensity (lux) received between 7 to 11 weeks (42 to 77 days) after planting was strongly correlated with pith expression in Lillian ($r = 0.93$, $p = 0.002$), which corresponds roughly to the time between the start of stem elongation and the end of flowering. During these critical growth stages, we hypothesize that the formation of pith must be highly coordinated with internode elongation, which begins with the basal node, and progresses

sequentially from node to node towards the top of the plant. Low light intensity during this period of plant development may inhibit cell division or growth within the pith tissue of the inner stem. Throughout most of the growing season of 2012, the Saskatoon and Lethbridge sites experienced the lowest light intensity of all testing environments, and subsequent pith expression in Lillian was poor. The highest average light intensity across testing environments was recorded at Lethbridge 2013, and corresponding pith expression in Lillian was the highest of any environment (average = 2.8). Taken together, these results suggest light intensity could be a major contributing factor towards the variation of pith expression in Lillian.

3.5. CONCLUSIONS

Modern durum cultivars CDC Fortitude and AAC Raymore, had stems that were significantly more solid than Golden Ball or the CWRS cultivar Lillian. When averaged over all cultivars, increasing sowing density tended to negatively influence pith expression. However, both new durum cultivars expressed superior stem solidness across all sowing density levels, above the recommended minimum threshold level to achieve effective sawfly resistance (Wallace et al., 1973). There was no negative association between stem solidness and grain yield in CDC Fortitude and AAC Raymore, as both produced grain yield similar to Strongfield. Yield was positively influenced by increasing sowing density in all cultivars, and stable yields were achieved at sowing densities greater than 150 seeds m^{-2}. These findings suggest that, unlike with CWRS solid-stemmed cultivars, it does not appear necessary to lower sowing densities for CDC Fortitude and AAC Raymore, as the critical threshold for optimum pith expression was maintained at all sowing density levels (i.e. $\geq$ 3.75). Our results reinforce the important role that both solid-stemmed cultivars and proper agronomics can offer to a holistic IPM strategy for WSS management.

4. HIGH DENSITY MAPPING AND HAPLOTYPE ANALYSIS OF THE MAJOR STEM-SOLIDNESS LOCUS *SSt1* IN DURUM AND COMMON WHEAT

ABSTRACT

Breeding for solid-stemmed durum *(Triticum turgidum* L. var *durum*) and common wheat (*Triticum aestivum* L.) cultivars is one strategy to minimize yield losses caused by the wheat stem sawfly (WSS, *Cephus cinctus* Norton). Major stem-solidness QTL have been localized to the long arm of chromosome 3B in both wheat species, but it is unclear if these QTL span a common genetic interval. In this study, we have improved the resolution of the QTL on chromosome 3B in a durum (Kofa/W9262-260D3) and common wheat (Lillian/Vesper) mapping population. Coincident QTL (LOD = 94 - 127, R^2 = 78 - 92 %) were localized near the telomere of chromosome 3BL in both mapping populations, which we designate *SSt1*. We further examined the *SSt1* interval by using available consensus maps for durum and common wheat and compared genetic to physical intervals by anchoring markers to the current version of the wild emmer wheat (WEW) reference sequence. These results suggest that the *SSt1* interval spans a physical distance of 1.6 Mb in WEW (positions 833.4 – 835.0 Mb). In addition, minor QTL were identified on chromosomes 2A, 2D, 4A, and 5A (LOD = 3.0 – 6.1, R^2 = 0.2 – 2.8 %) that were found to synergistically enhance expression of *SSt1* to increase stem-solidness. These results suggest that developing new wheat cultivars with improved stem-solidness is possible by combining *SSt1* with favorable alleles at minor loci within both wheat species.

Disclosure:

This chapter has been published in**:** Nilsen KT, N'Diaye A, MacLachlan PR, Clarke JM, Ruan Y, Cuthbert RD, et al. (2017) High density mapping and haplotype analysis of the major stem-solidness locus *SSt1* in durum and common wheat. PLoS ONE 12(4): e0175285. https://doi.org/10.1371/journal.pone.0175285

4.1. INTRODUCTION

The WSS (*Cephus cinctus* Norton) is a destructive insect pest of durum (*Triticum turgidum* L var *durum*) and common wheat (*Triticum aestivum* L.) in the northern Great Plains of North America. In Canada, severe infestations of WSS have been reported in southern Alberta, Saskatchewan and eastern Manitoba since the early 1920s (Criddle, 1923). In the United States, areas most prone to sawfly damage include north and eastern Montana, North Dakota, northern South Dakota and western Minnesota (Beres et al., 2011b). Severe damage has recently been observed in areas of Colorado, Wyoming and Nebraska.

The biology of the WSS has been extensively reviewed (Beres et al., 2011b; Wallace and McNeal, 1966). Briefly, WSS emerge from infested stubble of the previous cropping season, usually from around mid-June to mid-July. After mating, the female will select a suitable host plant to puncture using a specialized saw-like ovipositor to deposit an egg. Within five to seven days, the egg will hatch and the process of larval tunneling and feeding on plant tissue within the culm of the stem commences (Ainslie, 1920). Larval feeding damages vascular bundles and reduces photosynthetic ability (Macedo et al., 2007). Kernels harvested from infested plants have 5 to 30% lower mass, and are often of reduced grade (Wallace and McNeal, 1966). As the wheat host ripens, larvae move towards the base of the plant where they will chew a notch to girdle the stem, fill that region with frass and encase themselves in a hibernaculum to prepare for overwintering. The stem then easily topples over from wind and lodged plants are often not picked up at harvest, causing additional yield losses (Beres et al., 2007). A range of agronomic factors have been explored to reduce yield losses by WSS, such as insecticides, tillage, varietal blends, and altered sowing densities (Beres et al., 2009; Beres et al., 2011a; Beres et al., 2011d; Knodel et al., 2009; Nilsen et al., 2016). An integrated pest management approach centered around growing resistant solid-stemmed cultivars with increased pith in the stem is an effective management approach for WSS.

Growing solid-stemmed wheat cultivars that develop pith in the culm lumen has been the primary strategy to minimize yield losses (Beres et al., 2011b). Pith increases egg mortality through mechanical crushing (Holmes and Peterson, 1961), and acts as a physical barrier restricting larval movement inside the stem to within one or two internodes from the point of egg deposition (Holmes and Peterson, 1962). Consequently, WSS survivorship and yield losses are reduced in solid-stemmed cultivars (Carcamo et al., 2005). The expression of stem-solidness can

vary between and within common wheat and durum wheat. This may be explained by genetic differences between germplasm sources from which stem-solidness was derived, differences in ploidy between the two species, or other genetic factors.

Research on solid-stemmed wheat has primarily focused on common wheat. Most common wheat cultivars in North America derive their stem-solidness from the Portuguese landrace S-615. The underlying genetics of stem-solidness in the S-615 source are complex, and may include the action of a major gene coupled with four or more additional recessive genes (Larson, 1959a). Many of the S-615 derived cultivars suffer from inconsistent pith expression, because of genetic suppression effects in some wheat backgrounds (Larson and Macdonald, 1959). In addition, environmental factors such as reduced light intensity during stem elongation, can negatively influence pith development (Holmes, 1984). Several genetic mapping studies have localized genetic factors contributing to pith development to at least seven chromosomes in common wheat. In S-615, genes influencing stem-solidness were localized to chromosomes 3B, 3D, 5A, 5B, and 5D (Larson and Macdonald, 1959). The major QTL *Qss.msub-3BL* has been shown to explain at least 76% of the variation for stem-solidness in a winter wheat mapping population, and may contain multiple alleles conferring varying levels of stem solidness (Cook et al., 2004). A second minor QTL conferring stem-solidness, *Qss.msub-3DL,* was localized to chromosome 3DL in a mapping population derived from the semi-solid by solid cross MTHW9904/Choteau (Lanning et al., 2006). The strong expression of stem-solidness in Choteau over other cultivars is influenced by presence of both *Qss.msub-3BL* and *Qss.msub-3DL*. Finally, genome-wide association mapping identified novel minor QTL for stem-solidness on chromosomes 2A, 3A and 5B and 5D (Varella et al., 2015).

Durum wheat has greater stem-solidness compared to many common wheat cultivars (Clarke et al., 2002). Currently, the solid-stemmed durum cultivars registered for use in western Canada, CDC Fortitude (Pozniak et al., 2015), AAC Raymore (Singh et al., 2014), AAC Stronghold (unpublished), and AAC Cabri (Singh et al., 2016) all derive their stem-solidness from the German cultivar Biodur. To date, the only mapping work in durum wheat identified a single locus, which was later renamed solid-stem locus 1 (*SSt1*) (Beres et al., 2013a), that was responsible for conferring stem-solidness in the doubled haploid (DH) population Kofa/W9262-260D3, and recombinant-inbred line (RIL) populations Golden Ball/DT379//STD65 and G9580B-FE1C/AC Navigator (Houshmand et al., 2007). The authors suggested that W9262-260D3 (Kyle*2/Biodur)

and Golden Ball carry the same single dominant gene for stem-solidness on chromosome 3B, although they did note differences in polymorphisms for certain markers flanking the locus (Houshmand et al., 2007).

Identifying the genetic basis for stem-solidness will provide important insight to maximize phenotypic expression in cultivars grown in WSS prone areas. Although QTL conferring stem-solidness have been identified for both common and durum wheat, it is unclear if the genetic basis is the same in both. In addition, many of the existing genetic maps have poor resolution and use different sets of markers, which make them difficult to compare. In this study, we overcame these challenges by using the wheat 90K array, a standardized genotyping platform with high marker density (Wang et al., 2014). This technology allowed us to map the stem-solidness QTL in high resolution for both common and durum wheat, as well as compare genetic maps between common and durum wheat. Furthermore, comparison of markers from the wheat 90K array to the high quality WEW reference sequence allowed us to construct and compare physical map intervals of QTL for both common and durum wheat. Together, our findings shed light on the genetic basis of stem-solidness for both common and durum wheat. Resources developed from this study are currently being used in the development of new wheat cultivars with improved resistance to WSS.

4.2. MATERIALS AND METHODS

4.2.1. Plant materials

Two bi-parental DH mapping populations were used in this study, which consisted of either durum or common wheat. Both populations were developed at the Swift Current Research and Development Centre, Agriculture and Agri-Food Canada. The first consisted of 155 durum DH lines derived from the cross Kofa/W9262-260D3. Kofa is a hollow-stemmed cultivar from the United States, and W9262-260D3 is a solid-stemmed cultivar derived from the cross Kyle*2/Biodur (Houshmand et al., 2007). Biodur is a solid-stemmed cultivar of German origin that has been used as the predominant source of stem-solidness for modern Canadian solid-stemmed durum cultivars (Pozniak et al., 2015). The second DH mapping population consisted of 293 lines that were derived from the common wheat cross Lillian/Vesper. Lillian is a solid-stemmed cultivar derived from S-615 and has been widely grown in Western Canada for its WSS resistance, high yield, and grain protein content (DePauw et al., 2005).

To validate the results from the bi-parental mapping of the *SSt1* interval, two diversity panels were used for haplotype analysis that included either durum or common wheat. The durum set consisted of 103 cultivars, while the common wheat set contained 98 cultivars. The wheat cultivars in both diversity panels were primarily from North America, with some selections from around the world (Appendix 2 and 3).

4.2.2. Field experiments

All field plots were sown between May and mid-June with a target sowing density of 250 seeds / m^{-2} with 23.5 cm row spacing. The Kofa/W9262-260D3 mapping population was planted in plots located near Swift Current (SK) in a randomized complete block design in 2000 and an alpha lattice in 2001 and 2002, with two replications in each year. The Lillian/Vesper mapping population was planted in 3 m single rows in un-replicated trials near Swift Current (SK) in 2014 and 2015. In 2015, the Lillian/Vesper mapping population was planted as 1m single rows near Saskatoon (SK) in an alpha lattice design with three replications. In addition, the two diversity panels were grown in field nurseries near Saskatoon (SK) in an alpha lattice design in 2011 and 2012, with two replications in each year. Permission to use field sites located at Saskatoon, and Swift Current, was provided by the University of Saskatchewan, and Agriculture and Agri-Food Canada, respectively.

4.2.3. Phenotyping and statistical analysis of field experiments

The main stem from five to fifteen plants per plot were rated for stem-solidness at maturity using the rating system (1-5) described previously (Depauw and Read, 1982). Each internode was assigned a stem-solidness rating and averaged to obtain an overall rating per plot. Statistical analysis for replicated field trials was performed using the MIXED procedure of SAS/STAT® v9.4. Site years, replications, and blocks were considered as random effects, whereas genotype (i.e. each line) was considered as a fixed effect. Interactions between genotype and all random effects were set as random in the statistical model. Multi-environment least-square means (LS means) for stem-solidness were estimated for each DH line for subsequent use in QTL mapping. The same statistical models were used to generate LS means for each line in the diversity panels. Means separation was performed using Fisher's Least Significant Difference (LSD) test with a significance value of $p < 0.05$, implemented through the PDMIX800 SAS macro (Saxton, 1998).

4.2.4. Molecular analysis

Genomic DNA was extracted from fresh leaf tissue for each DH line and for the lines from the diversity panels using a modified CTAB approach (CIMMYT, 2005). DNA quality was examined on agarose gels and diluted to 50 ng/µL. All lines were genotyped using the wheat 90K array (Wang et al., 2014). The durum DH population was also genotyped using PCR based markers developed using primer3 software (Rozen and Skaletsky, 2000) to flank the *SSt1* locus: EK_02-292495 (F-CCACATCAAGGAAACTCAAACA, R-AGCTATAAGACGATGCAAGGCT) and EK_08-5169 (F-AAGCATGGGATGAGAGGAGATA, R-GCCATAGAGAATGCTCCTGTTC) (K. Nilsen, Unpublished data).

4.2.5. Linkage and QTL mapping

Genotypic data from the wheat 90K array for each mapping population were filtered against markers showing significant segregation distortion (deviating from the expected 1:1 ratio for DH populations) using a chi-square (χ^2) test. Markers missing 25% or more of the data were removed from the analysis. Draft maps were generated using the MSTMap software (Wu et al., 2008) with a *p*-value of $1E^{-10}$ and a maximum distance between markers of 15.0 cM for grouping SNPs into linkage groups. Maps were refined using the MapDisto v1.7.5 software (Lorieux, 2012) using a threshold LOD score of 3.0 and a cut off recombination value of 0.35. The best order of markers was estimated using both "AutoCheckInversions" and "AutoRipple" commands in MapDisto and distances between markers were calculated using the Kosambi function (Kosambi, 1943). Linkage groups (LGs) were scanned and corrected for double recombinants using MapDisto v1.7.5 (Lorieux, 2012). Final LGs were assigned to a chromosome based on the existing high density 90K wheat consensus maps (Maccaferri et al., 2015; Wang et al., 2014).

QTL analysis was performed using Windows QTL Cartographer software. Composite interval mapping (CIM) was implemented with a 1.0 cM walk speed. Cofactor selection was performed using forward and backward regression with a significance level of $p = 0.1$ with a 1 cM window size. QTL significance thresholds were determined by permutation tests (1000 permutations) at a significance level of $p = 0.05$. QTL intervals for haplotype analysis were defined by the entire CIM interval above which the LOD score was greater than the calculated threshold value.

4.2.6. QTL interaction tests

Two-way QTL interactions with *SSt1* were modeled as fixed effects influencing stem-solidness. The closest 90K probe to each QTL peak was used as a diagnostic marker testing for QTL interaction effects within each mapping population. Carriers were distinguished from non-carriers and the stem-solidness LS means were calculated for each. Data were analyzed using the Mixed procedure of SAS v9.4. Means separation was performed using Fisher's LSD test with a significance value of $p < 0.05$, implemented through the PDMIX800 SAS macro (Saxton, 1998).

4.2.7. In-silico mapping of 90K probe sequences to the wild emmer wheat reference

To determine the physical position of 90K probes along chromosome 3B, GMAP software (Wu and Watanabe, 2005) was used to align the 90K probe source sequences (Wang et al., 2014) to the complete WEW reference sequence (Avni et al., 2017). Filtering criteria was applied such that significant hits were required to obtain a minimum threshold sequence identity and coverage, of 95% and 90%, respectively. If probes mapped to multiple locations, only the highest scoring hit was retained.

4.2.8. Map comparison and 3B haplotype analysis

Probes from the 90k wheat array that mapped to the QTL intervals on chromosome 3B for the bi-parental DH populations of durum and common wheat were compared to their respective consensus maps (Maccaferri et al., 2015; Wang et al., 2014). The physical positions of the 90K probes within these intervals on WEW chromosome 3B were used to compare between genetic, and physical distance. Annotated genes falling within the physical intervals were extracted from the WEW gene annotation's gene transfer format (GTF) file: TRIDC_WEWseq_PGSB_20160501_HighConf.gtf (Avni et al., 2017).

Using the inferred QTL position on the consensus maps, we also aligned 90K genotypic data from the two diversity panels and identified haplotype groups containing historical recombination events within the *SSt1* interval. Two-dimensional hierarchical cluster analysis was performed using dendextend package of R. v3.3.1. to simultaneously cluster groups of markers, and cultivars based on genotypic similarity. Data were visualized using the Heatmap function of the ComplexHeatmap package of R v3.2.1.

4.3. RESULTS

4.3.1. Pith expression differences exist between durum and common wheat

The pattern of phenotypic variation differed for stem-solidness between the two DH mapping populations. The distribution of the stem-solidness phenotype in the Kofa/W9262-260D3 DH population was bimodal with scores ranging from one to five ($p < 0.05$), with two clear and distinct groups clustering near the extremes of the stem-solidness rating scale (Figure 4.1A). Some lines exhibited transgressive segregation for stem-solidness, either being hollower than Kofa (stem-solidness < 1.5), or more solid than W9262-260D3 (stem-solidness > 4.4). The pattern of segregation fit the expected 1:1 expected ratio ($X^2 = 0.007$, $p > 0.95$) for a single major gene in the DH population, which allowed stem-solidness to be mapped qualitatively as a genetic marker. The pattern of stem-solidness variation in the Lillian/Vesper population ranged from scores of 1.1 to 3.4 ($p < 0.05$). The distribution of stem-solidness followed an approximate bimodal distribution, but the difference between hollow and solid lines was less pronounced; therefore, discrete classification was not achievable (Figure 4.1B). The least solid lines were similar to the hollow parent Vesper (stem-solidness = 1.0), whereas the most solid lines exceeded stem-solidness in Lillian, although the difference was not statistically significant (stem-solidness > 2.8).

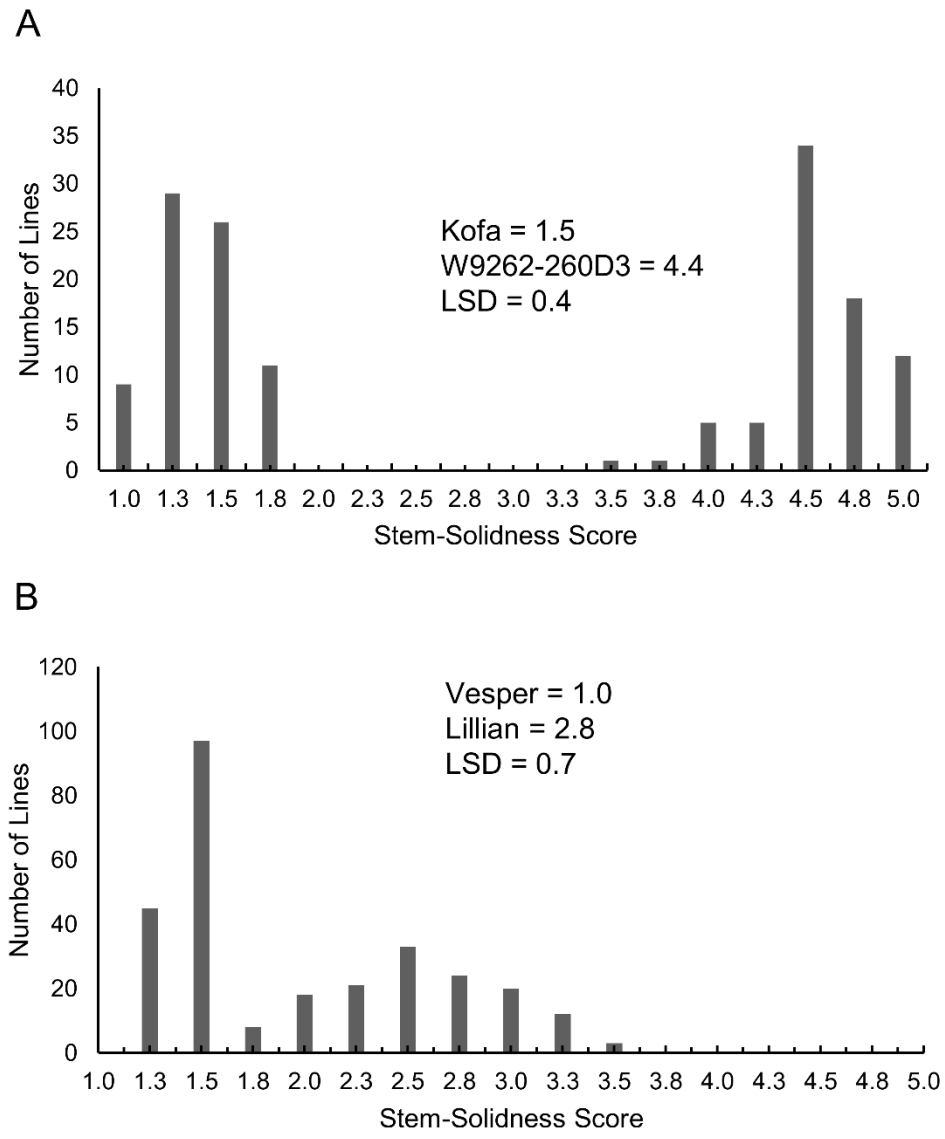

Figure 4.1. Frequency histograms displaying least-square means for stem-solidness. Scores are averaged across testing environments for DH lines in a) Kofa/W9262-260D3 (durum), and b) Lillian/Vesper (common wheat) mapping populations.

Stem-solidness scores from the durum haplotype diversity panel ranged from nearly completely solid (stem-solidness = 4.7) to completely hollow (stem-solidness = 1.0). Among the cultivars scoring highest for stem-solidness were the Biodur derivatives: W9262-260D3, CDC Fortitude and AAC Raymore. A high level of stem-solidness was also expressed in Golden Ball, Lesina, Colloseo, Camacho and Fortore. A large proportion of cultivars scored towards the hollow side of the rating scale, which notably included Kofa, the hollow parent of the durum mapping

population. A small number of lines expressed intermediate levels of pith (stem-solidness = 2.5 - 3.5).

Stems collected from the common wheat haplotype panel ranged from nearly solid to hollow (stem-solidness = 1.0 - 4.3). The only fully solid-stemmed cultivar was Choteau (stem-solidness = 4.3), whereas the remaining solid cultivars (Lillian, AC Eatonia, AC Abbey, Fortuna, Lancer) had intermediate pith expression (stem-solidness = 2.5 - 3.5). Several cultivars expressed small amounts of pith (stem-solidness = 1.5 - 2), which included McKenzie and Unity, and some members of the Canada Western Extra Strong market class such as Glenlea, CDN Bison and Burnside. Most cultivars in the panel were entirely hollow-stemmed (stem-solidness=1), which included Vesper, the hollow parent in the common wheat mapping population.

4.3.2. Stem-solidness is predominantly controlled by the *SSt1* in durum and common wheat

The wheat 90K array was used to construct a linkage map containing a total of 4227 markers in the Kofa/W9262-260D3 population, which spanned a total map distance of 2282 cM (Appendix 4A). Stem-solidness in the Kofa/W9262-260D3 population was scored qualitatively (hollow vs. solid) and mapped as a phenotypic marker to position 228.7 cM of chromosome 3B in the genetic map (Figure 4.2A). CIM localized significant QTL to chromosomes 3B (*SSt1*), 2A (*Qss.usw-2A1, Qss.usw-2A2*), and 4A (*Qss.usw-4A*) (Table 4.1). The majority of the phenotypic variation in this mapping population was explained by *SSt1* (R^2 = 92%, LOD = 127), which was localized near the telomere of chromosome 3BL (227.3-228.7 cM, peak = 228.7 cM) (Figure 4.2A). The peak of the *SSt1* QTL was at position 228.7 cM, which was the same position where *SSt1* was mapped as a phenotypic marker through linkage mapping. The allele conferring stem-solidness at *SSt1* was contributed by the solid parent W9262-260D3. The closest markers to the peak of *SSt1* were PCR-based markers *EK_02-292495*, *EK_08-5169*. The remaining QTL, *Qss.usw-2A1, Qss.usw-2A2* and *Qss.usw-4A*, had minor effects with LOD scores ranging from 3.0 - 5.1, and explained 0.2 – 0.3 % of the phenotypic variance. All three minor QTL had alleles for stem-solidness that were contributed by the hollow parent Kofa. Notably, two distinct QTL were detected on chromosome 2A separated by > 50 cM between the QTL peaks.

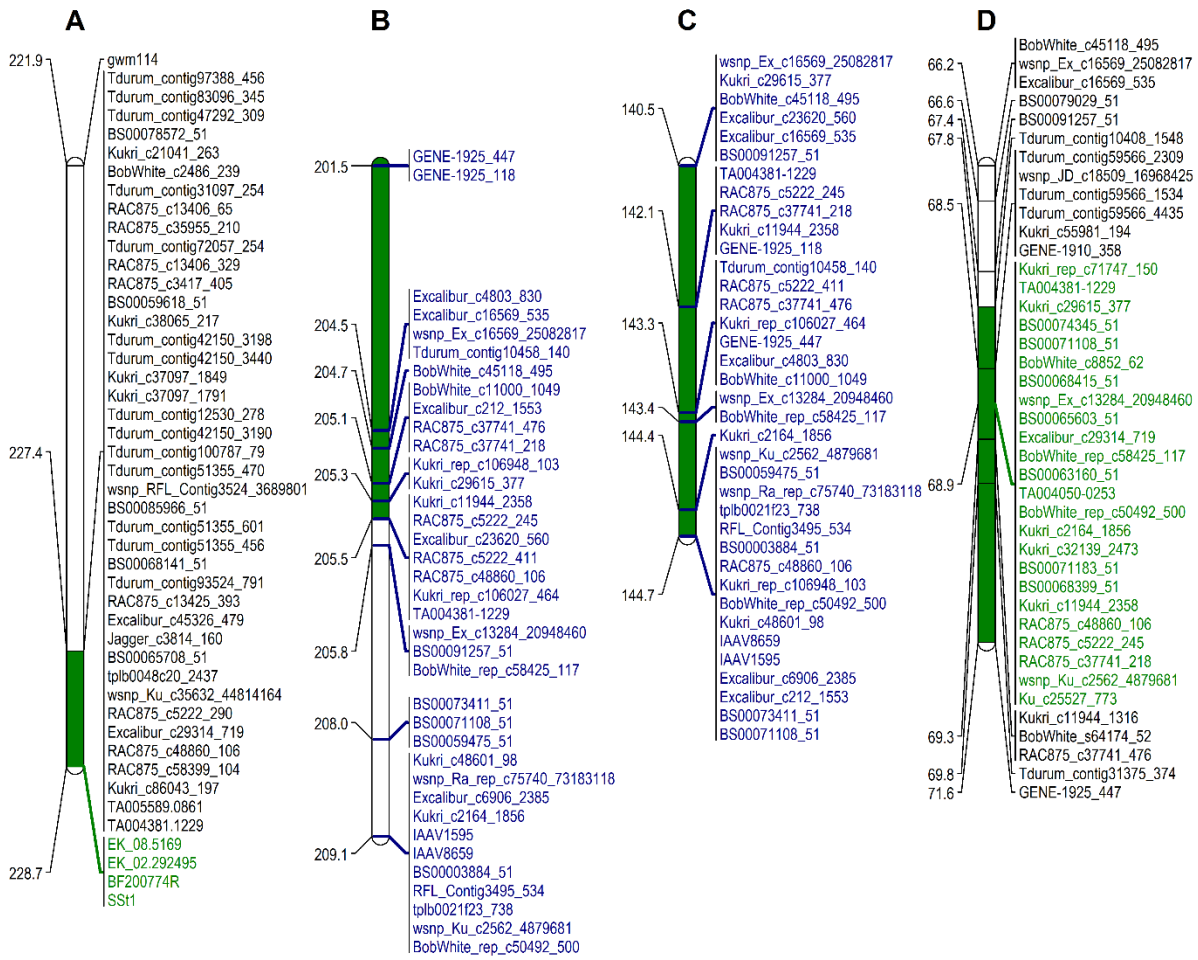

Figure 4.2. Genetic map interval of *SSt1* of chromosome 3BL. a) Kofa/W9262-260D3 DH population genetic map, b) durum wheat consensus map, c) common wheat consensus map, d) Lillian/Vesper DH population. The position of each QTL is indicated by green shading for each mapping population, and estimated in the consensus map. The markers associated with each QTL peak are highlighted in green text. Common markers between consensus maps are highlighted in blue text.

Table 4.1. Summary of CIM results. QTL were localized in the Kofa/W9262-260D3 (durum) and Lillian/Vesper (common wheat) mapping populations.

Population	QTL name	CHR	Interval (cM)	Peak position (cM)	LOD	R^2 (%)	Additive Effect [1]
Kofa/W9262-260D3	*Qss.usw.2A.1*	2A	81.11– 87.1	83.5	3.0	0.2	0.1 (K)
	Qss.usw.2A.2	2A	129.7 – 155.6	137.7	5.1	0.3	0.1 (K)
	SSt1	3B	227.3 – 228.7	228.7	126.9	92.1	1.6 (W)
	Qss.usw.4A	4A	112.2 – 137.1	125.5	3.0	0.2	0.1 (K)
Lillian/Vesper	*Qss.usw.2D*	2D	91.3-131.4	112.9	6.1	2.8	0.1 (L)
	SSt1	3B	67.8-71.6	68.9	94.0	77.8	0.6 (L)
	Qss.usw.5A	5A	88.5-100.3	92.3	3.9	1.3	0.1 (L)

CHR, Chromosome
LOD, Logarithm of Odds
[1]Parent contributing positive allele, K = Kofa, W = W9262-260D3, L = Lillian, V = Vesper

The Lillian/Vesper genetic map contained 7839 markers, which covered a total map distance of 3680 cM (Appendix 4B). Significant QTL were localized to chromosomes 3B (*SSt1*), 2D (*Qss.usw-2D*), and 5A (*Qss.usw-5A*) (Table 4.1). The majority of the phenotypic variation was explained by *SSt1* (LOD = 94.0, R^2 = 77.8%), which spanned from map position 67.8-71.6 cM (Peak position = 68.9 cM) (Table 4.1, Figure 4.2D). The remaining QTL, although significant, had only minor effects (R^2 = 1.3 – 2.8 %). The alleles conferring stem-solidness at all QTL in the Lillian/Vesper cross were contributed by the solid parent Lillian.

4.3.3. Synergistic QTL interactions enhance the effect of *SSt1*

The major locus *SSt1* on chromosome 3B, has been previously shown to interact epistatically with other minor QTL to synergistically enhance expression of stem-solidness (Lanning et al., 2006). In the present study, transgressive segregation was observed for stem-solidness in some cases, therefore the possibility of synergistic interaction between QTL was investigated in further detail. These results indicated that the two-way interactions between *SSt1* and all minor QTL were all strongly significant (p<0.01) in both mapping populations. In the Kofa/W9262-260D3 population, the combination of alleles conferring stem-solidness in two-way interactions (*SSt1*Qss.usw-2A.1*, *SSt1*Qss.usw-2A.2*, *SSt1*Qss.usw-4A)* conferred stem-solidness that exceeded the score in W9262-260D3 (stem-solidness > 4.4; Table 4.2). However, in the absence of *SSt1*, DH lines carrying solidness alleles at each minor QTL did not express significantly more pith than non-carriers. The only exception was lines carrying *Qss.usw-2A.1*,

which had some minor pith development independent of *SSt1* (stem-solidness = 1.4). In the Lillian/Vesper population, the presence of stem-solidness alleles at each minor QTL acted synergistically with *SSt1* to significantly increase pith density compared to lines carrying only *SSt1* ($p < 0.05$) (Table 4.2). However, no two-way interaction between *SSt1*, and minor QTL, yielded stem-solidness that exceeded that of Lillian (stem-solidness = 2.8,). In the absence of *SSt1*, none of the minor QTL had a significant effect on pith development in the Lillian/Vesper population.

Table 4.2. Synergistic two-way interactions between *SSt1* and minor QTL identified in the Kofa/W9262-260D3 (durum) and Lillian/Vesper (common wheat) mapping populations.

Kofa/W9262-260D3					
SSt1[1]	*Qss.usw-2A1*	*Qss.usw-2A2*	*Qss.usw-4A*	Stem-solidness[2]	SE
+	+			4.56[a]	0.04
+	-			4.33[b]	0.04
-	+			1.41[c]	0.05
-	-			1.21[d]	0.04
+		+		4.55[a]	0.04
+		-		4.34[b]	0.04
-		+		1.32[c]	0.05
-		-		1.30[c]	0.04
+			+	4.54[a]	0.04
+			-	4.35[b]	0.04
-			+	1.32[c]	0.04
-			-	1.29[c]	0.04
Lillian/Vesper					
SSt1	*Qss.usw-2D*	*Qss.usw-5A*			
+	+			2.51[a]	0.04
+	-			2.32[b]	0.04
-	+			1.34[c]	0.04
-	-			1.28[c]	0.04
+		+		2.54[a]	0.04
+		-		2.29[b]	0.04
-		+		1.34[c]	0.04
-		-		1.29[c]	0.04

[1]'+' denotes the group carries the stem-solidness allele for the specified QTL, whereas '-' denotes the group carries the stem-hollowness allele. Blank cells indicate the QTL was not considered for the comparison.
[2]LS means for stem-solidness for each two-way allele combination (1-5 scale). Letter groupings in superscript statistical significance between LS means determined through Fishers LSD test at $p < 0.05$.

4.3.4. Comparison of *SSt1* using wheat consensus maps

To facilitate the comparison between the *SSt1* interval in the Kofa/W9262-260D3 and Lillian/Vesper mapping populations, the position of 90K probes within each QTL interval were compared to the published durum and common wheat consensus maps (Figure 4.2B, 4.2C). Markers mapping within the *SSt1* interval in Kofa/W9262-260D3 spanned from positions 196.3 to 205.5 cM on the durum consensus map (Figure 4.2B). The remaining 90K probes distal to position 205.5 cM were not polymorphic between Kofa and W9262-260D3. The markers in the *SSt1* interval in Lillian/Vesper interval spanned 140.5 – 144.7 cM in the hexaploid consensus map (Figure 4.2C). Comparison of 90K probes common to the two consensus maps revealed that the two QTL span a similar genetic interval on chromosome 3B, and there were 22 common 90K

probes between the two consensus maps (Figure 4.2B and C). Overall, the co-localization of the markers for in the Kofa/W9262-260D3 linkage map agreed with their positions in the durum consensus map (Figure 4.2A and B). Similarly, the markers in the Lillian/Vesper linkage map agreed with the common wheat consensus map, although some minor differences in marker order were noted (Figure 4.2C and D).

4.3.5. 90k probes from *SSt1* are coincident in common and durum wheat

The relationship between physical and genetic map positions was assessed by mapping 90K probe sequences against the WEW chromosome 3B reference sequence. Probe sequences that did not meet the minimum sequence identity (>95%) and coverage requirements (> 90%) and were removed from the analysis. The physical location of markers closest to the peak of *SSt1* in Kofa/W9262-260D3 spanned positions 823.0 – 835.1 megabase pairs (Mb) on WEW chromosome 3B (Figure 4.3). The order of the probes on chromosome 3B was consistent with their position on the durum consensus map (Figure 4.3). The estimated position of the 3B QTL in the Lillian/Vesper population spanned positions 140.5 – 144.7 cM on the common wheat consensus map (Figure 4.2C). The 90K probes within this interval on chromosome 3B in WEW ranged from positions 830.6 – 841.0 Mb (Figure 4.4). Based on the 22 probes in *SSt1* that were shared between the common and durum wheat consensus maps, spanning 140.5 - 144.7 cM in common wheat and 204.5 - 209.1 cM in durum wheat, there is a region of overlap; this region corresponds to positions 830.2 - 837.5 Mb in WEW chromosome 3B.

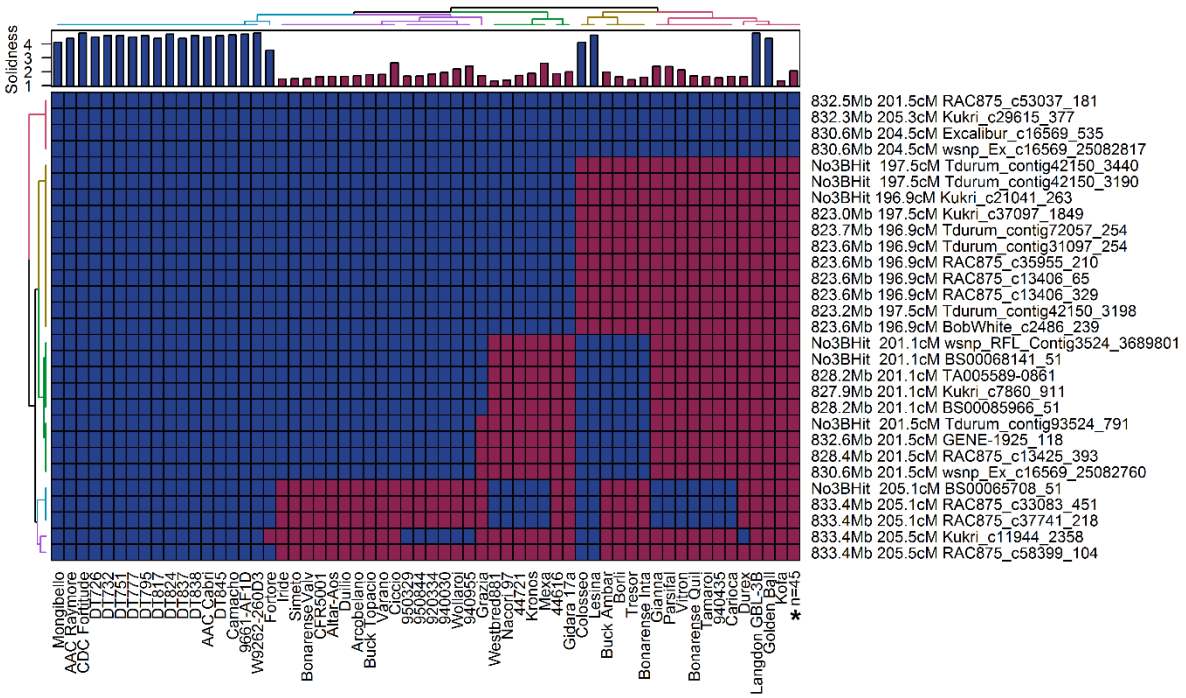

Figure 4.3. Haplotypes of 103 durum cultivars within the Kofa/W9262-260D3 *SSt1* QTL interval. Stem-solidness LS means for each line are shown in the bar chart along the top X-axis. The matrix consists of 90K genotypic data where cells shaded in blue denote expression of the W9262-260D3 (solid-stem) allele, whereas cells shaded in red denote expression of the Kofa (hollow-stem) allele. The name and position of each 90K probe, the anchored physical position on WEW chromosome 3B, and the corresponding position on the common wheat consensus map are shown. Two dimensional (row and column) hierarchical cluster analysis was performed to group lines into haplotypes as indicated by the colorized dendrogram along the top X-axis, whereas markers were grouped along the Y-axis.

*Lines showing identical haplotypes (n=45) were collapsed into a single haplotype (Appendix 2).

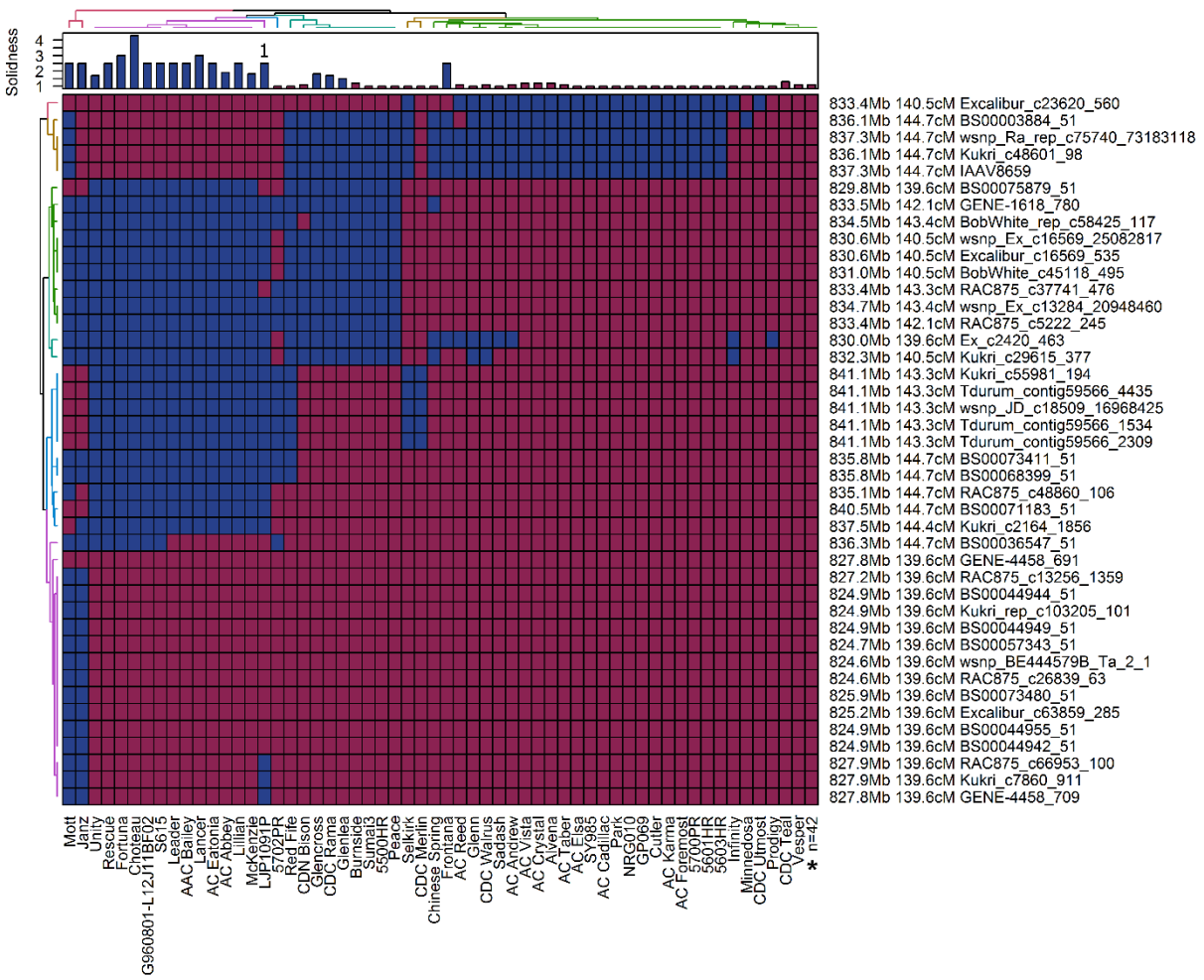

Figure 4.4. **Haplotypes of 98 common cultivars within the Lillian/Vesper *SSt1* QTL interval.** Stem-solidness LS means for each line are shown in the bar chart along the top X-axis. The matrix consists of 90K genotypic data where cells shaded in blue denote expression of the Lillian (solid-stem) allele, whereas cells shaded in red denote expression of the Vesper (hollow-stem) allele. The name and position of each 90K probe, the anchored physical position on WEW chromosome 3B, and the corresponding position on the common wheat consensus map are shown. Two dimensional (row and column) hierarchical cluster analysis was performed to group lines into groups as indicated by the colorized dendrogram along the top X-axis, whereas markers were grouped along the Y-axis.

*Lines showing identical haplotypes (n=45) were collapsed into a single haplotype (Appendix 3).

[1] Winter wheat, stem-solidness was evaluated on plants grown in a growth chamber.

4.3.6. Diversity panels reveal multiple *SSt1* haplotypes

Further investigation of the *SSt1* interval in the durum diversity panel identified six different haplotype groups within the Kofa/W9262-260D3 QTL interval (Figure 4.3). Most of the solid-stemmed Biodur derivatives, including the CDC Fortitude and AAC Raymore were part of a haplotype group that was identical to W9262-260D3. In addition, Camacho and 9661.AF1D also carried the haplotype identical to Biodur and the solid line Fortore was nearly identical to Biodur, except at the marker *Kukri_c11944_2358* (Figure 4.3). The solid Italian cultivars Lesina and Colloseo had unique haplotypes, and carried the Kofa allele between WEW chromosome 3B positions 823.0 – 823.7 Mb, and the W9262-260D3 allele at all remaining loci within the QTL interval. The majority of lines in the panel showed an identical haplotype to Kofa and had hollow stems, except for the solid-stemmed lines Langdon-GB-3B and Golden Ball (Figure 4.3). The only marker to properly differentiate all solid from hollow lines in the panel (except for Golden Ball, and Langdon-GB-3B) was *RAC875_c58399_104*, which was located at WEW position chromosome 3B 833.4 Mb (consensus 205 cM). Not only was this marker the most distally located marker in the dataset, but it was also the most distal marker in the durum consensus map that was polymorphic between the parents of the durum mapping population Kofa and W9262.

Within the common wheat QTL interval, a total of five different haplotype groups were identified through hierarchical cluster analysis (Figure 4.4). Most solid-stemmed derivatives of S-615, which included AAC Bailey, Unity, Rescue, Fortuna, Choteau, Leader, Lancer, Mckenzie, and AC Abbey, were nearly identical in haplotype to Lillian and carried the allele for stem-solidness between WEW 3B positions 830.0 – 841.1 Mb on chromosome 3B. A second haplotype was identified consisting of several members from the Canada Western Extra Strong (CWES) market class which carried the stem-solidness allele between 830.0 - 837.3 cM. This group also contained the hollow-stemmed lines Sumai 3, Peace, 5500HR, and Red Fife (Figure 4.4). The pattern of pith expression within this group was split between the CWES cultivars, which had low to intermediate pith development, and the other lines Sumai 3, Peace, 5500HR, and Red Fife which were entirely hollow-stemmed. Finally, there was a unique haplotype that consisted of the solid-stemmed lines Mott and Janz. The majority of lines in the panel consisted of hollow-stemmed cultivars, which had shared identical haplotype to Vesper (Figure 4.4).

4.3.7. Candidate genes contributing to stem-solidness in *SSt1*

Based on the peak of *SSt1* in common wheat (832.2 - 835.1 Mb) and durum wheat (833.5-833.6 Mb) (Table 4.1), and overlapping 90k probes and haplotypes for common and durum wheat (Figure 4.3 and 4.4), we could narrow the genetic interval for *SSt1* to 833.4 – 835.0 Mb in WEW chromosome 3B. This interval contained 43 genes, based on the current version of the WEW annotation. Of these, 23 were classified as having unknown function (Table 4.3). Of the 20 functionally annotated genes, notable candidates for the solid-stem phenotype include three ribosomal proteins (RPS17, RPS19 and RPS28), a Dof zinc finger transcription factor (Dof2), and a protein kinase superfamily protein (Table 4.3).

Table 4.3 High confidence annotated genes within the *SSt1* interval in WEW chromosome 3B.

Gene ID	Description	Emmer Start	Emmer End
TRIDC3BG086390	AP-3 complex subunit beta-2	833,410,411	833,417,858
TRIDC3BG086400	unknown function	833,418,228	833,419,311
TRIDC3BG086410	unknown function	833,447,122	833,448,100
TRIDC3BG086420	Dual-specificity RNA methyltransferase RlmN	833,471,636	833,473,995
TRIDC3BG086430	Protein kinase superfamily protein	833,499,650	833,502,363
TRIDC3BG086440	undescribed protein	833,500,052	833,501,188
TRIDC3BG086450	undescribed protein	833,568,672	833,569,127
TRIDC3BG086460	40S ribosomal protein S28	833,617,967	833,619,969
TRIDC3BG086470	undescribed protein	833,695,443	833,696,292
TRIDC3BG086480	unknown function	833,753,129	833,755,302
TRIDC3BG086490	unknown function	833,960,480	833,981,832
TRIDC3BG086500	undescribed protein	834,115,057	834,115,259
TRIDC3BG086510	Protein of unknown function (DUF506)	834,115,507	834,117,890
TRIDC3BG086520	undescribed protein	834,115,959	834,116,369
TRIDC3BG086530	NAD(P)H-quinone oxidoreductase subunit 6, chloroplastic	834,154,291	834,154,828
TRIDC3BG086540	undescribed protein	834,278,312	834,279,220
TRIDC3BG086550	undescribed protein	834,278,400	834,278,856
TRIDC3BG086560	Vacuolar protein sorting-associated protein 25	834,313,166	834,344,089
TRIDC3BG086570	Disease resistance protein RPM1	834,329,315	834,331,881
TRIDC3BG086580	12S seed storage globulin 2	834,354,104	834,355,541
TRIDC3BG086590	Accelerated cell death 11	834,398,396	834,398,890
TRIDC3BG086600	undescribed protein	834,399,338	834,400,223
TRIDC3BG086610	12S seed storage globulin 1	834,443,909	834,445,752
TRIDC3BG086620	undescribed protein	834,473,716	834,474,056
TRIDC3BG086630	undescribed protein	834,501,444	834,501,784
TRIDC3BG086640	undescribed protein	834,529,195	834,530,259
TRIDC3BG086650	30S ribosomal protein S17	834,546,892	834,549,240
TRIDC3BG086660	30S ribosomal protein S19	834,559,426	834,561,567
TRIDC3BG086670	unknown function	834,649,174	834,650,437
TRIDC3BG086680	Mitochondrial ATP synthase 6 kDa subunit	834,677,496	834,677,663
TRIDC3BG086690	undescribed protein	834,687,517	834,688,148
TRIDC3BG086700	undescribed protein	834,688,939	834,691,009
TRIDC3BG086710	Very-long-chain (3R)-3-hydroxyacyl-CoA dehydratase 2	834,691,153	834,693,605
TRIDC3BG086720	DOF zinc finger protein 2	834,983,287	834,984,049
TRIDC3BG086730	undescribed protein	835,036,191	835,036,444
TRIDC3BG086740	undescribed protein	835,037,520	835,037,765
TRIDC3BG086750	undescribed protein	835,075,268	835,075,570
TRIDC3BG086780	Transposon protein, putative, CACTA, En/Spm sub-class	835,127,161	835,133,343
TRIDC3BG086800	Transposon protein, putative, CACTA, En/Spm sub-class	835,129,795	835,130,231
TRIDC3BG086810	Ankyrin repeat family protein	835,176,160	835,177,639
TRIDC3BG086820	undescribed protein	835,177,635	835,178,250
TRIDC3BG086830	Cytochrome P450 superfamily protein	835,354,094	835,355,636
TRIDC3BG086840	unknown function	835,360,730	835,361,289

4.4. DISCUSSION

In this study, we localized coincident QTL conferring stem-solidness to chromosome 3BL in the durum population Kofa/W9262-260D3, and common wheat population Lillian/Vesper. The QTL interval on chromosome 3B in durum wheat was consistent with the previously reported location of *SSt1* (Houshmand et al., 2007); similarly, the QTL interval in Lillian/Vesper was consistent with the previously reported location of *Qss.msub-3BL* (Cook et al., 2004). Earlier work identified two 90K probes (*BS00065603* and *BS00074345_51*) in linkage disequilibrium (LD) with *Qss.msub-3BL* through association mapping (Varella et al., 2015). In the present study, both markers co-segregated with the peak of the Lillian/Vesper QTL (Figure 4.2D), indicating the Lillian/Vesper QTL is indeed coincident with *Qss.msub-3BL*. Comparison of the wheat consensus maps identified 22 common probes within the QTL intervals in durum and common wheat (Figure 4.2B, C), with probe sequences that spanned a physical interval of 830.2-837.5 Mb. Based on the peaks of the QTL, overlapping marker, and haplotype evidence, we have further defined this interval to approximately 2 Mb (833.4 – 835.1 Mb). Since these QTL are coincident in their physical and genetic maps, we suggest that they correspond to the same region in both wheat species, which we henceforth designate *SSt1*. If common and durum wheat carry a common gene within *SSt1* that confers stem-solidness on chromosome 3B, then it may be localized to this common physical interval between the two defined QTL.

Within the common interval in WEW, there are 43 putative high confidence annotated genes, several of which could be involved in biological processes related to stem-solidness. These include three ribosomal proteins (RPs) (RPS17, RPS19, RPS28), a Dof2, and a protein kinase superfamily protein. Increased expression of RPs would be expected in actively dividing tissues including the pith of solid-stemmed cultivars. There are 70-80 different types of RPs and are required to be in stoichiometric balance to make up the ribosomal complex responsible for protein synthesis (Naora, 1999). Defects in part of the ribosomal protein complex can result in cell-cycle arrest via apoptosis in animal systems (Warner and McIntosh, 2009). Therefore, it could be possible that mutations affecting the function of a specific RP could cause the hollow-stemmed phenotype. On the other hand, Dof proteins are a family of transcription factors specific to plants responsible positive and negative regulation of gene expression implicated in a wide variety of functions, including cell cycle regulation (Skirycz et al., 2008), cell cycle progression/cell expansion (Xu et al., 2016), photosynthesis and light response, and plant growth and plant

development (Yanagisawa and Sheen, 1998). Likewise, protein kinases are involved in post translational modification of proteins and signal transduction, and similar to the Dof transcription factor could be involved in a wide array of processes (Stone and Walker, 1995). Work is currently underway to determine whether these, or other genes, are differentially expressed in the pith of developing plants and if they contain genetic variants between hollow and solid-stemmed parents that could explain the differential phenotypic response.

In addition to *SSt1*, we also observed that synergistic two-way interactions between *SSt1* and other minor QTL on chromosomes conferred a greater level of stem-solidness than the presence of *SSt1* alone. We identified minor QTL on chromosomes 2A, and 4A in our durum mapping population (Kofa/W9262-260D3), and 2D, and 5A in the common wheat population (Lillian/Vesper). Previous studies have also identified minor QTL conferring stem-solidness. For example, a secondary QTL was identified on chromosome 3DL that enhances pith expression when combined with *SSt1* (Lanning et al., 2006). In the present study, the solid-stem alleles for the durum QTL on 2A and 4A were contributed by the hollow parent Kofa, which suggests that some hollow by solid parental combinations could be used to enhance expression of stem-solidness in durum wheat. This may not be of critical importance to durum wheat breeders because modern cultivars that carry *SSt1* have strong pith expression that exceeds the minimum threshold stem-solidness score of 3.75 proposed to achieve effective sawfly resistance (Wallace et al., 1973). In the present study, we observed that the additive effect of the *SSt1* resistance allele in durum wheat conferred three times more units of stem-solidness than it did in common wheat. In contrast, variable pith expression has often been an issue for many common wheat cultivars (Platt, 1941). The variability in common wheat can be caused by environmental conditions, particularly low light intensity during stem elongation, which can negatively impact pith development (Holmes, 1984). Some common wheat cultivars have been shown to express greater amounts of pith at early stages of development when WSS infestation typically occurs, followed by rapid pith retraction towards maturity (Varella et al., 2016). In some common wheat cultivars, the presence of *SSt1* alone may not be enough to ensure effective WSS resistance, therefore developing common wheat cultivars with improved WSS resistance remains a priority in breeding programs. We have shown here that some two-way combinations between *SSt1* and minor QTL in the Lillian/Vesper population resulted in stem-solidness that exceeded the effects of *SSt1* alone. These results indicate that future work should include attempts to pyramid *SSt1* with one or more secondary genes with

complementary additive effects. Such favorable interactions likely have already been inadvertently implemented by breeding programs through the selection of elite cultivars with increased stem-solidness.

Several different haplotypes were found within the *SSt1* interval in common and durum wheat. All known solid-stemmed cultivars in the durum haplotype panel, except for Golden Ball and Langdon-GB-3B, carried alleles for stem-solidness somewhere within the *SSt1* interval in the Kofa/W9262-260D3 mapping population. The lack of similarity between Golden Ball and the other solid durum lines was unexpected, because the gene conferring stem-solidness in Golden Ball was mapped to a similar region of 3B in a previous study (Houshmand et al., 2007). The solid-stemmed parent (W9262-260D3) of the durum mapping population derives its stem-solidness from the German cultivar Biodur, as do the four commercially registered Canadian durum cultivars CDC Fortitude (Pozniak et al., 2015), AAC Raymore (Singh et al., 2014), AAC Cabri (Singh et al., 2016), and AAC Stronghold (Unpublished data), and the majority of solid-stemmed Canadian durum breeding lines. Biodur (Valdur//Wascana/Durtal) may derive the solid allele from North African ancestors; the ancestry of Golden Ball is unknown, being a landrace introduced to North America from South Africa in the early 20th century. Therefore, these results could suggest that Golden Ball and Biodur represent different sources of stem-solidness on chromosome 3B. In the present study, a lack of polymorphic markers between Kofa and W9262-260D3 distal to the expected location of *SSt1* hindered comparison between the two putative sources. Therefore, future investigation will be required to confirm whether the gene in Golden Ball is allelic to Biodur.

Alternate haplotypes were also evident in the solid cultivars of Italian origin. Lesina (Capeiti/Creso//Trinakria/Valforte) and Colosseo (Creso/Mexa) expressed stem-solidness similar to Golden Ball, yet had different haplotypes than either the Biodur derivatives or Golden Ball. Fortore (Capeiti 8/Valforte) had a lower stem-solidness score than the Biodur derivatives, but similar haplotype, except at three loci. Conversely, Mongibello (Trinakria/Valforte) was very solid and had the Biodur haplotype, despite similar ancestry to the other solid Italian lines. Of the ancestral lines of these cultivars, we can only confirm stem-solidness in Trinakria (Clarke et al., 2012), although one could speculate that Creso, a cross between a Capelli short straw mutant and a CIMMYT semi-dwarf line (Clarke et al., 2012) is also solid-stemmed. Together, evidence indicates that Italian cultivars have solid-stem phenotypes, though they do not fully fall within either the Golden Ball or Biodur haplotypes.

Several notable haplotypes were also identified in the common wheat haplotype panel. Many North American common wheat cultivars studied, including Lillian, Rescue, AC Eatonia, AC Abbey, Leader, Lancer, McKenzie and Unity, derive their stem-solidness from the Portuguese landrace S-615 (Beres et al., 2013a). In the present study, most of the S-615 derivatives carried an identical haplotype to Lillian throughout the QTL interval. However, a distinct haplotype was identified in the solid-stemmed cultivars Mott and Janz. Mott is a spring wheat cultivar developed at North Dakota State University, with stem-solidness that is partially derived from S-615 via the cultivars Ernest, Fortuna and Tioga. In contrast, Janz is a white spring wheat that derives its stem-solidness from an alternative source, *Agropyron elongatum* (Beres et al., 2013b). Another interesting haplotype was identified in members of the Canada Western Extra Strong (CWES) market class (Glenlea, RL4452, Burnside, Glencross, CDN Bison, CDC Rama) which carry alleles for both solid and hollow stem within the QTL interval. Although this haplotype group consists of cultivars that were relatively hollow-stemmed, certain cultivars such as Glenlea, and CDC Rama did express some pith in the lower internodes, which could indicate they are carriers of *SSt1* with phenotypic suppression of stem-solidness. Several genes inhibiting the expression of stem-solidness have been identified in S-615 and its derivatives, including those carried by the D-genome (Larson and Macdonald, 1962).

4.5. CONCLUSIONS

In conclusion, the major QTL on chromosome 3BL identified in this study is coincident with the previously reported map positions of *Qss.msub-3BL* and *SSt1* (Houshmand et al., 2007). To elucidate the relationship between the genetic and physical maps of *SSt1*, we anchored 90K probes that mapped inside the QTL interval to the WEW reference sequence. Combined with haplotype analysis, the most probable location of *SSt1* is estimated to be between positions 833.4 - 835.1 Mb. The two sources of stem-solidness in durum wheat (Golden Ball and Biodur) are different in haplotype around *SSt1* although QTL have been mapped to 3B in both sources (Houshmand et al., 2007). Golden Ball carries the hollow haplotype throughout the *SSt1* interval, which will require further investigation to confirm whether it is allelic to *SSt1*. Common wheat cultivars that derived their stem-solidness from S-615 were similar in haplotype, though alternate haplotypes were identified. Despite sharing a common locus on chromosome 3B, phenotypic expression of stem-solidness differed between durum and common wheat. Minor QTL were shown

to synergistically enhance the expression of *SSt1* in both mapping populations, which suggests breeding efforts can improve pith expression through strategic parental selection, which may be particularly useful in breeding common wheat.

5. GENE EXPRESSION PROFILING AND COMPARATIVE GENOMIC ANALYSIS OF STEM-SOLIDNESS LOCUS *SSt1* IN DURUM AND COMMON WHEAT

ABSTRACT

Solid-stemmed wheat (*Triticum* spp.) cultivars are resistant to the wheat stem sawfly (WSS, *Cephus cinctus*). Previous mapping studies have identified the major stem-solidness locus *SSt1* on chromosome 3BL, and recent work has narrowed the interval to a physical distance less than 2 Mb on chromosome 3BL based on tetraploid genome sequence of wild emmer wheat (WEW). Since that time, additional draft genome assemblies have become available for the first tetraploid durum cultivar Svevo, the hexaploid wheat landrace Chinese Spring (Refseq v.1.0), in addition to draft assemblies for the hexaploid cultivars CDC Stanley and CDC Landmark. In this study, we identified discrepancies in the physical position of 90K probes between these reference sequences suggesting that structural variation may exist between some wheat lines, thereby affecting how the *SSt1* interval is defined, particularly in Refseq v.1.0. To correct this issue, we anchored all Refseq v.1.0 gene models to the Svevo reference sequence; the newly defined interval contained 32 candidate genes. We observed that many of the genes within the *SSt1* region have undergone a series of gene duplication events, and quantitative PCR confirmed that one gene that encodes for a DNA binding one finger (Dof) transcription factor, *TraesCS3B01G608800*, has copy number variation (CNV), with increased copies occurring in solid-stemmed cultivars. The number of gene copies correlate with increased gene expression determined by RNAseq. Furthermore, screening of an EMS mutant population derived from the solid-stemmed cultivar CDC Fortitude identified two mutant lines with a hollow-stemmed phenotype; the first mutant line appears to have a large deletion that includes *TraesCS3B01G608800*, and the second mutant shows significant lower expression of *TraesCS3B01G608800* when compared to CDC Fortitude. Together, these results provide intriguing new insights into the causal genetic factors contributing to the stem-solidness phenotype and indicate that *TraesCS3B01G608800* is a strong candidate for *SSt1*.

Disclosure:
This chapter is currently a manuscript in preparation: Gene expression profiling and comparative genomic analysis of the stem solidness locus *SSt1* in durum and common wheat
Nilsen, K.T., S. Walkowiak, K. Wiebe, A.T. Cory, A. N'Diaye, R.D. Cuthbert, P.R. MacLachlan, J.M. Clarke, A.G. Sharpe and C.J. Pozniak (2017). IN PREPARATION.

5.1. INTRODUCTION

The wheat stem sawfly (WSS), *Cephus cinctus* Norton (Hymenoptera: Cephidae), is a damaging pest of wheat (*Triticum aestivum* L., *Triticum turgidum* L. var *durum*) in North America (Beres et al., 2011b). Sawfly infestations occur throughout the southern parts of Alberta, Saskatchewan, Manitoba, Northern Montana, North Dakota and northern South Dakota (Beres et al., 2011b). This region includes almost the entire durum wheat growing region of North America.

Over the last century, the most effective way to minimize damage caused by the WSS in affected regions has been to grow solid-stemmed wheat cultivars that develop pith within the culm lumen (Beres et al., 2013a). Solid stems provide resistance to the WSS by deterring stem cutting, mechanically crushing eggs, and impeding larval development and growth inside the stem (Hayat et al., 1995). Under infestation, spring wheat fields sown to solid-stemmed cultivar AC Eatonia yielded 16% more, and were a grade unit higher, than hollow-stemmed cultivar AC Barrie (Beres et al., 2009).

The genetics conferring the stem-solidness trait have been well studied, but the underlying causal genes have not been identified. The trait is known to be partially controlled by a single locus, *SSt1*, located on chromosome 3B in both wheat species (Cook et al., 2004; Houshmand et al., 2007). The location of *SSt1* spans from positions 833.5-835.5 Mb on chromosome 3B in the current WEW reference sequence (Nilsen et al., 2017).

The release of the Chinese Spring (common wheat) survey sequence was a major step forward for wheat genomics, which was subsequently followed by the full assembly of the first chromosome (3B) in wheat (Mayer et al., 201l; Choulet et al., 2014). Since that time, several additional reference sequences have become available, including the complete assembled sequence for all chromosomes for wild emmer wheat (WEW) (Avni et al., 2017), Chinese Spring (Refseq v.1.0), the first durum cultivar Svevo, and two draft assemblies of two Canadian common wheat cultivars CDC Stanley and CDC Landmark. At the time of writing, only the assemblies of WEW, Svevo and Refseq v.1.0 have been finalized, whereas work continues towards improving the draft assemblies of CDC Landmark and CDC Stanley.

Identifying the genetic basis for stem-solidness is an important goal that will improve our understanding of the biological mechanism conferring stem-solidness. The goal of this research was to utilize these newly available genomic resources to better define the *SSt1* interval, identify candidate genes for *SSt1* by looking within the previously defined chromosome 3B interval (Nilsen

et al., 2017), and test for differential regulation of those genes between solid and hollow-stemmed durum and common wheat cultivars. In addition, we developed an ethyl-methane sulfonate (EMS) mutant population derived from the solid-stemmed durum cultivar CDC Fortitude as an attempt to disrupt expression of the *SSt1*. Global gene expression profiling was performed to identify possible downstream targets of *SSt1*.

5.2. MATERIALS AND METHODS

5.2.1. Comparative genomic analysis

The full genomic sequence for chromosome 3B was extracted from the following genomic assemblies: Svevo v1.0 (durum), Zavitan v2.0 (wild emmer wheat), Refseq v.1.0 (common wheat), CDC Stanley v0.4 (common wheat) and CDC Landmark v0.4. (common wheat). Each sequence was aligned to Svevo using the NUCmer tool from MUMmer v 3.0 software package, with a minimum alignment match length of 500 bp. Sequences were compared using MUMmerplot and plotted using gnuplot and circos software. GMAP software (Wu and Watanabe, 2005) was used to align the 90K probe source sequences (Wang et al., 2014) and GMAP was also used to align high confidence gene sequences from Refseq v.1.0 annotation, to each of the five assembled reference sequences. Filtering criteria were applied such that significant hits were required to obtain a minimum threshold sequence identity and coverage of 98%, and only the top scoring hit was selected. 90K probes mapping within the *SSt1* region were sorted based on physical position in each assembly and visualized using MapChart software (Voorrips, 2002). Homoeologous genes from the Refseq v.1.0 annotation mapping to chromosomes 3A, 3B and 3D were visualized using Mapchart software (Voorrips, 2002).

5.2.2. Generation of mutant population

An EMS mutant population was created from the solid-stemmed durum cultivar CDC Fortitude (Pozniak et al., 2015) to disrupt the expression of *SSt1*. Approximately 1.5 kg of seed was soaked in tubs containing 0.5% (v/v) EMS solution for four hours under gentle agitation, followed by four hours of continuous rinsing with fresh tap water. Next, seeds were dried overnight and were subsequently sown as space-planted field plots near Saskatoon (SK) the following day. A single spike was harvested from each plant at maturity, and were planted in 2376 M2 head-rows the following field season. 10 M3 spikes were harvested from each row and saved for future use. Plants from each row were cut in cross section and rated for stem-solidness, and any rows segregating for hollowness were noted.

5.2.3. Plant materials and growth conditions for RNA sequencing

Plant materials selected for RNA sequencing included three common wheat cultivars, five durum cultivars, and two loss-of-function mutants derived from the solid parent CDC Fortitude

that express the hollow phenotype (Table 5.1). Three seeds from each cultivar were planted in 4L pots and grown in a growth cabinet under T5 fluorescent lighting. Growth conditions were set to temperature cycles of 22°C during the day and 16°C at night, with a 16-hour photoperiod. Each pot was considered a treatment and each treatment was grown in three replications for a total of 30 treatments. The experiment was grown as a completely randomized design (CRD), and pots were randomly moved to a new position in the growth cabinet every seven days.

Table 5.1. Description of plant materials used for RNAseq experiments.

Name	Stem Type	Species	Source of Solidness
Vesper	Hollow	Wheat	-
Lillian	Solid	Wheat	S-615
McKenzie	Semi-Solid	Wheat	S-615
CDC Fortitude	Solid	Durum	Biodur
W9262	Solid	Durum	Biodur
Kofa	Hollow	Durum	-
Langdon	Hollow	Durum	-
Langdon-GB-3B	Solid	Durum	Golden Ball
M2.1184	Hollow EMS Knockout	Durum	CDC Fortitude
M2.2324	Hollow EMS Knockout	Durum	CDC Fortitude

5.2.4. Tissue sampling for RNA extraction

The main stems of three plants from each treatment were sampled at Zadoks stage 32, the point at which two nodes are present on the main stem (Appendix 3). Approximately 0.5 cm of the stem was sampled measuring from the bottom of the lowermost node towards the uppermost node on (Figure 5.1). Samples were immediately placed in 1.5 mL micro-centrifuge tubes, flash-frozen in liquid nitrogen and stored at -80°C prior to RNA extraction. Stem tissue was ground under liquid nitrogen with a sterilized mortar and pestle. Total RNA extraction was performed using the Qiagen RNeasy Plant Mini Kit (Qiagen) per the manufacturer's supplied protocol. RNA integrity was evaluated using an Agilent Bioanalyser RNA 6000 nano chip, and RNA quantitation was performed using the Qubit Broad Range assay kit (Thermofisher).

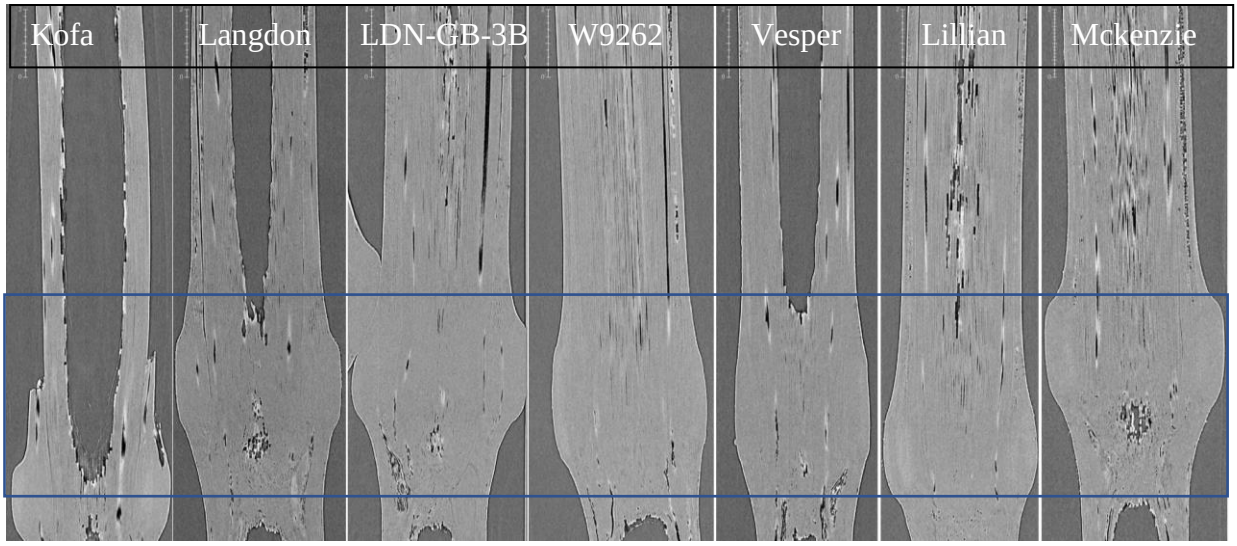

Figure 5.1. Synchrotron radiation micro-computed tomography (SR-µCT) imaging from a selection of lines of the RNAseq panel. Two-dimensional transmission images were captured at the Biomedical Imaging-Therapy beamline at the Canadian Light Source Synchrotron (Saskatoon, SK, Canada). The region contained within the blue box shows the pith transition zone that was sampled for RNAseq.

5.2.5. RNAseq library preparation and sequencing

Individually barcoded cDNA libraries were prepared using the Truseq v2 unstranded kit (Illumina) per the manufacturer's recommended protocol. Library integrity was checked on an Agilent Bioanalyser using the high sensitivity DNA analysis kit. Library quantitation was performed using the Qubit High Sensitivity assay kit. Individually barcoded libraries were diluted to 10 ng/µl, pooled into groups of six, and sequenced across five lanes on the Illumina HiSeq4000 platform with 2 x 150 bp PE chemistry.

5.2.6. RNAseq bioinformatics analysis pipeline

An overview of the bioinformatics pipeline used in this analysis, and the scripts used to run the programs are presented in Appendix 5 and 6. Adaptor and quality trimming was performed using Trimmomatic version 0.27 (Bolger et al., 2014) with the parameters ILLUMINACLIP:TruSeq3-PE:2:30:10 LEADING:3 TRAILING:3 SLIDINGWINDOW:4:20 MINLEN:75. Trimmed reads were checked for adaptor contamination and quality using FastQC and were aligned to the Refseq v.1.0 reference sequence using STAR version 2.5 (Dobin et al., 2013) with default parameters, except the maximum mismatch rate (--outFilterMismatchNmax) was set to 6 (minimum 96% sequence identity) and the maximum intron length (--alignIntronMax)

was set to 10,000 bp. Binary Alignment Map (BAM) files containing aligned reads were inputted into StringTie (Pertea et al., 2016) to count reads mapping to genes in the Refseq v.1.0. A matrix of raw read counts was analyzed by DESeq2 (Love et al., 2014) for analysis of differential expression between hollow and solid lines. In total, 15 pairwise comparisons were made between the three hollow and five solid-stemmed lines (Table 5.1). Differential gene expression testing was also performed between CDC Fortitude and the two EMS mutant lines M2.1184 and M2.2324. Genes were considered differentially expressed if they had a $\log_2$ fold change > +2 or < -2, and adjusted p-value < 0.001.

5.2.7. Gene ontology enrichment testing

Gene ontology (GO) enrichment testing was performed to identify GO terms that were disproportionally represented in the differential gene expression dataset from the RNAseq. Separate GO analyses were performed for biological process (BP), molecular function (MF) and cellular component (CC). GO terms were extracted from the Refseq v.1.0 annotation and used to create a background set of genes against which to test for enrichment using the topGO package in R. Enrichment testing was performed using Fisher's exact test with a significance level of $p < 0.05$. A summary of significant GO terms was explored using REVIGO software (Supek et al., 2011).

5.2.8. Structural variation of *SSt1* by Chromium 10x Genomics whole genome sequencing

To examine structural variation around the *SSt1* interval, whole genome sequencing was performed on Svevo, CDC Landmark, CDC Fortitude, and the EMS deletion line M2.1184 using the Chromium 10x Genomics platform. Nuclei were isolated from ≈30 seedlings from each line as per the procedures outlined in Zhang et al. (2012). High molecular-weight genomic DNA was extracted from nuclei using a modified CTAB extraction protocol (CIMMYT, 2005). Genomic DNA was quantified was by fluorometry using Qubit 2.0 Broad Range (Thermofisher) and size selection to remove fragments <40 kb using pulsed field electrophoresis on a Blue Pippin (Sage Science) according to the manufacturers specifications. Final DNA integrity and size were determined using a Tapestation 2200 (Agilent), and Qubit 2.0 Broad Range (Thermofisher), respectively.

Library preparation was performed per the 10x Genome Library protocol (10x Genomics). Four uniquely barcoded libraries were prepared for each sample and multi-plexed on Illumina

HiSeqX and HiSeq 2500 platforms. De-multiplexing was performed using the specialized 10x Genomics Software Supernova, and fastq files were generated using LongRanger sofware. Reads from CDC Fortitude and M2.1184 were aligned to the Svevo reference sequence, whereas reads from CDC Landmark were aligned to the CDC Landmark v0.4 and CDC Stanley v0.4 reference sequences. All alignments were performed using LongRanger WGS. Structural variants were visualized using Loupe software. Confirmation of the deletion of *TraesCS3B01G608800* and surrounding regions in M2.1184 were determined by PCR (Appendix 8).

5.2.9. Exome capture and bulked segregant analysis

DNA was extracted and pooled from 20 solid-stemmed lines and 20 hollow-stemmed lines from the Kofa /W9262-260D3 mapping population (Nilsen et al., 2017) to create *SSt1+* and *SSt1-* samples for bulked segregant analysis (BSA). DNA was enriched for coding regions using the wheat exome capture array according to the procedures outlined in Jordan et al. (2015). High-throughput sequencing was performed on the Illumina HiSeq2500 platform with 2 x 100 bp PE chemistry. Raw sequence reads were processed in Trimmomatic v0.32 and processed reads were aligned to the genome of Svevo using Novoalign v3.02.05. Duplicate read mappings and improper read pairs were removed using Picard-Tools. SNP variants were called using the SAMtools v1.2.1 mpileup command. Filters were applied requiring each bulk to be homozygous, and carrying a different allele from the other, and the remaining SNPs were plotted as a frequency histogram with a bin size of 25 kb.

5.2.10. Characterizing CNV around *TraesCS3B01G60880*

The sequence for the candidate gene *TraesCS3B01G608800* was extracted from each of the five assemblies and aligned using MUSCLE to identify possible sequence variation (Appendix 7); the *TraesCS3B01G608800* sequence was also run through FGENESH software to validate the open reading frame (ORF) predicted in the Refseq v1.0 annotation. The conserved domain was extracted from *TraesCS3B01G608800* and used to identify additional members of the Dof gene family in the CS annotation using TBLASTX (Appendix 9). The sequences of all Dof genes were aligned using MUSCLE with default parameters, and was clustered into a phylogenetic tree using the neighbor joining clustering method of Simple Phylogeny software.

For CNV analysis of *TraesCS3B01G608800*, PCR was used to assay a polymorphic GAGA element upstream of the TSS for *TraesCS3B01G608800* for members of the Kofa/W9262-260D3 and Lillian/Vesper mapping populations (Nilsen et al., 2017), all lines in the RNAseq panel, and lines from hexaploid and tetraploid diversity panels (Appendix 8) (Nilsen et al., 2017). PCR fragments were then visualized on single strand conformation polymorphism (SSCP) gels. A quantitative PCR (qPCR) assay was also developed to test for CNV at *TraesCS3B01G608800* (Appendix 8). qPCR reactions were performed in 10µl reactions in a 384-well microtiter plate and quantification was performed using SYBR green fluorescence measured in a BioRAD CFX384 cycler. The relative number of copies of *TraesCS3B01G608800* was determined using the ΔΔCT method using *TraesCS3B01G61220* as an endogenous control gene with a single copy. These results were validated using 10x Genomics sequencing data from CDC Landmark aligned to the Landmark assembly v0.4 using LongRanger WGS, followed by analysis of structural variation via Loupe software. A list of all primers used for both SSCP an qPCR is presented in Appendix 8.

5.3. RESULTS

5.3.1. Comparative genomic analysis reveals structural variation around the *SSt1* interval

Based on the position of 90K probes previously identified as being associated with the peak of *SSt1* in wild emmer wheat (833.5 - 835.5 Mb) (Nilsen et al., 2017), the corresponding *SSt1* interval in the other assemblies were: Svevo, 827.5 - 830 Mb; Refseq v.1.0 821.7 - 830 Mb; CDC Landmark 796.6 - 800 Mb; and CDC Stanley 804.5 - 806.5 Mb. Analysis of whole chromosome alignments using NUCmer revealed that the telomere of chromosome 3BL was associated with substantial structural/sequence variation (Figure 5.2 a-e) relative to other parts of the chromosome (Appendix 10). A region containing a peak of increased SNPs from the BSA was observed between Svevo position 827.5 – 828.5 Mb (Figure 5.2e), which was also a region of poor sequence similarity between Svevo and the other four assemblies. Despite these observations, there was strong collinearity between the order of genes around *SSt1* in Svevo and the other assemblies (Appendices 11-14); the only exception was Refseq v.1.0, which showed extensive structural variation including sequence duplications, small translocations, and inversions around *SSt1* relative to the other assemblies. The combined effect of the sequence rearrangements had a major impact when using the Refseq v.1.0 assembly as a guide for the positional cloning of *SSt1*. For example, a portion of the genomic sequence in Refseq v.1.0 located between 828.1 - 830.6 Mb was inverted relative to Svevo and the other assemblies; therefore, the genes present within this region of Refseq v.1.0 co-localize with the peak of the *SSt1* QTL in Svevo (Figure 5.3, Appendix 12). Conversely, the sequence in Refseq v.1.0 between 822.6 - 824.4 Mb is localized distally in Svevo, outside of the QTL interval (Figure 5.3, Appendix 12). To investigate this in more detail, we examined the syntenic regions of chromosomes 3A, 3B, and 3D in the Refseq v1.0 assembly. These results supported our finding that chromosome 3B carries a large inversion relative to its A and D genome counterparts (Figure 5.4).

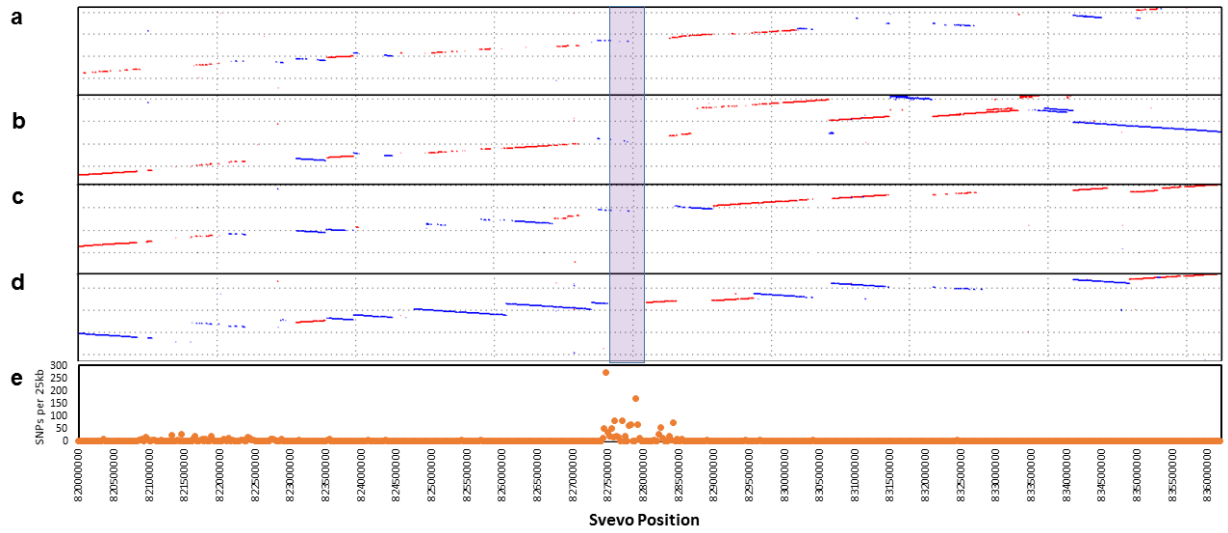

Figure 5.2. Structural variation exists in the *SSt1* interval between genome assemblies. Dot plots representing NUCmer alignments of the last 20 Mb of chromosome 3BL between Svevo and a) Zavitan; b) Refseq v.1.0; c) CDC Stanley; d) CDC Landmark. Red lines indicate alignment in the correct orientation and blue lines indicate inversions. A region of poor alignment between Svevo and other genomes is indicated by a purple shaded box. e) Exome capture BSA SNP frequency distribution in the Kofa/W9262-260D3 bulks.

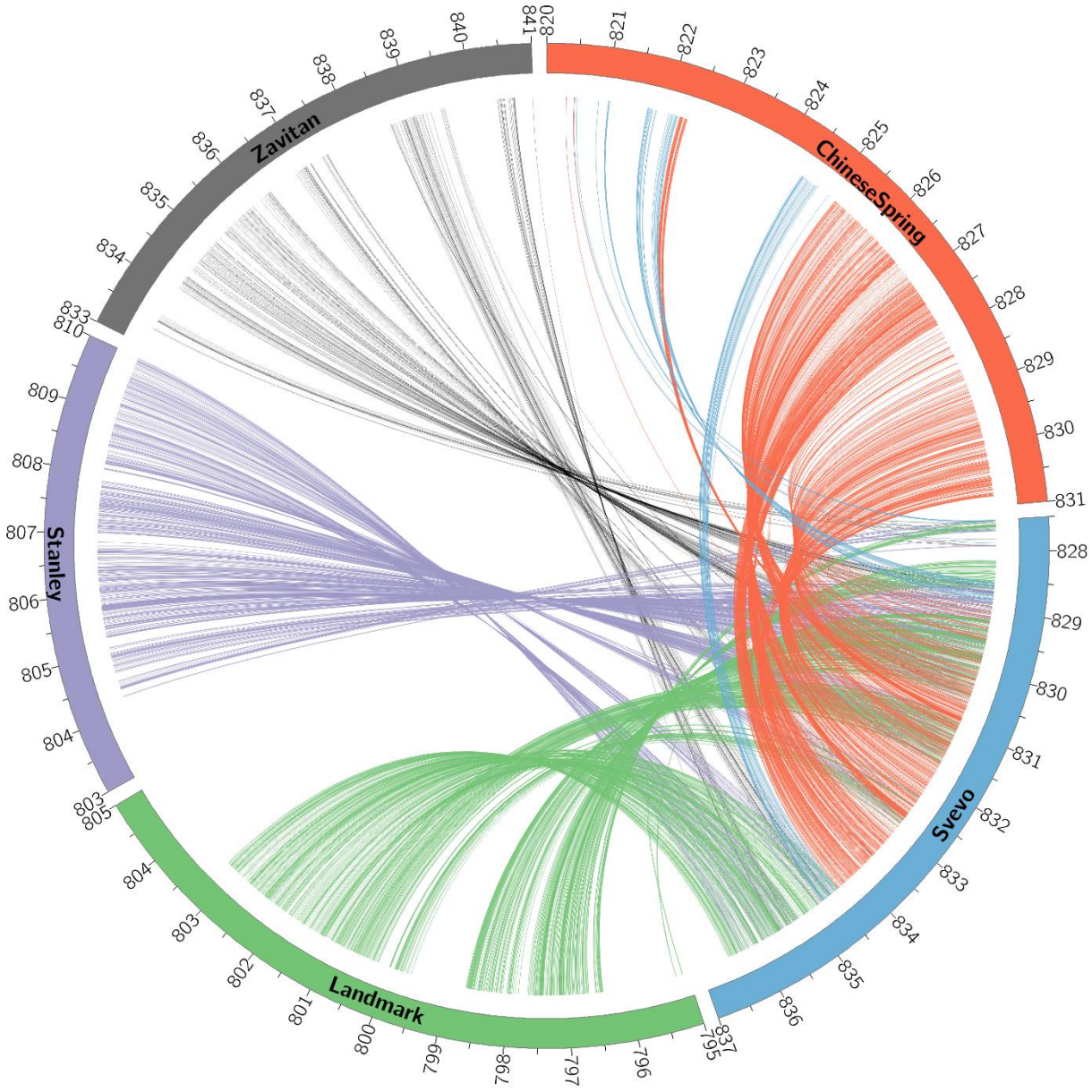

Figure 5.3. Comparative genomic analysis of the *SSt1* region in 5 genomic assemblies. Links between genomes are based on syntenic blocks from alignments in NUCmer. All comparisons are performed using Svevo as a reference, with each comparison represented as a different colour; the rearrangement in Refseq v.1.0 is shown in blue lines. Positions are in Mb.

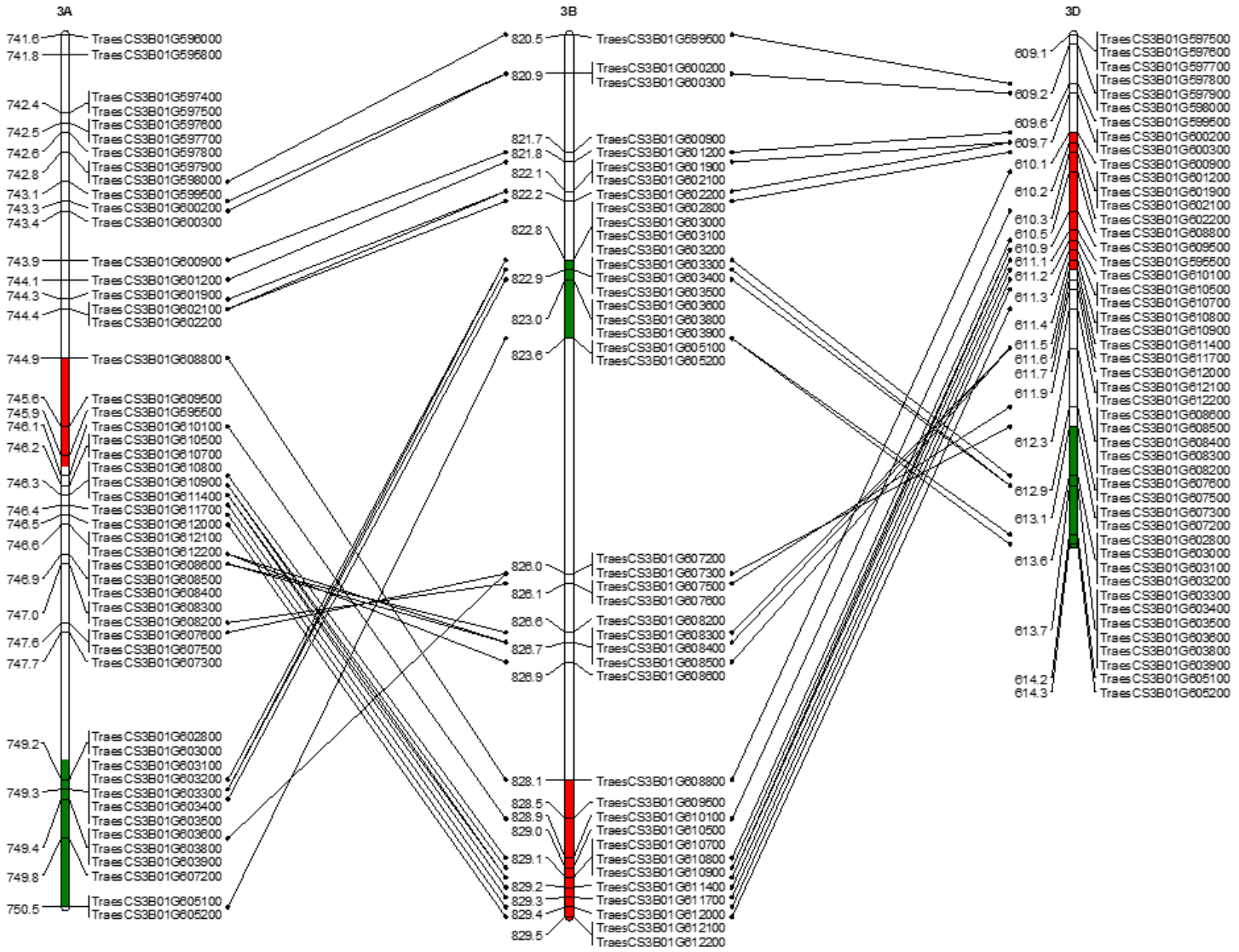

Figure 5.4. Refseq v.1.0 genes in and around the *SSt1* interval on chromosome 3B, and their corresponding homoeologous positions on chromosomes 3A and 3D. The green and red regions highlight major sequence rearrangements. Positions to the left of linkage maps are in Mb.

Other small differences were noted between Svevo and the other assemblies, but these differences were minor in comparison to the differences to observed with Refseq v.1.0. These differences were predominantly scaffold orientation conflicts, characterized by a group of markers in the same location with inverse ordering. The CDC Landmark assembly showed high collinearity to Svevo but was shorter than that of the other assemblies, indicative of sequence which was not incorporated into the assembly. In addition, the genomic region in Landmark between 798.8 - 799.0 Mb appeared to map to chromosome 2A in the other assemblies; this is likely a chimeric scaffold in the assembly or a miss-assembled scaffold. The comparison between Svevo and CDC Stanley indicate that the assemblies were highly co-linear, with a strong relationship in 90K markers and Refseq v.1.0 gene models.

5.3.2. RNAseq analysis reveals differentially expressed genes within the *SSt1* interval

The number of differentially expressed genes (DEGs) across the whole genome for each hollow by solid comparison ranged from 78 to 7174 (Figure 5.5). The fewest number of DEGs (n = 78) was observed when comparing EMS knockout line M2.1184 to its parent CDC Fortitude, whereas the highest number of DEGs were observed in hexaploid comparison Vesper/Lillian (7174).

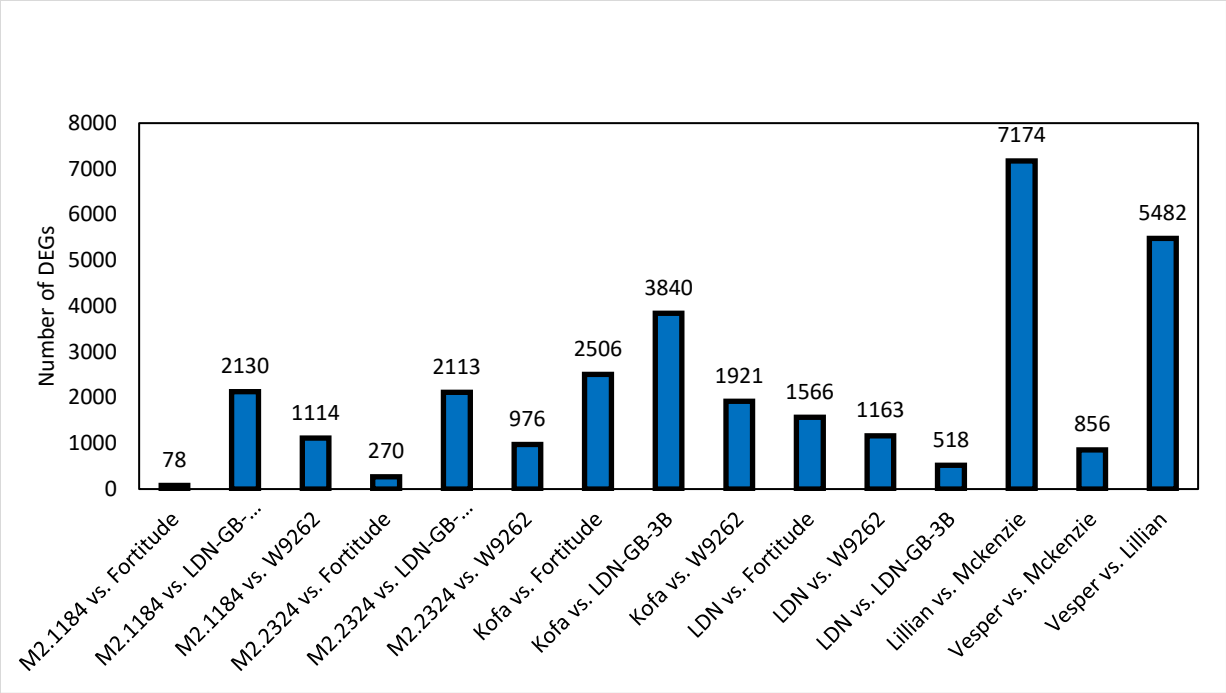

Figure 5.5. Number of differentially expressed genes between hollow vs. solid comparisons in the RNAseq panel.

There were 32 high confidence genes from the Refseq v.1.0 gene models which anchored within the *SSt1* region in Svevo (827.5 - 830 Mb), (Figure 5.6). This interval also contained the highest frequency of polymorphic SNPs between the *SSt1*+ and *SSt1*- bulks identified with exome capture and BSA (Fig. 5.2); several of these SNPs were localized inside genes within the *SSt1* interval (Fig. 5.6). Several genes within the *SSt1* interval were functionally related and tandemly duplicated; including three ankyrin repeat-containing domain proteins (ANK), four metallothionein (MT), two RPS28, three Dof transcription factors, and five pectin acetylesterases (PAEs). At Svevo position 829.2 Mb, a gene encoding a putative Dof (*TraesCS3B01G608800*) was significantly upregulated ($p < 0.001$) in all solid-stemmed lines in the RNAseq panel except Mckenzie, and was the only one of the three Dof genes that was expressed across lines in the RNAseq panel. There were no reads that mapped to *TraesCS3B01G608800* in M2.1184, and the expression of all genes between positions 828.6 and 829.2 were severely impaired in the mutant, indicating a possible deletion of this region (Figure 5.6). PCR fragments were not detected from the mutant M2.1184 both within *TraesCS3B01G608800* and flanking regions (Figure 5.7C), suggesting that the entire gene is deleted. Other notable genes that were differentially expressed in some, but not all pairwise comparisons included a protein kinase (*TraesCS3B01G600300*), a dual-

specificity RNA methyltransferase (*TraesCS3B01G6002000*), and the MYB transcription factor (*TraesCS3B01G612200*), which was localized just outside the *SSt1* interval (830.6 Mb), but was consistently down-regulated in all solid-stemmed lines.

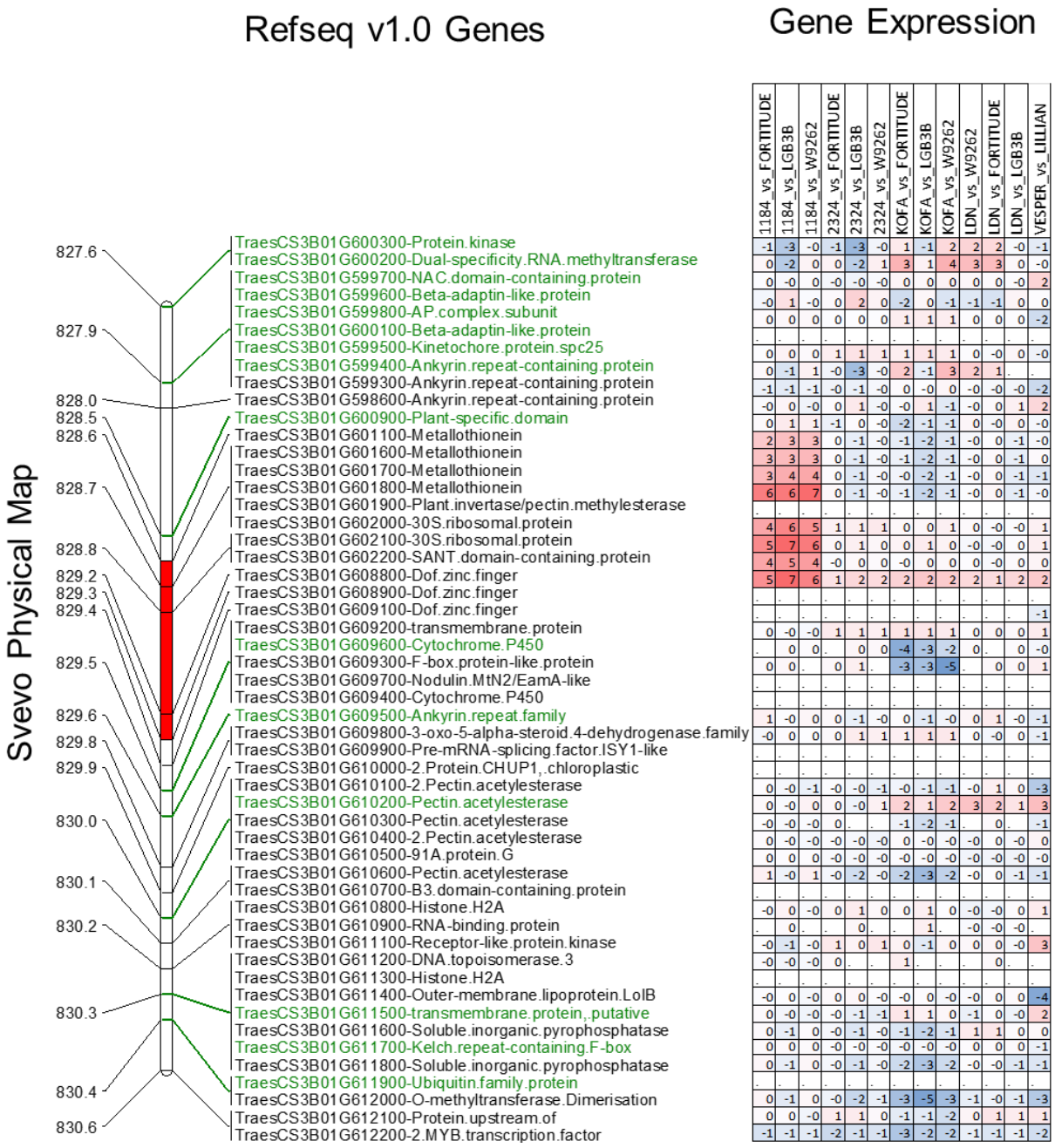

Figure 5.6. Gene expression comparison within the *SSt1* interval in the Svevo reference. Refseq v1.0 genes were anchored and ordered based on the Svevo reference sequence. Physical positions are shown to the left of map in Mb. The deleted region in M2.1184 is highlighted in red shading along the physical map. Genes that contained polymorphic SNPs from exome BSA are highlighted in green font. Gene expression differences between hollow vs. solid stemmed comparisons are shown as a heatmap on the right. Positive fold changes shown in blue shading indicate greater expression in the solid line, whereas negative fold changes shown in red shading indicate greater expression in the hollow line. Expression values are expressed as $\log_2$ fold change. '.' indicates no expression was detected.

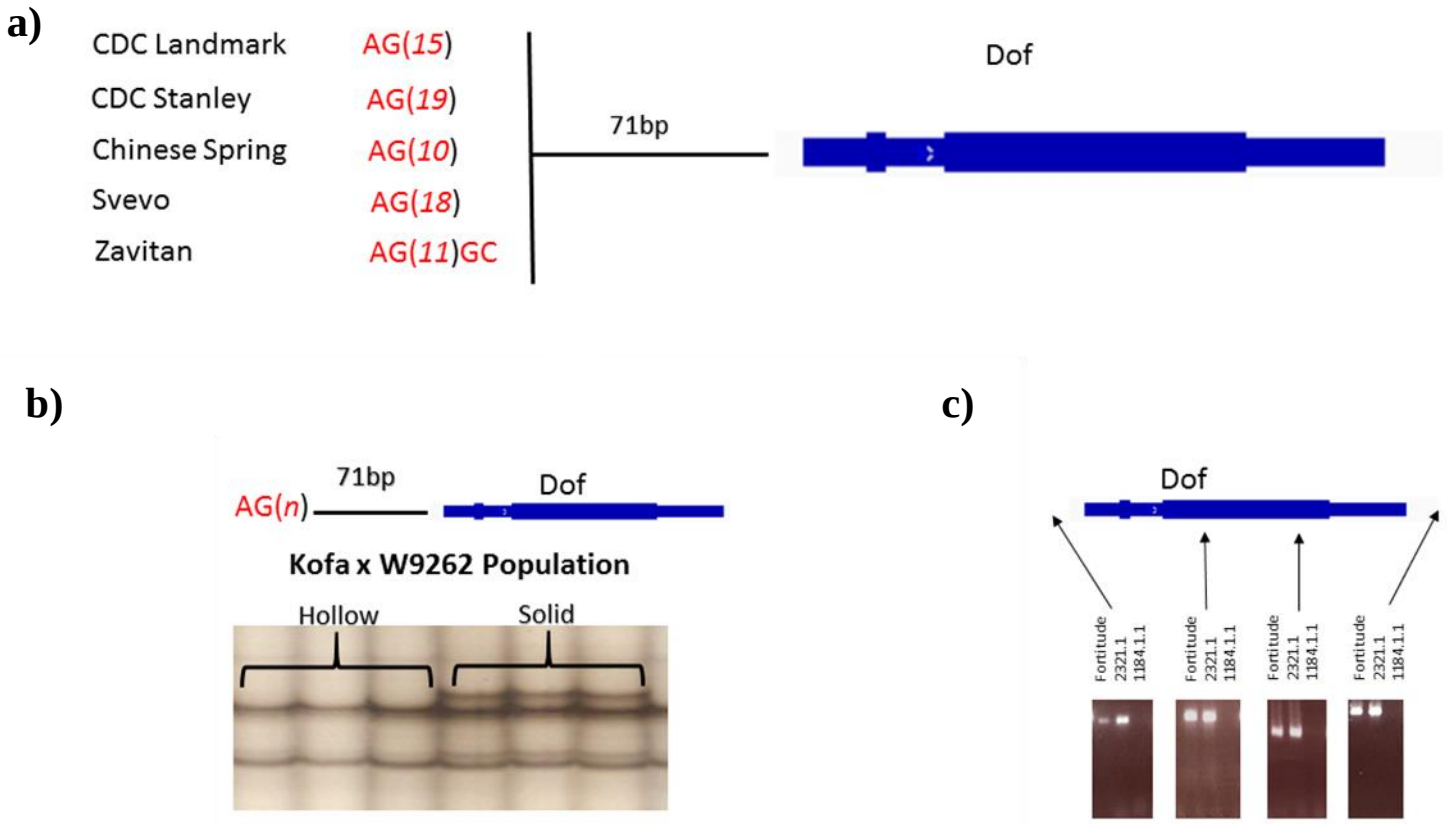

Figure 5.7. Variation around the *TraesCS3B01G60880* (Dof) gene. a) Polymorphic GAGA repeat in the promoter of Dof. **b)** SSCP gel image showing double banding in the AG repeat element in solid lines from Kofa/W9262-260D3 mapping population. **c)** Agarose gel image showing a deletion in mutant M2.1184 using as series of primers designed in and around the Dof gene.

5.3.3. Functional enrichment reveals that differentially expressed genes are involved in a variety of biological processes

Significant GO terms showing functional enrichment based on DEGs between hollow vs solid comparisons were identified for BP (12), CC (5), and MF (18) (Appendix 15), several of which can be plausibly linked to the role of *SSt1*. These included the biological processes GO:0006950 (response to stress), GO:0042546 (cell wall biogenesis), and GO:0071554 (cell wall organization or biogenesis). Many of the functionally enriched genes from the Refseq v.1.0 annotation that contained GO terms associated with cell wall modification were enzymes of the class xyloglucan endotransglucosylases/hydrolase (XTH), which are known regulator targets of Dof (Xu et al., 2016), while the remainder were galactoside 2-alpha-L-fucosyltransferases (FUT). The most enriched GO terms under Molecular Function was GO:008171 (O-methyltransferase activity), which included activity of genes encoding O-methyltransferase (OMT) and caffeoyl-CoA O-methyltransferase (CCOMT).

5.3.4. Comparative analysis reveals both sequence variation and CNV at *TraesCS3B01G608800*

To investigate possible sequence variation around *TraesCS3B01G608800*, the gene sequence from Refseq v.1.0 was aligned to the draft sequences of CDC Landmark (*SSt1*+), and CDC Stanley, Zavitan, Refseq v.1.0, and Svevo (*SSt1*-) using GMAP, and the complete gene sequence including 1Kb upstream and downstream of the gene were aligned using Muscle (Edgar, 2004). The *TraesCS3B01G608800* transcript is 2068 bp long and includes one intron. The predicted open reading frame (ORF) is 1134 bp, which encodes for a putative protein with 378 amino acids (Appendix 16). The analysis of sequence variation revealed that the transcript sequence of *TraesCS3B01G608800* shared 100% sequence identity between CDC Landmark and CDC Stanley (Appendix 7). Investigation into sequence variation within the promoter of *TraesCS3B01G608800* identified a polymorphic GAGA repeat 71 bp upstream of the transcriptional start site (TSS). Further investigation revealed the number of GA copies in each assembly was as follows: Refseq v1.0: 10; Zavitan: 11; CDC Landmark: 15; Svevo: 18; and CDC Stanley: 19 (Figure 5.7A).

Primers designed to flank the GAGA repeat upstream of *TraesCS3B01G60880* were used to screen a larger panel of lines for association analysis. The resulting PCR product was visualized

on SSCP gels, which unexpectedly identified additional fragments amplifying in solid-stemmed lines of the Kofa/W9262 and Lillian/Vesper mapping populations (Figure 5.7B). This led to the hypothesis of a sequence duplication in *TraesCS3B01G60880* could be associated with stem-solidness. Because the primer sequences map uniquely in the Landmark assembly, thus should not be amplifying any non-target fragments, the duplication must be collapsed. This polymorphic banding pattern was scored as a presence/absence polymorphism and was re-mapped in both mapping populations and found to co-segregate with the *SSt1* (data not shown), confirming that the polymorphism we observed was indeed from the *SSt1* region of 3BL.

5.3.5. Validation of structural variation using 10x sequencing

To investigate the possibility of a collapsed duplication in the Landmark assembly, we aligned the 10x sequence data for CDC Landmark, against the CDC Landmark and CDC Stanley reference sequences. Visualization of sequence read information identified a four-fold increase in read coverage in the region within the *SSt1* interval that contained *TraesCS3B01G60880* (Figure 5.8A and B), consistent with a collapsed gene duplication. However, the size of the duplicated region differed between alignments to the two assemblies. When CDC Landmark reads were aligned to CDC Stanley, the duplicated region spanned 34.1 kb (Figure 5.8B), whereas when aligned to CDC Landmark it spanned just 4.3 kb (Figure 5.8A). The only gene contained within either duplicated interval was *TraesCS3B01G60880.*

10x sequence data was also generated for Svevo, CDC Fortitude and M2.1184 and was aligned against the Svevo reference sequence. Visualization of the Svevo read data showed consistent read coverage around the region containing *TraesCS3B01G60880,* and a strong diagonal line with respect to molecule association did not show significant evidence of structural variation, which validates the Svevo assembly within the interval (Figure 5.9A). Visualization of the CDC Fortitude 10x data (Figure 5.9B) identified a peak in read coverage spanning 34.8 kb similar to the peak observed in CDC Landmark (34.1 kb). Similarly, this interval contained *TraesCS3B01G60880* and surrounding region. Molecule associations spanning the region were consistent with a duplication in a tandem configuration. Within the same interval, a largescale deletion spanning 674 kb was detected in M2.1184 (Figure 5.9C). Molecule associations spanning this gap were also identified consistent with a deletion. Additional structural variations, including

an additional series of possible deletions, common to the CDC Fortitude genetic background, were noted upstream of the *TraesCS3B01G60880* duplication interval.

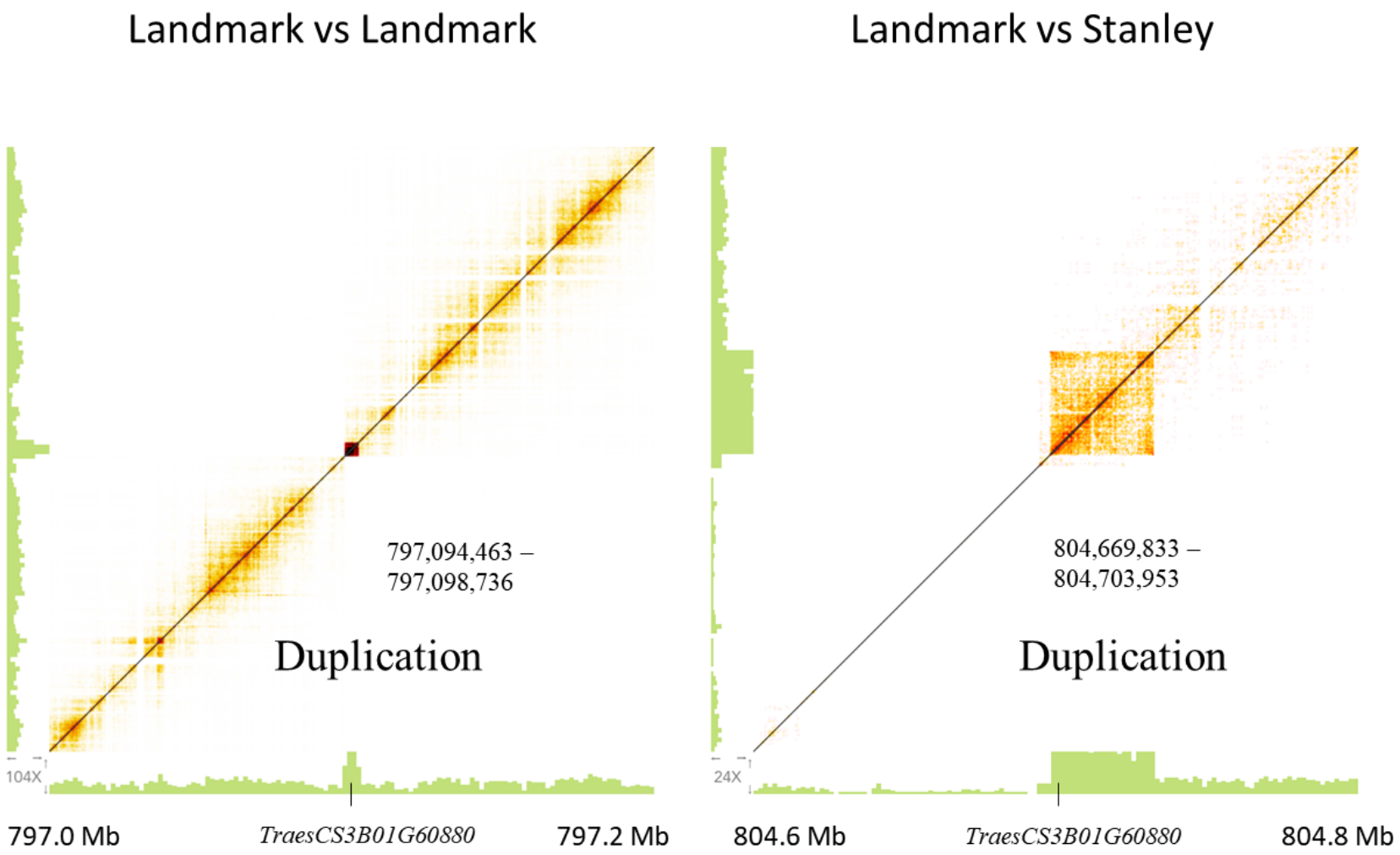

Figure 5.8. Loupe visualization of CDC Landmark 10x reads aligned to a) CDC Landmark and b) CDC Stanley. Read coverage is plotted on the X and Y axes, whereas the diagonal red line represents 10x molecule association. Deviations from the main diagonal suggest putative structural variations.

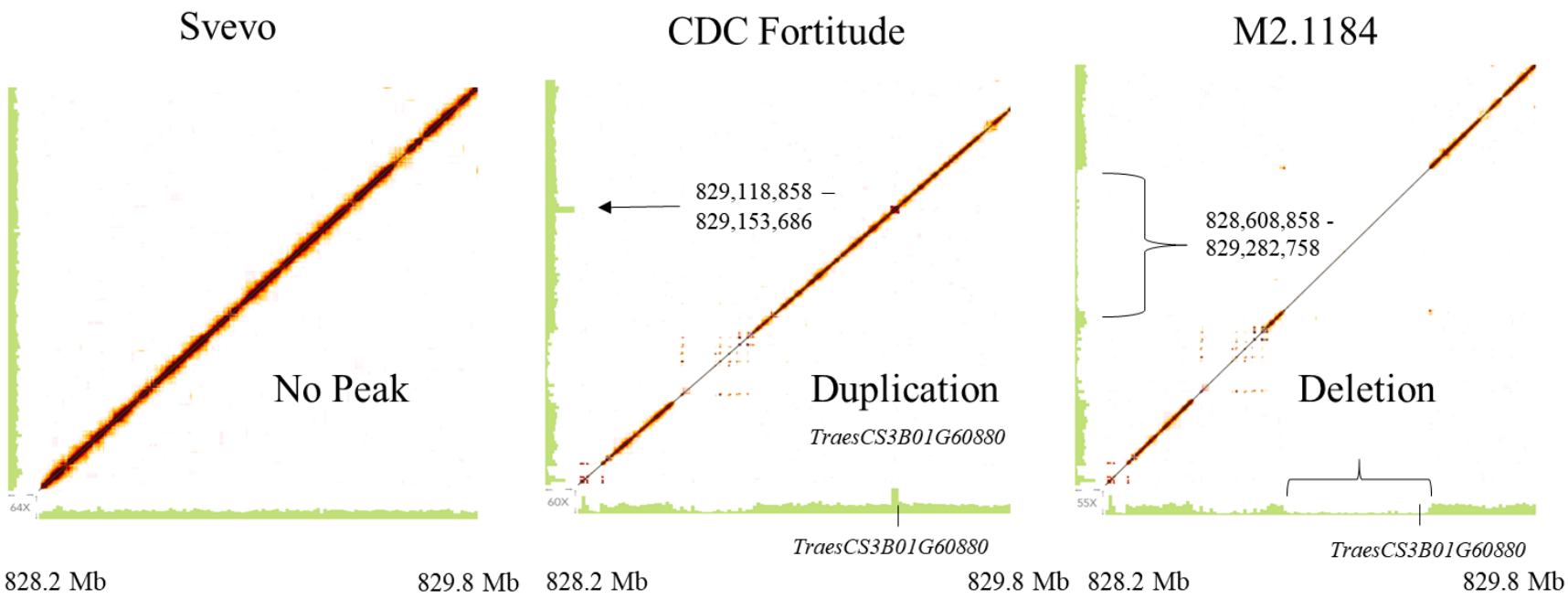

Figure 5.9 Loupe visualization of 10x reads aligned to the Svevo reference from: a) Svevo, b) CDC Fortitude and c) M2.1184. Read coverage is plotted on the X and Y axes, whereas the diagonal red line represents 10x molecule association. Deviations from the main diagonal suggest putative structural variations.

A qPCR assay was developed to interrogate copy number variation (CNV) of *TraesCS3B01G60880* in an expanded set of lines, including all five lines for which reference assemblies were available (Landmark, Stanley, Svevo, Zavitan and Refseq v1.0, Figure 5.10A). In addition, all lines in the RNAseq panel were screened (Figure 5.10B), in addition to an extended set of tetraploid and hexaploid cultivars (Appendix 17 and 18). Of the five reference lines, CDC Landmark (*SSt1+*) had a three to four-fold greater number of copies than Stanley, Svevo, Zavitan, and Refseq v.1.0. In the RNAseq panel, Lillian had a similar number of copies as CDC Landmark that was about three to four times greater than in Vesper. The solid-stemmed durum's W9262-260D3, CDC Fortitude, and LDN-GB-3B had a similar number of copies of *TraesCS3B01G60880* that was three to four-fold times greater than the hollow cultivar Kofa. The mutant M2.2324 had a similar number of copies to its parent, CDC Fortitude, however a complete lack of amplification for *TraesCS3B01G60880* was detected in M2.1184, providing additional evidence of a deletion in that line. The number of copies experimentally validated through qPCR were moderately correlated (r = 0.43) to the normalized reads count from DESeq2 analysis (Figure 5.10C). The number of copies of *TraesCS3B01G60880* in the expanded set of cultivars had nearly a perfect association with known phenotypic expression of stem-solidness, although the threshold for determining the cut-off point differed between durum and common wheat (Figure 5.10D). The only obvious exceptions were Janz, a solid hexaploid which expresses a solid-stem derived from *T. ponticum*, but appears to carry only a single copy of *TraesCS3B01G60880*, and Durex, a hollow-stemmed durum that expresses multiple copies of *TraesCS3B01G60880*.

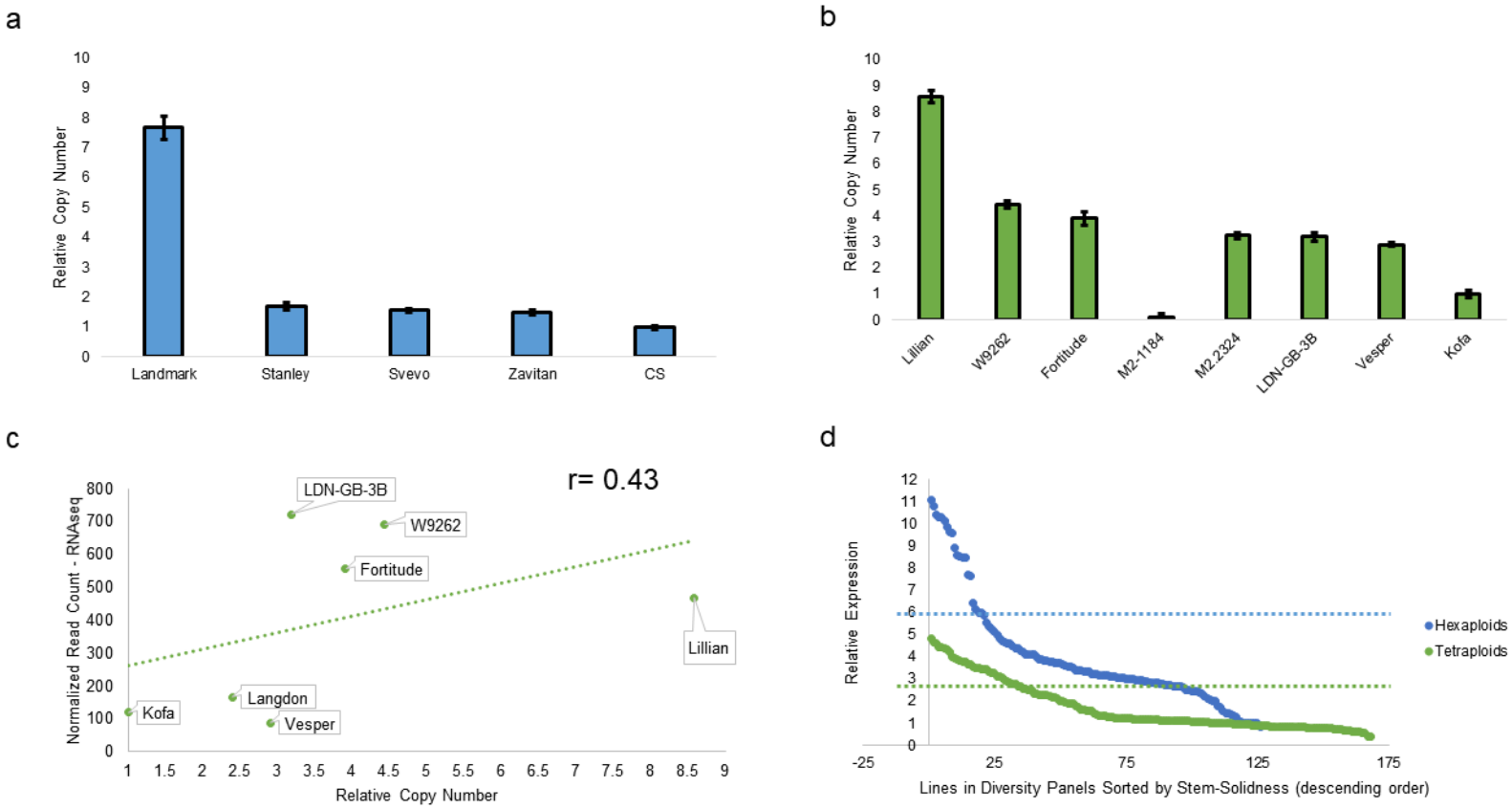

Figure 5.10. Copy number analysis for the *TraesCS3B01G60880* (Dof) gene. Copy number was determined by qPCR. a) Relative copy number of *TraesCS3B01G60880* in each of the five genome assemblies, and b) Relative copy number of *TraesCS3B01G60880* in lines from RNAseq panel. c) Correlation between relative copy number of *TraesCS3B01G60880*, and normalized read count from RNAseq. d) Distribution of CNV for *TraesCS3B01G60880* in a diverse set of hexaploid and tetraploid lines. The color-coded dotted lines show the cut-off point differentiating hollow from solid cultivars based on phenotypic screening. The full data summary is shown in (Appendix 17 and 18).

5.4. DISCUSSION

Growing wheat cultivars that express the solid-stem phenotype is the most effective way to minimize damage caused by the WSS. Identifying the genetic factors responsible for conferring stem-solidness is important towards maximizing pith expression in wheat, especially for common wheat where pith expression can be below the threshold required to achieve effective resistance to WSS. The *SSt1* locus on chromosome 3B contributes to most of the phenotypic variation in stem-solidness in both wheat species. In this study, we report on several key findings that will help guide future research in breeding for resistance to the WSS.

We identified major sequence variation around and within the *SSt1* locus, including major rearrangements, CNV, regions of dissimilar sequence, and other small translocations or inversions. The rearrangements in Refseq v.1.0 make this reference sequence problematic to use for the positional cloning of *SSt1*. For example, previous association mapping work in common wheat had identified the peak of the QTL to be close to the marker *BS00074345_51* (Varella et al., 2015); this marker is located at Refseq v.1.0 position 829.2 Mb, nearly 10 Mb distal from where the peak of the QTL was localized in durum wheat, near the marker *EK02_292495* (Refseq v.1.0 position 821.0 Mb) (Nilsen et al., 2017). This led us to initially question whether durum and common wheat carry two different genes at *SSt1*, until the release of the assembly for Svevo shed new light on the problem. The *TraesCS3B01G60880* gene is localized close to *BS00074345_51* in physical distance, but when we mapped our *TraesCS3B01G60880* CNV as a molecular marker in the Lillian/Vesper and Kofa/W9262-260D3 mapping populations, it was found to co-segregate with *EK02_292495*. This finding was supported by the fact that when the Refseq v.1.0 gene models were anchored to Svevo, and positioned accordingly, both *EK02-292495* and *BS00074345_51* mapped to a much smaller interval of 2.5 Mb interval (827.5 - 830.2 Mb) and co-segregated with the peak of the QTL in both species. The arrangement of *EK02-292495* and *BS00074345_51* was consistent across the other four assemblies, therefore the re-arrangement appears to be specific to Refseq v.1.0. Furthermore, comparison between the homoeologous gene order on 3A and 3D in Refseq v.1.0 also showed an inversion on 3BL around the same region. Taken together, these findings suggest that the gene order in Refseq v.1.0 does not reflect the true order of genes in the other assemblies, which is more accurately represented by the order in Svevo, and supported by the other assemblies and the wheat 90K consensus map. It remains unclear whether the

rearrangement in Refseq v.1.0 is the result of an error in the assembly of the pseudomolecule or a true structural variation.

Many of the PCR based markers that were previously developed to saturate the *SSt1* locus (data not shown) functioned only as dominant markers (presence absence of an amplified fragment), and the amplification pattern for these markers was opposite in common wheat versus durum wheat (i.e. solid durum's and hollow hexaploids amplified a band, whereas, hollow durum's and solid hexaploids did not). This led us to hypothesize that hollow durum's and solid hexaploids carried a deletion of approximately 500 kb in length. However, in the present study, comparative genomic analysis revealed that this region does not carry a deletion, but rather is a region of dissimilar sequence between the assemblies. This same region was also associated with the peak of SNP frequency differentiating the exome bulks (*SSt1+*, *SSt1-*) and is likely in linkage disequilibrium with the causal gene(s) conferring stem-solidness, positioned just proximal to the peak of the *SSt1* QTL in durum and common wheat. If common wheat and durum wheat do in fact share a common gene conferring stem-solidness, then it's likely that a historical recombination event has occurred at some point in evolutionary history between this region of dissimilarity, and the causal gene.

The *SSt1* region has undergone a series of gene duplication events. Several clusters of between two and four genes were discovered within *SSt1*, consisting of genes encoding putative ANK, MT, RPS28, Dof and PAEs. These gene clusters occurred within tight physical intervals along the Svevo reference sequence which suggests they were tandemly duplicated. Results presented here suggest CDC Landmark carries multiple copies of one the Dof genes, *TraesCS3B01G60880*, that were collapsed into a single copy in the current CDC Landmark assembly. This was in addition to the two additional Dof genes that were resolved in the CDC Landmark assembly. Within the CDC Landmark assembly, *TraesCS3B01G60880* was positioned near the edge of a scaffold break point, which suggests that this region is particularly difficult to assemble, possibly because of the sequence duplication.

In the present study, we found the *SSt1* interval in Svevo (827.5 - 830 Mb) contains 32 annotated genes, of which only 10 were differentially regulated in at least one hollow vs. solid comparison. The QTL interval was independently verified using wheat exome capture coupled with bulked segregant analysis, which localized the highest frequency of polymorphic markers between *SSt1+* and *SSt1-* bulks to the same location. Although exome capture may not be directly

suitable towards the identification of causal mutations because of large gaps in probe coverage, these results do show the approach was capable of saturating our target interval with additional markers that may be useful for marker-assisted selection or genetic mapping experiments. Based on the cumulative analysis of multiple differential expression analyses, the strongest candidate gene for *SSt1* was *TraesCS3B01G608800*, which encodes a putative Dof transcription factor. Dof proteins are a family of transcription factors specific to plants that are responsible for the positive and negative regulation of genes implicated in a wide variety of functions, including cell cycle regulation (Skirycz et al., 2008), C4 carbohydrate metabolism via phosphoenolpyruvate carboxylase (PEPC) (Yanagisawa, 2000), plant growth and development, photosynthesis, light response (Yanagisawa and Sheen, 1998), and cell cycle progression/cell expansion (Xu et al., 2016). Dof proteins regulate target genes by binding to the sequence AAAAG, which is ubiquitously found in the promoters of many plant genes (Yanagisawa and Izui, 1993), including in the promoter of *TraesCS3B01G60880* itself, which could suggest *TraesCS3B01G60880* is a self-regulating transcription factor. Although there was no evidence of sequence variation within the *TraesCS3B01G60880* transcript that would impair gene function between hollow vs. solid-stemmed cultivars, we discovered that the *TraesCS3B01G60880* promoter carries a GAGA element within 100bp of the TSS that has between 10 and 21 AG repeats depending on the assembly. This ultimately led to the discovery that *TraesCS3B01G60880* itself was duplicated and was not fully resolved in the assembly of Landmark. In other systems, GAGA binding proteins have been suggested to influence gene expression by binding to GAGA sites in the promoter (Sangwan and O'Brian, 2002).

Supporting evidence for *TraesCS3B01G60880* as a candidate gene for *SSt1* was provided by our EMS knockout line M2.1184, which we believe carries a substantial deletion around the *TraesCS3B01G60880* gene based on several lines of evidence. First, we observed a complete lack of PCR amplification using a variety of primers specifically designed around the *TraesCS3B01G60880* gene. Second, we did not detect evidence that the gene was expressed in RNAseq experiments, or with qPCR analysis. And third, based on whole genome sequence data using the Chromium 10x sequencing platform, which showed a substantial reduction of read coverage within a region spanning 673 kb, with evidence of molecule associations that appear to span the putative deletion. Previous research has also found that large scale deletions between 150 and 750 kb were generated using EMS as a chemical mutagen in wheat (Henry et al., 2014). The

genes immediately distal to *TraesCS3B01G60880* also have severe impairment of their expression in M2.1184, including two RPS28 copies, a SANT-domain-containing protein, four copies of ANK, and four MT encoding proteins. A small number of reads were found to be mapping to these genes, possibly due to cross-mapping during the RNAseq assembly, which was also observed with 10x dataset. Therefore, based on this analysis it is possible the deletion in M2.1184 could be as large as 673 kb spanning Svevo position 828.6 -829.2 Mb. In addition, a second mutant line, M2.2324, had reduced expression of *TraesCS3B01G60880* in our RNAseq analyses, providing additional support for this gene as a candidate for *SSt1*. Given that *TraesCS3B01G60880* was consistently upregulated in solid-stemmed cultivars, we consider it the strongest candidate gene for *SSt1*. However, the possibility that additional genes contained within the deletion in M2.1184 MTs, RPS28, Sant Domain containing protein) are also involved cannot be ruled out presently.

The remaining genes within the interval could be also be involved in conferring stem-solidness. Plant metallothionein's are a diverse family of protein primarily involved in heavy metal detoxification and reactive oxygen species (ROS) scavenging (Hassinen et al., 2011). Previous studies have shown RNAi knockdowns of the OsMT2b gene in rice resulted in increased epidermal cell death, whereas the epidermal cells of normal plants undergoing cell death were found to have downregulation of OsMT2b in the presence of H_20_2 and ethylene (Steffens and Sauter, 2009). Pith autolysis is a normal process by which pith is broken down and cell wall components recycled, particularly during periods of stress such as low light intensity or drought stress (Huberman et al., 1993). Therefore, it could be plausible that metallothioneins could be involved in the normal development of the hollow-stem. However, if this were true we would expect to have seen consistent down-regulation of the metallothionein genes, which was not observed through RNAseq analysis.

Ribosomal protein genes were also observed in the *SSt1* interval, and are required to be in stoichiometric balance to make up the ribosomal complex responsible for protein synthesis (Naora, 1999). The coordination of RP production is even more important in polyploidy species where the presence of additional homoeologous gene copies are likely. In addition to their primary roles, several RPs have been implicated in extra-ribosomal functions. For example, inhibiting the expression of RPS3a can initiate apoptosis, whereas the gene is expressed at very high levels in some human tumor cells (Naora et al., 1998). RPS28 can also bind to the 3' UTR of its own mRNA as a post-transcriptional regulation mechanism (Badis et al., 2004). In humans, L26 can bind to

the 5’ UTR of the tumor suppressor gene p53 thereby enhancing its translation (Takagi et al., 2005). Stem-solidness likely arises from increased cell division, cell elongation or a combination of the two. Conversely, stem-hollowness, which is the predominant form in modern wheat cultivars, could be caused by a deficiency in the production of RPS28 leading to an initiation of cell cycle arrest or the induction of programmed cell death.

Previous research suggested O-methyltransferase (OMT, *TraesCS3B01G612000*) as a possible candidate gene for *SSt1* due to strong differential expression in hollow vs solid cultivars (Oiestad et al., 2017). Although this gene was not found within our defined QTL interval that is shared between durum and common wheat, it fell just outside (Svevo position 830.4 Mb) and was within the QTL interval of the Lillian/Vesper mapping population. The gene was strongly up-regulated in hollow-stemmed cultivars (log_2 fold change = 3-5), except in comparisons with the hollow-stemmed cultivar Langdon. However, OMT was not differentially expressed in comparisons with the EMS mutant M2.1184, which suggests that it is not a strong candidate, at least in the context of durum wheat. GO enrichment analysis did identify significant functional enrichment of O-methyltransferase across many hollow-solid comparisons. O-methyltransferase is thought to be involved in lignin biosynthesis. True pith cells are composed of undifferentiated, un-lignified parenchyma, whereas the cells surrounding vascular bundles consist mainly lignified sclerenchyma that provide mechanical support to the stem. (McNeal et al., 1965) found no significant difference in lignin content between the hollow-stemmed cultivar Thatcher and the solid-stemmed cultivar Rescue, which would suggest the lignified portion of the stem is the same in both lines. Therefore, one possible explanation is that the detection of differential expression of O-methyltransferase is more related to disproportionate sampling of cell types as opposed to a true differential expression response. In the present study, we attempted to avoid such bias by sampling the pith transition zone located above the node where both hollow and solid-stemmed cultivars have pith cells present, in contrast to Oiestad et al. (2017) who sampled the entire internode region for expression analysis. Despite having a more precise sampling method, we detected differential expression of OMT in some comparisons, which could warrant future investigation.

5.5. CONCLUSIONS

Defining the *SSt1* interval has been problematic because small discrepancies in gene order exist between assemblies, particularly in Refseq v.1.0, therefore caution must be taken when using

a reference guided approach towards positional cloning of genes, which highlights the need for a high-quality assembly of an *SSt1* carrier. A region of dissimilar sequence between Svevo and the other assemblies corresponded to an increase in SNP frequency identified by exome capture and BSA; these SNPs will serve as an important source of markers for additional mapping experiments or marker-assisted selection in wheat. We corrected the order of Refseq v.1.0 genes within the *SSt1* interval using the Svevo sequence, which contains 32 genes. Of these, a gene encoding a Dof transcription factor (*TraesCS3B01G60880)* was consistently differentially expressed across all hollow by solid comparisons. During attempts to characterize the promoter of the *TraesCS3B01G60880* gene, we unexpectedly amplified multiple copies in solid-stemmed lines. We developed a qPCR assay that confirmed CNV in *TraesCS3B01G60880,* which was found to be associated with stem-solidness in a diverse set of hexaploid and tetraploid cultivars. A large EMS induced deletion was also identified in and EMS mutation line, M2.1184, which included the entire *TraesCS3B01G60880* gene, providing further evidence towards its involvement in conferring stem-solidness.

6. GENERAL DISCUSSION

Wheat is currently the world's most widely grown food crop, and accounts for 20% of the daily calories consumed by a current population estimated to be around 7.5 billion people. The United Nations projects the global population will reach 10 billion people by the year 2056, thus the corresponding demand for wheat is expected to increase significantly over the same period. Wheat production is currently limited by several biotic and abiotic stresses, which will need to be addressed to ensure global food security in the near future. The WSS is a damaging insect pest across the major wheat growing regions in North America. The most effective way to control the WSS is to deploy cultivars that express the solid-stem phenotype. The goal of this thesis was to comprehensively examine the expression of stem-solidness trait wheat. This research was facilitated by the major advances that have been made in wheat genomics over the past decade, including the development of new high throughput SNP genotyping platforms such as the wheat 90K array and the first fully assembled reference sequences for durum and common wheat.

6.1. Increased sowing density decreases pith expression in common and durum wheat

Optimizing management practices that maximize agronomic performance can have a major impact on a producer's bottom line, particularly regarding yield and grain quality. In regions that are prone to sawfly damage, maximizing the expression of stem-solidness could help protect against yield and quality losses from lodging and downgrading caused by the WSS. However, it can be difficult to predict when WSS infestation will occur. Thus, it is essential to find the right balance between management practices which optimize yield and stem-solidness, both in the absence or presence of WSS infestation. Previous research has shown that the expression of stem-solidness in common wheat is influenced by environmental factors, the most important of which is light intensity/quality. The effect of light quality on the expression of stem-solidness in durum wheat had not been evaluated prior to this research, but was presumed to be less of a concern due to the strong pith expression across environments observed in most durum cultivars. It was hypothesized that under higher commercial sowing densities, a reduction in the amount of light penetrating through the canopy could negatively affect pith development in some solid-stemmed wheat cultivars. Thus, determining the optimum sowing density is important to ensure effective WSS resistance. Such interactions are likely cultivar specific, which highlights the need of continued agronomic research as new solid-stemmed cultivars are released.

In this study, we showed that the expression of stem-solidness in the durum cultivars Golden Ball, and the Biodur derivatives CDC Fortitude, and AAC Raymore, was not heavily affected by sowing density, as all three cultivars had stems that were nearly completely solid. This contrasted with the common wheat cultivar Lillian, which developed significantly less pith than the durum lines, and was well below the minimum threshold or 3.75 proposed by (Wallace et al., 1973) required to achieve effective resistance to WSS. In this study, we were not able to observe significant WSS cutting, therefore additional research is necessary to ensure the resistance in these lines would be sufficient under infestation. We observed a negative correlation between sowing density and the expression of stem-solidness, and positive correlation with yield across cultivars in the study. Both CDC Fortitude and AAC Raymore were similar in grain yield to the check cultivar Strongfield. Although this does not necessarily mean there is not a yield penalty associated with stem-solidness per se, it does indicate that breeding efforts have been successful in overcoming any potential yield drag in durum wheat.

6.2. *SSt1* maps to a coincident locus on chromosome 3B in mapping populations Kofa/W9262-260D3 and Lillian/Vesper

Advances in high-throughput genotyping platforms such as the iSelect 90K array allowed the dissection of the major stem-solidness QTL on chromosome 3BL at a higher resolution than was previously possible. Using this approach, two coincident QTL were identified on chromosome 3BL near the previously reported location of *Qss.msub-3BL* (Cook et al., 2004) and *SSt1* (Houshmand et al., 2007). At the time when this experiment was conducted, the only available genome assembly was the sequence for the WEW accession Zavitan (Avni et al., 2017). Anchoring of 90K probes associated with the peak of *SSt1* to the WEW reference sequence allowed for precise comparison between genetic and physical intervals for both mapping populations. Based on the overlapping portion of the QTL interval in Kofa/W9262-260D3 and the Lillian/Vesper mapping populations, the *SSt1* interval spanned positions 833.4 – 835.1 Mb on WEW chromosome 3B. This finding was supported by haplotype evidence using common wheat and durum wheat diversity panels.

In the present study, differences in haplotypes observed in some lines in the diversity panels, which supported the hypothesis that multiple sources of stem-solidness exist (Beres et al., 2013a). Stem-solidness likely evolved in Europe, either prior to the global expansion of wheat

from the fertile crescent. Alternatively, stem-solidness may have evolved multiple times independently, either before or after expansion from the fertile crescent. The reason that stem-solidness has persisted may be due to a selective advantage associated with having a solid stem, either as a mechanism of insect resistance, or for its role in stress response. In North America, *C. cinctus* is the only economically important pest of wheat, but does not currently exist in Europe. However, the closely related species *C. pygmaeus* does cause crop losses in Europe, and has similar life cycle and biology to *C. cinctus.* If infestations of *C. pygmaeus* occurred during the domestication of wheat, then it is likely that stem-solidness was inadvertently selected for by early hunter and gatherers, as hollow-stemmed counterparts would have been susceptible to lodging.

In the present study, the two known sources of stem-solidness in durum wheat (Golden Ball and Biodur) had different haplotypes, despite QTL having previously been mapped to a similar region of chromosome 3BL (Houshmand et al., 2007). Golden Ball carried the hollowness allele throughout the entire interval, thus it is presently unclear whether the stem-solidness gene it carries is allelic to *SSt1*. In a previous study, Cook et al. (2017) found 26 different haplotypes within the *SSt1* interval in durum and common wheat. In the present study, most common wheat lines derived from S-615 all carried a similar haplotype, with a few exceptions, such as Janz and Mott, both of which share a similar haplotype that is quite different from S-615. Janz derives its stem solidness from *Thinopyrum ponticum* (Beres et al., 2013b), whereas Mott is a derivative of S-615. At this point it remains unclear whether the different sources of stem-solidness carry different genes, or different alleles of the same gene. Research in common wheat suggests there could be multiple alleles at *SSt1* based on observations in the winter wheat cultivar Conan (Talbert et al., 2014). Conan was derived from the cross: Westbred-Rambo/Westbred-906-R, where Westbred-906-R was derived from the cross Fortuna/Westbred-906-R//Golden-86. Fortuna is a derivative of S-615, thus Conan itself should be an S-615 derivative.

Conan is unique because it exhibits temporal expression of stem-solidness, having a very solid-stem during early stem elongation, but becomes more hollow-stemmed towards maturity (Varella et al., 2016). The traditional approach to rate for stem-solidness in breeding programs has been to examine stems at maturity, which was also the rating approach used throughout this thesis. This could explain why several hollow-stemmed lines in the common wheat diversity panel carried haplotypes that would have suggested they are solid-stemmed. For example, the cultivar Mckenzie carries the S-615 haplotype, but has sometimes been described as a hollow-stemmed cultivar

(Beres et al., 2013a). At maturity, Mckenzie had a low level of stem-solidness (stem-solidness < 2), yet was entirely solid-stemmed at the time of sampling for RNAseq during early stem-elongation. Other similar examples include the CWES cultivars Glenlea and Burnside, which carry novel (possibly solid-stemmed) haplotypes within the *SSt1* interval. Further research is required to characterize the extent of temporal pith expression in Canadian germplasm.

6.3. Major structural variation exists around the *SSt1* locus in some genomic assemblies

Since the release of the WEW genome sequence (Avni et al., 2017), additional completed reference sequences have become available at a spectacular rate, even during the writing of this thesis. At the time or writing, there are complete assemblies now available for common wheat (Refseq v.1.0), and durum wheat (Svevo). While reference sequences can be important tools to define QTL intervals, they can also be challenging, particularly because small differences in gene order exist between assemblies. This is particularly true near the telomeres, as was the case for *SSt1*. Assembly of the wheat genome is hindered by the allopolyploid nature of its genome, and large amount of repetitive sequences. Therefore, it can often be difficult to determine whether structural variation between assemblies is real, or an artifact of the assembly process. Furthermore, the possibility that unique sequence variation or structure exists in solid-stemmed lines highlights the need for an assembled sequence of an *SSt1* carrier. To address this concern, work is currently underway finalize the draft assembly of the *SSt1* carrier CDC Landmark.

6.4. The *SSt1* interval contains several possible candidate genes

One of the major objectives of this thesis was to define the *SSt1* interval and the genes contained within it. A high degree of collinearity between the genes and gene order was observed between the assemblies Zavitan, Svevo, CDC Stanley and CDC Landmark. However, this research identified largescale structural variation in Refseq v.1.0 relative to the other assemblies with major implications towards defining the *SSt1* interval. Considering a large amount of the work in this thesis was done in durum wheat, the only available durum reference sequence, Svevo, was examined. The Refseq v.1.0 gene models were re-ordered by anchoring the transcript sequences to Svevo. Based on the Svevo order, there are 32 high confidence genes contained within the *SSt1* interval. Many of the genes within the interval are functionally duplicated, including clusters of genes encoding putative ANK, MT, Dof, RPS28 and PAE proteins.

Gene expression analysis through RNAseq identified many differentially expressed genes between hollow and solid cultivars, both genome-wide, and contained within the *SSt1* interval. One gene, *TraesCS3B01G60880*, encoding a putative Dof transcription factor was differentially expressed across all hollow by solid comparisons. The ORF of *TraesCS3B01G60880* did not show significant sequence variation to account for its differential expression, however, a polymorphic GAGA element was identified 71 BP upstream of its TSS, and a different number of GA repeats was found in each of the five genome assemblies. Primers were designed to flank this polymorphism, however the amplification of multiple PCR fragments in solid-stemmed cultivars suggested additional copies of the gene could be associated with stem-solidness. In the current version of the CDC Landmark assembly, there is only a single copy of *TraesCS3B01G60880* and the gene is localized at the edge of a scaffold with a breakpoint immediately upstream of the GAGA element.

Further investigation using 10x sequencing data showed that the entire *TraesCS3B01G60880* gene and surrounding sequence was duplicated, spanning a physical distance of ~35 kb. No additional genes were present within the duplication. Because there is approximately four-fold greater 10x read coverage within the duplication, there are likely to be four copies of *TraesCS3B01G60880* in a tandemly duplicated configuration. Similar number of copies are found in the other gene clusters within the *SSt1* interval. Because the additional copies are not being resolved in the CDC Landmark assembly, it is reasonable to assume that they are either identical in their nucleotide sequence, or nearly so. This was supported by the fact that additional SNPs were not detected among stacked 10x reads (data not shown). The occurrence of a scaffold breakpoint in such proximity to the edge of the duplicated region would also suggest that the duplication is causing problems in the assembly process.

To examine the frequency of CNV at *TraesCS3B01G60880* a qPCR assay was developed and used to screen the common wheat and durum wheat diversity panels. These results showed a strong association between the number of copies of *TraesCS3B01G60880* and stem-solidness, although a few exceptions were noted. Among these was the Australian cultivar Janz, which derives its stem solidness from *Thinopyrum ponticum* (Beres et al., 2013a). Janz only carried a single copy of *TraesCS3B01G60880* yet expressed a solid-stem similar to S-615. These findings again highlight the need for further research to fully understand the different sources of stem-solidness in wheat.

The identification of a large-scale EMS induced mutation within the *SSt1* QTL interval in M2.1184 provided further evidence of the involvement of *TraesCS3B01G60880* in conferring stem-solidness. The deletion spanned approximately 673 kb, which was estimated by examining the coverage of 10x sequencing reads and 10x molecule associations that spanned the gap. Previously research has also identified EMS deletions ranging in size up to 760 kb (Henry et al., 2014). Thus, wheat appears to be quite tolerant of large deletions, likely due to the buffering effect caused by allopolyploidy. The deletion in M2.1184 also include seven other genes, including four MTs, two RPS28 and a SANT-domain-containing protein. Based on stable differential expression in most hollow vs solid comparisons, *TraesCS3B01G60880* is the strongest candidate, however further experiments will be required to confirm it as the causal gene.

7. CONCLUSIONS AND FUTURE RESEARCH DIRECTIONS

This research was conducted to investigate the expression of stem-solidness in durum and common wheat. Experiments were performed to evaluate the expression of stem-solidness primarily controlled by the *SSt1* locus on chromosome 3BL at the field level under commercial sowing densities. To improve the resolution of the *SSt1* interval on 3BL, QTL mapping was performed in two bi-parental mapping populations derived from the crosses Kofa/W9262-260D3 (durum wheat), and Lillian/Vesper (common wheat), using high density mapping using the iSelect 90K assay. Haplotype analysis was performed using markers associated with the peak of *SSt1* in a diverse set of durum and common wheat lines. Given the availability of several new genome assemblies in wheat, the map position of the peak *SSt1* markers were compared to their physical intervals on chromosome 3BL. The accompanying high confidence gene annotations allowed for whole transcriptome analysis of gene expression from the stem tissue sampled from several wheat cultivars from tissue sampled during the critical points of stem elongation when pith development occurs. The major conclusions from this thesis are as follows:

- Stem-solidness increased as sowing densities decreased, however, the stems of CDC Fortitude and AAC Raymore were significantly more solid across all sowing densities than common wheat cultivar Lillian.
- Lowering sowing densities may be beneficial to common wheat producers aiming to maximize resistance to the WSS, however, in durum wheat, WSS resistance is not likely to be affected.
- Optimal yield was achieved in all lines at sowing densities greater than 150 seeds m^{-2}.
- These results highlight the importance that both solid-stemmed cultivars and proper agronomics can offer to a holistic IPM strategy for WSS management.
- The position of the major QTL derived from S-615 in common wheat (*Qss.msub-3BL*) is coincident with the Biodur derived QTL in durum wheat (*SSt1*), and was designated throughout this thesis as *SSt1*.
- Several novel haplotypes were identified in common wheat and durum wheat diversity panels, including in several of the alternate sources of stem-solidness which included Golden Ball, and Janz.
- Over the course of this research, the expression of stem-solidness was almost always lower than the recommended threshold of 3.75 required to achieve effective resistance.

- Minor QTL were shown to synergistically enhance the expression of *SSt1* in durum and common wheat mapping populations, which suggests strategic parental selection for crossing coupled with phenotypic selection should be an effective strategy to maximize the effect of minor alleles and increase stem-solidness in common wheat.
- The physical interval of *SSt1* spans a physical interval of 827.5 – 830 Mb, and contains 32 high confidence genes based on the Svevo reference.
- One gene encoding a Dof transcription factor (*TraesCS3B01G60880*) was consistently differentially expressed across all hollow by solid comparisons.
- CNV in *TraesCS3B01G60880* was associated with stem-solidness in a diverse set of hexaploid and tetraploid cultivars.
- A large EMS induced deletion was identified in the mutant line M2.1184, which included the entire *TraesCS3B01G60880* gene, providing further evidence towards its involvement in conferring stem-solidness.

7.1. Future Research Directions

This research identified several genes contained within the *SSt1* interval, of which the strongest candidate encodes a putative Dof transcription factor (*TraesCS3B01G60880).* Additional functional validation work will be required to rule out the possibility of other genes as candidates, and to confirm the loss of phenotypic expression of pith when *TraesCS3B01G60880* is silenced. The best strategy moving forward will include: 1) knock-down the expression of candidate genes in *SSt1* carriers using Clustered Regularly Interspaced Short Palindromic Repeats (CRISPR-Cas9), or virus-induced gene silencing (VIGS) approaches and subsequent phenotypic evaluation; 2) complementation (add-back) of *TraesCS3B01G60880*, and other candidates in the mutant to restore the phenotype. Given that complementation can often result in multiple copies of the target gene being inserted into the host plant, it might be a particularly effective strategy given the CNV may be involved in conferring stem solidness. 3) Additional screening of EMS populations derived from solid-stemmed lines would also be an effective strategy to identify causal SNPs within the gene.

In this study, we co-localized the *SSt1* QTL to a common region on chromosome 3BL in durum and common wheat. Fine-mapping the locus in both species could further delineate the locus, point to a specific candidate gene, and rule out other gene candidates. Fine mapping work

is currently underway using an F2 mapping populations derived from the durum cross Kofa/W9262-260D3, and common wheat cross CDC Landmark/CDC Stanley.

The EMS mutant line M2.1184 carries a large deletion within the *SSt1* interval. Although there is a high likelihood that the deletion is responsible for the loss of phenotypic expression in this line, it could also be possible that the causal mutation is located elsewhere in the genome. To confirm the causal mutation does indeed derive from the deletion on 3BL, crosses were made between M2.1184 and the parent CDC Fortitude to generate an F2 fine-mapping population. This work is currently in progress.

Several studies, and some anecdotal evidence, have suggested stem-solidness is associated with a yield penalty, but this has not been sufficiently examined using the proper genetic experiments. The argument could be made either way. The sequestration of carbon in the stem could be diverting carbon from the developing grain. On the other hand, the remobilization of WSCs, and/or water, could contribute to grain fill under periods of stress. It remains unclear if the yield drag observed in many cultivars is caused by linkage drag from the inferior genetic background from which stem-solidness was derived. Further research is needed using NILs (common genetic background) differing only for the presence or absence of *SSt1*. These experiments are needed in durum and common wheat (spring and winter) to determine if this phenomenon is specific to a certain species or growth habit.

Further research is needed to better understand the relationship between different sources of stem-solidness. These include the two durum sources Biodur and Golden Ball, the common wheat lines S-615 and Conan, and the tall wheatgrass source *Thinopyrum ponticum*. Although the results presented throughout this thesis support the hypothesis that multiple sources of stem-solidness exist, it remains unclear whether stem-solidness arose independently, or can be traced back to a common ancestor. There are expression differences between sources with the durum sources being the strongest and most stable. Furthermore, some lines may exhibit temporal expression differences between early stem elongation and maturity. A better understanding of the different sources of stem-solidness could allow breeders to develop new cultivars with improved stem-solidness and resistance to the WSS.

The main goal of this thesis was to improve our understanding of solid-stem expression at the phenotypic and genotypic levels in durum and common wheat. The literature review should benefit researchers and breeders working on WSS resistance in wheat. One outcome of this

research was the identification of several markers from the 90K iSelect wheat array that could be suitable for marker-assisted selection in breeding programs. The haplotypes presented in Chapter 4 will allow breeders to select markers that are most useful across diverse genetic backgrounds to implement in marker-assisted selection schemes. In Chapter 3, we showed the expression of pith in durum wheat is stable across multiple environments, therefore marker-assisted selection for *SSt1* alone should be an effective strategy in durum wheat. A major problem that has yet to be addressed is the instability in pith expression in common wheat, and levels of pith expression below the threshold to achieve effective WSS resistance. While marker-assisted selection for *SSt1* should be generally effective for tracking in breeding programs, additional rounds of phenotypic selection for pith expression in multiple field nurseries is strongly encouraged. Selecting lines that produce the highest amounts of pith with greater stability across environments will help breeders exploit favourable genetic interactions between *SSt1* and minor loci. Future research is still needed to confirm the causal gene conferring stem-solidness, which will lead to a better of understanding of the biological mechanism conferring stem-solidness. Rapid advances in the field of wheat genomics will undoubtedly aid research on WSS resistance in the coming years.

8. REFERENCES

Ainslie, C.N. 1920. The western grass-stem sawfly, pp. 32. United States Department of Agriculture, Washington, D.C.

Avni, R., M. Nave, O. Barad, K. Baruch, S.O. Twardziok, H. Gundlach, I. Hale, M. Mascher, M. Spannagl, K. Wiebe, K.W. Jordan, G. Golan, J. Deek, B. Ben-Zvi, G. Ben-Zvi, A. Himmelbach, R.P. MacLachlan, A.G. Sharpe, A. Fritz, R. Ben-David, H. Budak, T. Fahima, A. Korol, J.D. Faris, A. Hernandez, M.A. Mikel, A.A. Levy, B. Steffenson, M. Maccaferri, R. Tuberosa, L. Cattivelli, P. Faccioli, A. Ceriotti, K. Kashkush, M. Pourkheirandish, T. Komatsuda, T. Eilam, H. Sela, A. Sharon, N. Ohad, D.A. Chamovitz, K.F.X. Mayer, N. Stein, G. Ronen, Z. Peleg, C.J. Pozniak, E.D. Akhunov, and A. Distelfeld. 2017. Wild emmer genome architecture and diversity elucidate wheat evolution and domestication. Science 357:93-97.

Badis, G., C. Saveanu, M. Fromont-Racine, and A. Jacquier. 2004. Targeted mRNA degradation by deadenylation-independent decapping. Molecular cell 15:5-15.

Beres, B.L., H.A. Carcamo, and J.R. Byers. 2007. Effect of wheat stem sawfly damage on yield and quality of selected Canadian spring wheat. Journal of Economic Entomology 100:79-87.

Beres, B.L., H.A. Carcamo, and E. Bremer. 2009. Evaluation of alternative planting strategies to reduce wheat stem sawfly (Hymenoptera: Cephidae) damage to spring wheat in the Northern Great Plains. Journal of Economic Entomology 102:2137-2145.

Beres, B.L., H.A. Carcamo, R.C. Yang, and D.M. Spaner. 2011a. Integrating spring wheat sowing density with variety selection to manage wheat stem sawfly. Agronomy Journal 103:1755-1764.

Beres, B.L., L.M. Dosdall, D.K. Weaver, H.A. Carcamo, and D.M. Spaner. 2011b. Biology and integrated management of wheat stem sawfly and the need for continuing research. Canadian Entomologist 143:105-125.

Beres, B.L., H.A. Carcamo, L.M. Dosdall, R.C. Yang, M.L. Evenden, and D.M. Spaner. 2011c. Do interactions between residue management and direct seeding system affect wheat stem sawfly and grain yield? Agronomy Journal 103:1635-1644.

Beres, B.L., B.D. Hill, H.A. Cárcamo, J.J. Knodel, D.K. Weaver, and R.D. Cuthbert. 2017. An artificial neural network model to predict wheat stem sawfly cutting in solid-stemmed wheat cultivars. Canadian Journal of Plant Science 97:329-336.

Beres, B.L., R.H. McKenzie, H.A. Carcamo, L.M. Dosdall, M.L. Evenden, R. Yang, and D.M. Spaner. 2012. Influence of seeding rate, nitrogen management, and micronutrient blend applications on pith expression in solid-stemmed spring wheat. Crop Science 52:1316-1329.

Beres, B.L., H.A. Cárcamo, J.R. Byers, F.R. Clarke, C.J. Pozniak, S.K. Basu, and R.M. DePauw. 2013a. Host plant interactions between wheat germplasm source and wheat stem sawfly *Cephus cinctus* Norton (Hymenoptera: Cephidae) I. Commercial cultivars. Canadian Journal of Plant Science 93:607-617.

Beres, B.L., H.A. Cárcamo, J.R. Byers, F.R. Clarke, Y. Ruan, C.J. Pozniak, S.K. Basu, and R.M. DePauw. 2013b. Host plant interactions between wheat germplasm source and wheat stem sawfly *Cephus cinctus* Norton (Hymenoptera: Cephidae) II. Other germplasm. Canadian Journal of Plant Science. 93:1169.

Beres, B.L., H.A. Carcamo, D.K. Weaver, L.M. Dosdal, M.L. Evenden, B.D. Hill, R.H. McKenzie, R.C. Yang, and D.M. Spaner. 2011d. Integrating the building blocks of agronomy and biocontrol into an IPM strategy for wheat stem sawfly. Prairie Soils and Crops 4:54-65.

Bolger, A.M., M. Lohse, and B. Usadel. 2014. Trimmomatic: a flexible trimmer for Illumina sequence data. Bioinformatics 30:2114-2120.

Bozzini, A., and S. Avanzi. 1962. Solid stem: A radiation induced mutation in *Triticum durum* Desf. Caryologia 15:525-535.

Bradshaw, J., S. Harvey, and C. McCullough. 2014. Nebraska wheat stem sawfly report - 2014 [Online] http://agronomy.unl.edu/Baenziger/Nebraska%20Wheat%20Stem%20Sawfly%20Project%20Report%202014%20-%20final.pdf.

Brenchley, R., M. Spannagl, M. Pfeifer, G.L.A. Barker, R. D'Amore, A.M. Allen, N. McKenzie, M. Kramer, A. Kerhornou, D. Bolser, S. Kay, D. Waite, M. Trick, I. Bancroft, Y. Gu, N. Huo, M.-C. Luo, S. Sehgal, B. Gill, S. Kianian, O. Anderson, P. Kersey, J. Dvorak, W.R. McCombie, A. Hall, K.F.X. Mayer, K.J. Edwards, M.W. Bevan, and N. Hall. 2012. Analysis of the bread wheat genome using whole-genome shotgun sequencing. Nature 491:705-710.

Carcamo, H.A., B.L. Beres, F. Clarke, R.J. Byers, H.H. Mundel, K. May, and R. DePauw. 2005. Influence of plant host quality on fitness and sex ratio of the wheat stem sawfly (Hymenoptera : Cephidae). Environmental Entomology 34:1579-1592.

Cárcamo, H.A., B.L. Beres, C.E. Herle, H. McLean, and S. McGinne. 2011. Solid-stemmed wheat does not affect overwintering mortality of the wheat stem sawfly, *Cephus cinctus*. Journal of Insect Science 11:129.

Cavanagh, C.R., S.M. Chao, S.C. Wang, B.E. Huang, S. Stephen, S. Kiani, K. Forrest, C. Saintenac, G.L. Brown-Guedira, A. Akhunova, D. See, G.H. Bai, M. Pumphrey, L. Tomar, D.B. Wong, S. Kong, M. Reynolds, M.L. da Silva, H. Bockelman, L. Talbert, J.A. Anderson, S. Dreisigacker, S. Baenziger, A. Carter, V. Korzun, P.L. Morrell, J. Dubcovsky, M.K. Morell, M.E. Sorrells, M.J. Hayden, and E. Akhunov. 2013. Genome-wide comparative diversity uncovers multiple targets of selection for improvement in hexaploid wheat landraces and cultivars. Proceedings of the National Academy of Sciences of the United States of America 110:8057-8062.

Chen, Y., B.F. Carver, S. Wang, F. Zhang, and L. Yan. 2009. Genetic loci associated with stem elongation and winter dormancy release in wheat. Theoretical and Applied Genetics 118:881-889.

Choulet, F., A. Alberti, S. Theil, N. Glover, V. Barbe, J. Daron, L. Pingault, P. Sourdille, A. Couloux, E. Paux, P. Leroy, S. Mangenot, N. Guilhot, J. Le Gouis, F. Balfourier, M. Alaux, V. Jamilloux, J. Poulain, C. Durand, A. Bellec, C. Gaspin, J. Safar, J. Dolezel, J. Rogers, K. Vandepoele, J.M. Aury, K. Mayer, H. Berges, H. Quesneville, P. Wincker, and C. Feuillet. 2014. Structural and functional partitioning of bread wheat chromosome 3B. Science 345.

CIMMYT. 2005. Laboratory Protocols: CIMMYT applied molecular genetics laboratory. Third Edition ed. CIMMYT, Mexico, D.F.

Clark, J., C. Ball, and J. Martin. 1922. Classification of american wheat varieties, pp. 310. United States Department of Agriculture, Washington, D.C. .

Clarke, F.R., J.M. Clarke, and R.E. Knox. 2002. Inheritance of stem solidness in eight durum wheat crosses. Canadian Journal of Plant Science 82:661-664.

Clarke, F.R., R.M. DePauw, and T. Aung. 2005a. Registration of sawfly resistant hexaploid spring wheat germplasm lines derived from durum. Crop Science 45:1665.

Clarke, J., E. De Ambrogio, R. Hare, and P. Roument. 2012. Genetics and breeding of durum wheat, *In* M. Sissons, et al., eds. Durum Wheat: Chemistry and Technology, 2nd Ed. ed. AACC International, St. Paul, MN, USA.

Clarke, J.M., T.N. McCaig, R.M. DePauw, R.E. Knox, F.R. Clarke, M.R. Fernandez, and N.P. Ames. 2005b. Strongfield durum wheat. Canadian Journal of Plant Science 85:651-654.

Cook, J.P., D.M. Wichman, J.M. Martin, P.L. Bruckner, and L.E. Talbert. 2004. Identification of microsatellite markers associated with a stem solidness locus in wheat. Crop Science 44:1397-1402.

Cook, J.P., N.K. Blake, H.Y. Heo, J.M. Martin, D.K. Weaver, and L.E. Talbert. 2017. Phenotypic and haplotype diversity among tetraploid and hexaploid wheat accessions with potentially novel insect resistance genes for wheat stem sawfly. Plant Genome 10.

Criddle, N. 1923. The life habits of *Cephus Cinctus* Norton in Manitoba. The Canadian Entomologist 55:1-4.

Delaney, K.J., D.K. Weaver, and R.K.D. Peterson. 2010. Photosynthesis and yield reductions from wheat stem sawfly (Hymenoptera: Cephidae): interactions with wheat solidness, water stress, and phosphorus deficiency. Journal of Economic Entomology 103:516-524.

Depauw, R.M., and D.W.L. Read. 1982. The effect of nitrogen and phosphorus on the expression of stem solidness in Canuck wheat at 4 Locations in Southwestern Saskatchewan. Canadian Journal of Plant Science 62:593-598.

DePauw, R.M., J.G. McLeod, J.M. Clarke, T.N. McCaig, M.R. Fernandez, and R.E. Knox. 1994. AC Eatonia hard red spring wheat. Canadian Journal of Plant Science 74:821.

DePauw, R.M., J.M. Clarke, R.E. Knox, M.R. Fernandez, T.N. McCaig, and J.G. McLeod. 2000. AC Abbey hard red spring wheat. Canadian Journal of Plant Science 80:123.

DePauw, R.M., T.F. Townley-Smith, G. Humphreys, R.E. Knox, F.R. Clarke, and J.M. Clarke. 2005. Lillian hard red spring wheat. Canadian Journal of Plant Science 85:397.

DePauw, R.M., R.E. Knox, F.R. Clarke, H. Wang, M.R. Fernandez, J.M. Clarke, and T.N. McCaig. 2007. Shifting undesirable correlations. Euphytica 157:409-415.

Dobin, A., C.A. Davis, F. Schlesinger, J. Drenkow, C. Zaleski, S. Jha, P. Batut, M. Chaisson, and T.R. Gingeras. 2013. STAR: ultrafast universal RNA-seq aligner. Bioinformatics 29:15-21.

Eckroth, E.G., and F.H. McNeal. 1953. Association of plant characters in spring wheat with resistance to the wheat stem sawfly. Agronomy Journal 45:400.

Edgar, R.C. 2004. MUSCLE: multiple sequence alignment with high accuracy and high throughput. Nucleic Acids Res 32:1792-7.

FAO. 2017. World food situation [Online] http://www.fao.org/worldfoodsituation/csdb/en/.

Ford, M.A., R.D. Blackwell, M.L. Parker, and R.B. Austin. 1979. Associations between stem solidity, soluble carbohydrate accumulation and other characters in wheat. Annals of Botany 44:731-738.

Funk, C.C., and M.E. Brown. 2009. Declining global per capita agricultural production and warming oceans threaten food security. Food Security 1:271-289.

Grains Canada. 2017a. Grain varieties by acreage insured [Online] https://www.grainscanada.gc.ca/statistics-statistiques/variety-variete/varieties-en.htm.

Grains Canada. 2017b. Canadian wheat class modernization [Online] http://www.grainscanada.gc.ca/consultations/classes-en.htm.

Grant, M.N., and H. McKenzie. 1964. Registration of Chinook wheat. Crop science 4:235 p.
Hassinen, V.H., A.I. Tervahauta, H. Schat, and S.O. Karenlampi. 2011. Plant metallothioneins--metal chelators with ROS scavenging activity? Plant Biology 13:225-32.
Hayat, M.A., J.M. Martin, S.P. Lanning, C.F. McGuire, and L.E. Talbert. 1995. Variation for stem solidness and its association with agronomic traits in spring wheat. Canadian Journal of Plant Science 75:775-780.
Henry, I.M., U. Nagalakshmi, M.C. Lieberman, K.J. Ngo, K.V. Krasileva, H. Vasquez-Gross, A. Akhunova, E. Akhunov, J. Dubcovsky, T.H. Tai, and L. Comai. 2014. Efficient genome-wide detection and cataloging of EMS-induced mutations using exome capture and next-generation sequencing. Plant Cell 26:1382-1397.
Heun, M., R. Schäfer-Pregl, D. Klawan, R. Castagna, M. Accerbi, B. Borghi, and F. Salamini. 1997. Site of Einkorn Wheat Domestication Identified by DNA Fingerprinting. Science 278:1312-1314.
Holmes, N.D. 1954. Food relations of the wheat stem sawfly, *Cephus cinctus* Nort. (Hymenoptera: Cephidae). The Canadian Entomologist 86:159-167.
Holmes, N.D. 1977. The effect of the wheat stem sawfly, *Cephus cinctus* (Hymenoptera: Cephidae), on the yield and quality of wheat. Canadian Entomologist 109:1591-1598.
Holmes, N.D. 1979. The wheat stem sawfly, pp. 2-13 Proceedings of the twenty-sixth annual meeting of the Entomological Society of Alberta, Lethbridge, Alberta.
Holmes, N.D. 1984. The effect of light on the resistance of hard red spring wheats to the wheat stem sawfly, *Cephus cinctus* (Hymenoptera, Cephidae). Canadian Entomologist 116:677-684.
Holmes, N.D., and C.W. Farstad. 1956. Effects of field exposure on immature stages of the wheat stem sawfly, *Cephus Cinctus* Nort. (Hymenoptera: Cephidae). Canadian Journal of Agricultural Science 36:196-202.
Holmes, N.D., and L.K. Peterson. 1957. Effect of continuous rearing in Rescue wheat on survival of the wheat stem sawfly, *Cephus cinctus* Nort. (Hymenoptera: Cephidae). Canadian Entomologist 89:363-364.
Holmes, N.D., and L.K. Peterson. 1960. The influence of the host on oviposition by the wheat stem sawfly, *Cephus cinctus* Nort. (Hymenoptera: Cephidae). Canadian Journal of Plant Science 40:29-46.
Holmes, N.D., and L.K. Peterson. 1961. Resistance of spring wheats to the wheat stem sawfly, *Cephus cinctus* Nort. (Hymenoptera: Cephidae): I. Resistance to the egg. The Canadian Entomologist 93:250-260.
Holmes, N.D., and L.K. Peterson. 1962. Resistance of spring wheats to the wheat stem sawfly, *Cephus cinctus* Nort. (Hymenoptera: Cephidae) II. Resistance to the larva. The Canadian Entomologist 94:348-365.
Holmes, N.D., and L.K. Peterson. 1963. Heptachlor as a systemic insecticide against the wheat stem sawfly, *Cephus cinctus* Nort. The Canadian Entomologist 95:792-796.
Houshmand, S., R.E. Knox, F.R. Clarke, and J.M. Clarke. 2007. Microsatellite markers flanking a stem solidness gene on chromosome 3BL in durum wheat. Molecular Breeding 20:261-270.
Housley, T.L. 2000. Role of fructans redistributed from vegetative tissues in grain filling of wheat and barley. Developments in Crop Science 26:207-221.

Huberman, M., E. Pressman, and M.J. Jaffe. 1993. Pith autolysis in plants: IV. The activity of polygalacturonase and cellulase during drought stress induced pith autolysis. Plant and Cell Physiology 34:795-801.

Ivie, M.A. 2001. On the geographic origin of the wheat stem sawfly (Hymenoptera: Cephidae): A new hypothesis of introduction from Northeastern Asia. American Entomologist 47:84-97.

Jackson, B.N., S. Aluru, and P.S. Schnable. 2005. Consensus genetic maps: A graph theoretic approach. 2005 IEEE Computational Systems Bioinformatics Conference, Proceedings:35-43.

Jia, J., S. Zhao, X. Kong, Y. Li, G. Zhao, W. He, R. Appels, M. Pfeifer, Y. Tao, X. Zhang, R. Jing, C. Zhang, Y. Ma, L. Gao, C. Gao, M. Spannagl, K.F. Mayer, D. Li, S. Pan, F. Zheng, Q. Hu, X. Xia, J. Li, Q. Liang, J. Chen, T. Wicker, C. Gou, H. Kuang, G. He, Y. Luo, B. Keller, Q. Xia, P. Lu, J. Wang, H. Zou, R. Zhang, J. Xu, J. Gao, C. Middleton, Z. Quan, G. Liu, J. Wang, H. Yang, X. Liu, Z. He, L. Mao, and J. Wang. 2013. *Aegilops tauschii* draft genome sequence reveals a gene repertoire for wheat adaptation. Nature 496:91-5.

Jordan, K.W., S.C. Wang, Y.N. Lun, L.J. Gardiner, R. MacLachlan, P. Hucl, K. Wiebe, D. Wong, K.L. Forrest, A.G. Sharpe, C.H.D. Sidebottom, N. Hall, C. Toomajian, T. Close, J. Dubcovsky, A. Akhunova, L. Talbert, U.K. Bansal, H.S. Bariana, M.J. Hayden, C. Pozniak, J.A. Jeddeloh, A. Hall, and E. Akhunov. 2015. A haplotype map of allohexaploid wheat reveals distinct patterns of selection on homoeologous genomes. Genome Biology 16.

Kassa, M.T., S. Haas, E. Schliephake, C. Lewis, F.M. You, C.J. Pozniak, I. Kramer, D. Perovic, A.G. Sharpe, P.R. Fobert, M. Koch, I.L. Wise, P. Fenwick, S. Berry, J. Simmonds, D. Hourcade, P. Senellart, L. Duchalais, O. Robert, J. Forster, J.B. Thomas, W. Friedt, F. Ordon, C. Uauy, and C.A. McCartney. 2016. A saturated SNP linkage map for the orange wheat blossom midge resistance gene *Sm1*. Theoretical and Applied Genetics 129:1507-1517.

Kemp, H.J. 1934. Studies of solid stem wheat varieties in relation to wheat stem sawfly control. Scientific Agriculture 15:30-38.

Knodel, J.J., P.B. Beauzay, E.D. Eriksmoen, and J.D. Pederson. 2009. Pest management of wheat stem maggot (Diptera: Chloropidae) and wheat stem sawfly (Hymenoptera: Cephidae) using insecticides in spring wheat. Journal of Agricultural and Urban Entomology 26:183-197.

Knott, D.R. 1995. Durum wheat. Pages 67-81 in A. E. Slinkard and D. R. Knott, eds. Harvest of gold - The history of field crop breeding in Canada. Saskatoon, Sask. University Extension Press, University of Saskatchewan, Saskatoon, Sask.

Kosambi, D.D. 1943. The estimation of map distances from recombination values. Annals of Eugenics 12:172-175.

Lanning, S.P., P. Fox, J. Elser, J.M. Martin, N.K. Blake, and L.E. Talbert. 2006. Microsatellite markers associated with a secondary stem solidness locus in wheat. Crop Science 46:1701-1703.

Larson, R.I. 1959a. Cytogenetics of solid stem in common wheat. I. Monosomic F2 analysis of the variety S-615. Canadian Journal of Botany 37:135-56.

Larson, R.I. 1959b. Inheritance of the type of solid stem in Golden Ball (*Triticum durum*). I. Early generations of a hybrid with Rescue *T. aestivum*. Canadian Journal of Botany 37:889-96.

Larson, R.I., and M.D. Macdonald. 1959. Cytogenetics of solid stem in common wheat. II. Stem solidness of monosomic lines of the variety S-615. Canadian Journal of Botany 37:365-378.

Larson, R.I., and M.D. Macdonald. 1962. Cytogenetics of solid stem in common wheat. IV. Aneuploid lines of the variety Rescue. Canadian Journal of Genetics and Cytology 4:97-104.

Larson, R.I., and M.D. Macdonald. 1963. Inheritance of the type of solid stem in Golden Ball (*Triticum durum*). III. The effect of selection for solid stem beyond F5 in hexaploid segregates of the hybrid Rescue (*T. aestivum*) x Golden Ball. Canadian Journal of Genetics and Cytology 5:437-44.

Larson, R.I., and Macdonald. 1966. Cytogenetics of solid stem in common wheat .V. Lines of S-615 with whole chromosome substitutions from Apex. Canadian Journal of Genetics and Cytology 8:64-70.

Lebsock, K.L., and E.J. Koch. 1968. Variation of stem-solidness in wheat. Crop Science 8:225-229.

Littell, R.C., G.A. Milliken, W.W. Stroup, and R.D. Wolfinger. 2006. SAS® System for Mixed Models. Second ed. SAS Institute Inc, Cary, NC.

Lorieux, M. 2012. MapDisto: fast and efficient computation of genetic linkage maps. Molecular Breeding 30:1231-1235.

Love, M.I., W. Huber, and S. Anders. 2014. Moderated estimation of fold change and dispersion for RNA-seq data with DESeq2. Genome Biology 15:1-21.

Luginbill, P., and F.H. McNeal. 1959. Influence of seeding density and row spacings on the resistance of spring wheats to the wheat stem sawfly. Journal of Economic Entomology 51:804-808.

Maccaferri, M., A. Ricci, S. Salvi, S.G. Milner, E. Noli, P.L. Martelli, R. Casadio, E. Akhunov, S. Scalabrin, V. Vendramin, K. Ammar, A. Blanco, F. Desiderio, A. Distelfeld, J. Dubcovsky, T. Fahima, J. Faris, A. Korol, A. Massi, A.M. Mastrangelo, M. Morgante, C. Pozniak, A. N'Diaye, S. Xu, and R. Tuberosa. 2015. A high-density, SNP-based consensus map of tetraploid wheat as a bridge to integrate durum and bread wheat genomics and breeding. Plant Biotechnology Journal 13:648-663.

Macedo, T.B., D.K. Weaver, and R.K.D. Peterson. 2007. Photosynthesis in wheat at the grain filling stage is altered by larval wheat stem sawfly (Hymenoptera: Cephidae) injury and reduced water availability. Journal of Entomological Science 42:228-238.

Macedo, T.B., R.K.D. Peterson, D.K. Weaver, and W.L. Morrill. 2005. Wheat stem sawfly, *Cephus cinctus* Norton, impact on wheat primary metabolism: an ecophysiological approach. Environmental Entomology 34:719-726.

Mayer, K.X., International Wheat Genome Sequencing Consortium (IWGSC), et al. 2014. A chromosome-based draft sequence of the hexaploid bread wheat (*Triticum aestivum*) genome. Science 345.

McCallum, B.D., and R.M. DePauw. 2008. A review of wheat cultivars grown in the Canadian prairies. Canadian Journal of Plant Science 88:649-677.

McKenzie, H. 1965. Inheritance of sawfly reaction and stem solidness in spring wheat crosses: stem solid-ness. Canadian Journal of Plant Science 45:591-600.

McMaster, G.S. 1997. Phenology, development, and growth of the wheat (*Triticum aestivum* L) shoot apex: A review. Advances in Agronomy 59:63-118.

McNeal, F.H. 1961. Segregation for stem solidness in a *Triticum aestivum* * *T.durum* wheat cross. Crop Science 1:111-114.
McNeal, F.H., and L.E. Wallace. 1967. Stem-solidness stability in spring wheat, Triticum aestivum L. Em. Thell. Agron. J. 59:472-3.
McNeal, F.H., and M.A. Berg. 1979. Stem solidness and its relationship to grain yield in 17 spring wheat crosses. Euphytica 28:89-91.
McNeal, F.H., C.A. Watson, M.A. Berg, and L.E. Wallace. 1965. Relationship of stem solidness to yield and lignin content in wheat selections. Agronomy Journal 57:20-21.
McNeal, F.H., K.L. Lebsock, M.A. Berg, and L.E. Wallace. 1966. Stem-solidness in parents and crosses of Rescue with 25 foreign wheats *Triticum aestivum* L Em Thell. Crop Science 6.
Morrill, W.L., J.W. Gabor, and G.D. Kushnak. 1992a. Wheat stem sawfly (Hymenoptera: Cephidae): damage and detection. Journal of Economic Entomology 85:2413-2417.
Morrill, W.L., J.W. Gabor, E.A. Hockett, and G.D. Kushnak. 1992b. Wheat stem sawfly (Hymenoptera: Cephidae) resistance in winter wheat. Journal of Economic Entomology 85:2008-2011.
Morrill, W.L., G.D. Kushnak, P.L. Bruckner, and J.W. Gabor. 1994. Wheat stem sawfly (Hymenoptera: Cephidae). Damage, rates of parasitism, and overwinter survival in resistant wheat lines. Journal of Economic Entomology 87:1373-1376.
MSU. 2015. Insecticide now available to fight wheat stem sawfly in Montana [Online] http://www.montana.edu/news/15597/insecticide-now-available-to-fight-wheat-stem-sawfly-in-montana (verified 10/18/2017).
Naora, H. 1999. Involvement of ribosomal proteins in regulating cell growth and apoptosis: translational modulation or recruitment for extraribosomal activity? Immunology and Cell Biology 77:197-205.
Naora, H., I. Takai, M. Adachi, and H. Naora. 1998. Altered cellular responses by varying expression of a ribosomal protein gene: sequential coordination of enhancement and suppression of ribosomal protein S3a gene expression induces apoptosis. The Journal of Cell Biology 141:741-53.
Nelson, W.A., and C.W. Farstad. 2012. Biology of *Bracon cephi* (Gahan) (Hymenoptera: Braconidae), An important native Parasite of the wheat stem sawfly, *Cephus cinctus* Nort. (Hymenoptera: Cephidae), in Western Canada. The Canadian Entomologist 85:103-107.
Nilsen, K.T., J.M. Clarke, B.L. Beres, and C.J. Pozniak. 2016. Sowing density and cultivar effects on pith expression in solid-stemmed durum wheat. Agronomy Journal 108:219-228.
Nilsen, K.T., A. N'Diaye, P.R. MacLachlan, J.M. Clarke, Y. Ruan, R.D. Cuthbert, R.E. Knox, K. Wiebe, A.T. Cory, S. Walkowiak, B.L. Beres, R.J. Graf, F.R. Clarke, A.G. Sharpe, A. Distelfeld, and C.J. Pozniak. 2017. High density mapping and haplotype analysis of the major stem-solidness locus *SSt1* in durum and common wheat. PLOS ONE 12:e0175285.
Oiestad, A.J., J.M. Martin, J. Cook, A.C. Varella, and M.J. Giroux. 2017. Identification of candidate genes responsible for stem pith production using expression analysis in solid-stemmed wheat. The Plant Genome 10:1-10.
Peng, J.H., D. Sun, and E. Nevo. 2011. Domestication evolution, genetics and genomics in wheat. Molecular Breeding 28:281-301.
Pertea, M., D. Kim, G.M. Pertea, J.T. Leek, and S.L. Salzberg. 2016. Transcript-level expression analysis of RNA-seq experiments with HISAT, StringTie and Ballgown. Nature Protocols 11:1650-1667.

Platt, A., and R.I. Larson. 1944. An attempt to transfer solid-stem from *Triticum durum* to *T. vulgare* by hybridization. Scientific Agriculture 24:214-220.
Platt, A., C.W. Farstad, and J.A. Callenbach. 1948. The reaction of Rescue wheat to sawfly damage. Scientific Agriculture 28:154-161.
Platt, A.W. 1941. The influence of some environmental factors on the expression of the solid stem character in certain wheat varieties. Scientific Agriculture 22:139-51.
Platt, A.W., J.G. Darroch, and H.J. Kemp. 1941. The inheritance of solid stem and certain other characters in crosses between varieties of *Triticum vulgare*. Scientific Agriculture 22:216-224.
Pozniak, C.J., K. Nilsen, J.M. Clarke, and B.L. Beres. 2015. CDC Fortitude durum wheat. Canadian Journal of Plant Science 95:1013-1019.
Putnam, L.G. 1942. A study of the inheritance of solid stems in some tetraploid wheats. Scientific Agriculture 22:594-607.
Ray, D.K., N.D. Mueller, P.C. West, and J.A. Foley. 2013. Yield trends are insufficient to double global crop production by 2050. PLOS ONE 8:e66428.
Roberts, D.W.A., and C. Tyrrell. 1961. Sawfly resistance in wheat : IV. Some effects of light intensity on resistance. Canadian Journal of Plant Science 41:457-465.
Rozen, S., and H. Skaletsky. 2000. Primer3 on the WWW for general users and for biologist programmers. Methods in Molecular Biology 132:365-86.
Runyon, J.B., W.L. Morrill, D.K. Weaver, and P.R. Miller. 2002. Parasitism of the wheat stem sawfly (Hymenoptera: Cephidae) by *Bracon cephi* and *B. lissogaster* (Hymenoptera: Braconidae) in wheat fields bordering tilled and untilled fallow in Montana. Journal of Economic Entomology 95:1130-1134.
Runyon, J.B., R.L. Hurley, W.L. Morrill, and D.K. Weaver. 2012. Distinguishing adults of *Bracon cephi* and *Bracon lissogaster* (Hymenoptera: Braconidae), parasitoids of the wheat stem sawfly (Hymenoptera: Cephidae). The Canadian Entomologist 133:215-217.
Ruuska, S.A., G.J. Rebetzke, A.F. van Herwaarden, R.A. Richards, N.A. Fettell, L. Tabe, and C.L.D. Jenkins. 2006. Genotypic variation in water-soluble carbohydrate accumulation in wheat. Functional Plant Biology 33:799-809.
Saint Pierre, C., R. Trethowan, and M. Reynolds. 2010. Stem solidness and its relationship to water-soluble carbohydrates: association with wheat yield under water deficit. Functional Plant Biology 37:166-174.
Sangwan, I., and M.R. O'Brian. 2002. Identification of a soybean protein that interacts with GAGA element dinucleotide repeat DNA. Plant Physiology 129:1788-1794.
Saxton, A. 1998. A macro for converting mean separation output to letter groupings in Proc Mixed. In Proc. 23rd SAS Users Group Intl., SAS Institute, Cary, NC, pp1243-1246.:1243-1246.
Seamans, H.L. 1944. The effect of wheat stem sawfly (*Cephus cinctus*) on the heads and grain of infested stems. Seventy-fifth Annual Report of the Entomolological. Society of Ontario, 75: 10–15.
Seamans, H.L. 1945. A preliminary report on the climatology of the wheat stem sawfly (*Cephus cinctus* Nort.) on the Canadian Prairies. Scientific Agriculture 25:432-457.
Sharbatkhari, M., Z.-S. Shobbar, S. Galeshi, and B. Nakhoda. 2016. Wheat stem reserves and salinity tolerance: molecular dissection of fructan biosynthesis and remobilization to grains. Planta 244:191-202.

Sherman, J.D., D.K. Weaver, M.L. Hofland, S.E. Sing, M. Buteler, S.P. Lanning, Y. Naruoka, F. Crutcher, N.K. Blake, J.M. Martin, P.F. Lamb, G.R. Carlson, and L.E. Talbert. 2010. Identification of novel QTL for sawfly resistance in wheat. Crop Science 50:73-86.

Sherman, J.D., N.K. Blake, J.M. Martin, K.D. Kephart, J. Smith, D.R. Clark, M.L. Hofland, D.K. Weaver, S.P. Lanning, H.-Y. Heo, M. Pumphrey, J. Chen, and L.E. Talbert. 2015. Agronomic impact of a stem solidness gene in near-isogenic lines of wheat. Crop Science 55:514-520.

Shewry, P.R. 2009. Wheat. Journal of Experimental Botany 60:1537-53.

Singh, A.K., R.M. DePauw, R.E. Knox, J.M. Clarke, T.N. McCaig, R.D. Cuthbert, and Y. Ruan. 2016. AAC Cabri durum wheat. Canadian Journal of Plant Science 97:135-143.

Singh, A.K., J.M. Clarke, R.E. Knox, R.M. DePauw, T.N. McCaig, R.D. Cuthbert, F.R. Clarke, and M.R. Fernandez. 2014. AAC Raymore durum wheat. Canadian Journal of Plant Science 94:1289-1296.

Singh, R.P., D.P. Hodson, J. Huerta-Espino, Y. Jin, S. Bhavani, P. Njau, S. Herrera-Foessel, P.K. Singh, S. Singh, and V. Govindan. 2011. The emergence of Ug99 races of the stem rust fungus is a threat to world wheat production. Annual Review of Phytopathology 49:465-481.

Skirycz, A., A. Radziejwoski, W. Busch, M.A. Hannah, J. Czeszejko, M. Kwasniewski, M.I. Zanor, J.U. Lohmann, L. De Veylder, I. Witt, and B. Mueller-Roeber. 2008. The DOF transcription factor OBP1 is involved in cell cycle regulation in *Arabidopsis thaliana*. The Plant Journal 56:779-92.

Somers, D.J., P. Isaac, and K. Edwards. 2004. A high-density microsatellite consensus map for bread wheat (*Triticum aestivum* L.). Theoretical and Applied Genetics 109:1105-1114.

Spiegel, B. 2014. Wheat stem sawflies head into winter wheat states [Online] http://www.agriculture.com/crops/wheat/production/wheat-stem-sawflies-head-into-winter_145-ar45791.

Statistics Canada. 2017. Production of principal field crops, July 2017 [Online] http://www.statcan.gc.ca/daily-quotidien/170831/dq170831c-eng.htm.

Steffens, B., and M. Sauter. 2009. Epidermal cell death in rice is confined to cells with a distinct molecular identity and is mediated by ethylene and H2O2 through an autoamplified signal pathway. Plant Cell 21:184-96.

Stone, J.M., and J.C. Walker. 1995. Plant protein kinase families and signal transduction. Plant Physiology 108:451-457.

Supek, F., M. Bošnjak, N. Škunca, and T. Šmuc. 2011. REVIGO Summarizes and Visualizes Long Lists of Gene Ontology Terms. PLOS ONE 6:e21800.

Taegar, A., S.M. Blank, and A.D. Liston. 2010. World catalog of Symphyta (Hymenoptera) Magnolia Press.

Takagi, M., M.J. Absalon, K.G. McLure, and M.B. Kastan. 2005. Regulation of p53 translation and induction after DNA damage by ribosomal protein L26 and nucleolin. Cell 123:49-63.

Talbert, L.E., J.D. Sherman, M.L. Hofland, S.P. Lanning, N.K. Blake, R. Grabbe, P.F. Lamb, J.M. Martin, and D.K. Weaver. 2014. Resistance to *Cephus cinctus* Norton, the wheat stem sawfly, in a recombinant inbred line population of wheat derived from two resistance sources. Plant Breeding 133:427-432.

Tester, M., and P. Langridge. 2010. Breeding technologies to increase crop production in a changing world. Science 327:818-822.

Uauy, C. 2017. Wheat genomics comes of age. Current Opinion in Plant Biology 36:142-148.

Varella, A.C., L.E. Talbert, M.L. Hofland, M. Buteler, J.D. Sherman, N.K. Blake, H.-Y. Heo, J.M. Martin, and D.K. Weaver. 2016. Alleles at a quantitative trait locus for stem solidness in wheat affect temporal patterns of pith expression and level of resistance to the wheat stem sawfly. Plant Breeding 135:546-551.

Varella, A.C., D.K. Weaver, J.D. Sherman, N.K. Blake, H.Y. Heo, J.R. Kalous, S. Chao, M.L. Hofland, J.M. Martin, K.D. Kephart, and L.E. Talbert. 2015. Association analysis of stem solidness and wheat stem sawfly resistance in a panel of North American spring wheat germplasm. Crop Science 55:2046-2055.

Voorrips, R.E. 2002. MapChart: software for the graphical presentation of linkage maps and QTLs. The Journal of Heredity 93:77-78.

Wallace, L.E., and F.H. McNeal. 1966. Stem sawflies of economic importance in grain crops in the United States, pp. 1-50, *In* U. S. D. o. Agriculture, (ed.), Vol. Technical Bulletin No. 1350, Washington, D.C.

Wallace, L.E., F.H. Mcneal, and M.A. Berg. 1973. Minimum stem solidness required in wheat for resistance to wheat stem sawfly Hymenoptera-Cephidae. Journal of Economic Entomology 66:1121-1123.

Wang, S.C., D.B. Wong, K. Forrest, A. Allen, S.M. Chao, B.E. Huang, M. Maccaferri, S. Salvi, S.G. Milner, L. Cattivelli, A.M. Mastrangelo, A. Whan, S. Stephen, G. Barker, R. Wieseke, J. Plieske, M. Lillemo, D. Mather, R. Appels, R. Dolferus, G. Brown-Guedira, A. Korol, A.R. Akhunova, C. Feuillet, J. Salse, M. Morgante, C. Pozniak, M.C. Luo, J. Dvorak, M. Morell, J. Dubcovsky, M. Ganal, R. Tuberosa, C. Lawley, I. Mikoulitch, C. Cavanagh, K.J. Edwards, M. Hayden, E. Akhunov, and I.W.G. Sequencing. 2014. Characterization of polyploid wheat genomic diversity using a high-density 90 000 single nucleotide polymorphism array. Plant Biotechnology Journal 12:787-796.

Warner, J.R., and K.B. McIntosh. 2009. How common are extra-ribosomal functions of ribosomal proteins? Molecular Cell 34:3-11.

Weaver, D.K., S.E. Sing, J.B. Runyon, and W.L. Morrill. 2004. Potential impact of cultural practices on wheat stem sawfly (Hymenoptera: Cephidae) and associated parasitoids. Journal of Agricultural and Urban Entomology 21:271-287.

Weaver, D.K., C. Nansen, J.B. Runyon, S.E. Sing, and W.L. Morrill. 2005. Spatial distributions of *Cephus cinctus* Norton (Hymenoptera: Cephidae) and its braconid parasitoids in Montana wheat fields. Biological Control 34:1-11.

Weiss, M.J., and W.L. Morrill. 1992. Wheat stem sawfly (Hymenoptera: Cephidae) revisited. American Entomologist 38:241-245.

Weiss, M.J., N.R. Riveland, L.L. Reitz, and T.C. Olson. 1990. Influence of resistant and susceptible cultivar blends of hard red spring wheat on wheat stem sawfly (Hymenoptera: Cephidae) damage and wheat quality parameters. Journal of Economic Entomology 83:255-259.

Wheat Initiative, W. 2016. 10 wheat genomes project [Online] http://www.wheatinitiative.org/activities/associated-programmes/10-wheat-genomes-project.

Whitechurch, E.M., G.A. Slafer, and D.J. Miralles. 2007. Variability in the duration of stem elongation in wheat and barley genotypes. Journal of Agronomy and Crop Science 193:138-145.

Wu, T.D., and C.K. Watanabe. 2005. GMAP: a genomic mapping and alignment program for mRNA and EST sequences. Bioinformatics 21:1859-1875.

Wu, Y., P.R. Bhat, T.J. Close, and S. Lonardi. 2008. Efficient and accurate construction of genetic linkage maps from the minimum spanning tree of a graph. PLOS Genetics 4:e1000212.

Xu, P., H. Chen, L. Ying, and W. Cai. 2016. AtDOF5.4/OBP4, a DOF transcription factor gene that negatively regulates cell cycle progression and cell expansion in *Arabidopsis thaliana*. Scientific Reports 6:27705.

Yamashita, K. 1937. Genetic investigations of the pith content of wheat stems. In: Memoirs of the College of Agriculture. Vol 39. Kyoto Imperial University.

Yanagisawa, S. 2000. Dof1 and Dof2 transcription factors are associated with expression of multiple genes involved in carbon metabolism in maize. The Plant Journal 21:281-8.

Yanagisawa, S., and K. Izui. 1993. Molecular cloning of two DNA-binding proteins of maize that are structurally different but interact with the same sequence motif. Journal of Biological Chemistry 268:16028-36.

Yanagisawa, S., and J. Sheen. 1998. Involvement of maize Dof zinc finger proteins in tissue-specific and light-regulated gene expression. Plant Cell 10:75-89.

Yuan, Y., P.E. Bayer, J. Batley, and D. Edwards. 2017. Improvements in genomic technologies: application to crop genomics. Trends in Biotechnology 35:547-558.

Zhang, M., Y. Zhang, C.F. Scheuring, C.C. Wu, J.J. Dong, and H.B. Zhang. 2012. Preparation of megabase-sized DNA from a variety of organisms using the nuclei method for advanced genomics research. Nature Protocols 7:467-78.

9. APPENDICES

Appendix 1. Stem-solidness rating scale.

Description of the method

Stems are either split longitudinally, or in cross section at multiple locations within each internode. Ratings are individually assigned for each internode, beginning at the basal internode moving upwards until the penultimate internode. In some applications, it may be useful to compare stem-solidness from the top of the plant down. A rating may be assigned for the peduncle however the rating can sometimes be confounded by the small stem diameter. Analysis may be performed separately for each internode, or combined across all internodes by taking the average across all internodes. Generally, only the main stem is selected for rating, as tillers may not give a true indication of the solidness of the plant.

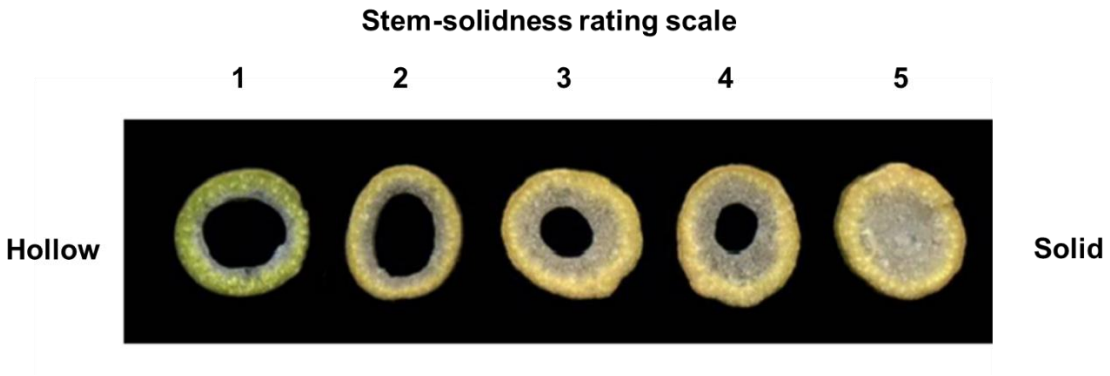

Appendix 2. Diversity panel haplotypes in the tetraploid wheat panel.

Name	Origin	Haplotype Group
Janz	Canada	1
Mott	USA - ND	1
AAC Bailey	Canada	2
AC Abbey	Canada	2
AC Eatonia	Canada	2
Choteau	USA - Montana	2
Fortuna	US - ND	2
G960801-L12J11BF02	Canada	2
Lancer	Canada	2
Leader	Canada	2
Lillian	Canada	2
LJP1091P	?	2
McKenzie	Canada	2
Rescue	Canada	2
S615	Portugal	2
Unity	Canada	2
5702PR	Canada	3
5500HR	Canada	4
Burnside	Canada	4
CDN Bison	Canada	4
CDC Rama	Canada	4
Glencross	Canada	4
Glenlea	Canada	4
Peace	Canada	4
Red Fife	Canada (source unknown)	4
Sumai 3	China	4
CDC Merlin	Canada	5
Chinese Spring	China	5
Selkirk	Canada	5
AC Reed	Canada	6
CDC Walrus	Canada	6
Frontana	Brazil	6
Glenn	USA - ND	6
Sadash	Canada	6
5601HR	Canada	6
5603HR	Canada	6
5700PR	Canada	6
AC Andrew	Canada	6
AC Cadillac	Canada	6
AC Crystal	Canada	6
AC Elsa	Canada	6

AC Foremost	Canada	6
AC Karma	Canada	6
AC Taber	Canada	6
AC Vista	Canada	6
Alvena	Canada	6
CDC Teal	Canada	6
CDC Utmost	Canada	6
Cutler	Canada	6
GP069	?	6
Infinity	Canada	6
Minnedosa	Canada	6
NRG010	Canada	6
Park	Canada	6
Prodigy	Canada	6
SY985	Canada	6
Vesper	Canada	7
5600HR	Canada	8
5602HR	Canada	8
5604HR CL	Canada	8
5701PR	Canada	8
AC Barrie	Canada	8
AC Domain	Canada	8
AC Intrepid	Canada	8
AC Splendor	Canada	8
Alikat	Canada	8
Carberry	Canada	8
CDC Abound	Canada	8
CDC Alsask	Canada	8
CDC Bounty	Canada	8
CDC Go	Canada	8
CDC Imagine	Canada	8
CDC Kernen	Canada	8
CDC Osler	Canada	8
CDC Stanley	Canada	8
CDC Thrive	Canada	8
Goodeve VB	Canada	8
Harvest	Canada	8
Helios	Canada	8
Journey	Canada	8
Kane	Canada	8
Katepwa	Canada	8
Laser	Canada	8
Laura	Canada	8

Lovitt	Canada	8
Muchmore	Canada	8
Neepawa	Canada	8
PT559	Canada	8
RL4137	Canada	8
Roblin	Canada	8
Snowbird	Canada	8
Snowstar	Canada	8
Somerset	Canada	8
Stanley	Canada	8
Stettler	Canada	8
Superb	Canada	8
Thatcher	Canada	8
Waskada	Canada	8

Appendix 3. Diversity panel haplotypes in the common wheat panel.

Name	Origin	Haplotype Group
9661-AF1D	Canada	1
AAC Cabri	Canada	1
AAC Raymore	Canada	1
Camacho	Spain	1
CDC Fortitude	Canada	1
DT726	Canada	1
DT732	Canada	1
DT751	Canada	1
DT777	Canada	1
DT795	Canada	1
DT817	Canada	1
DT824	Canada	1
DT837	Canada	1
DT838	Canada	1
DT845	Canada	1
Fortore	Italy	1
Mongibello	Italy	1
W9262-260D3	Canada	1
920334	Australia	2
940030	Australia	2
940955	Australia	2
950329	Australia	2
950844	Australia	2
Altar-Aos	Spain	2
Arcobelano	Italy	2
Bonarense Valv	Argentina	2
Buck Topacio	Argentina	2
CFR5001	New Zealand	2
Ciccio	Italy	2
Duilio	Italy	2
Grazia	Italy	2
Iride	Italy	2
Simeto	Italy	2
Varano	Italy	2
Wollaroi	Australia	2
44616	Iran	3
44721	Iran	3
Gidara 17A	Morocco	3
Kronos	USA	3
Mexa	Spain	3
Nacori 97	CIMMYT	3

Westbred881	USA	3
Bonarense Inta	Argentina	4
Borli	Spain	4
Buck Ambar	Argentina	4
Colosseo	Italy	4
Lesina	Italy	4
Tresor	Italy	4
940435	Australia	5
Bonarense Quil	Argentina	5
Carioca	France	5
Gianna	Italy	5
Parsifal	Italy	5
Tamaroi	Australia	5
Vitron	Italy	5
D95580	USA	6
9661-CA5E	Canada	6
AC Avonlea	Canada	6
AC Melita	Canada	6
AC Morse	Canada	6
AC Navigator	Canada	6
Agridur	France	6
Ariesol	France	6
Arrivato	New Zealand	6
Bronte	Italy	6
CDC Verona	Canada	6
Commander	Canada	6
D24-1773	Canada	6
D-73-15	Iran	6
D940027	USA	6
D940098	USA	6
D941038	USA	6
Demetra	Italy	6
DHTON 1	Morocco	6
DT513	Canada	6
DT536	Canada	6
DT691	Canada	6
DT695	Canada	6
DT696	Canada	6
DT704	Canada	6
DT705	Canada	6
DT707	Canada	6
DT709	Canada	6
DT710	Canada	6

DT711	Canada	6
Durabon	Germany	6
Durafit	Germany	6
Durex	USA	6
Golden Ball	South Africa	6
Green27	CIMMYT	6
Green34	CIMMYT	6
K-39099	Russia	6
Kofa	USA	6
Kyle	Canada	6
Langdon	USA	6
Langdon GBL-3B	USA	6
Marjak	Morocco	6
Ocotillo	USA	6
Plaza	USA	6
RABD 93.40	France	6
Strongfield	Canada	6
Svevo	Italy	6
Tetradur	France	6

Appendix 4. High density genetic linkage maps: (A) Kofa/W9262-260D3. (B) Lillian/Vesper populations.

https://ndownloader.figshare.com/articles/4866245/versions/1

Appendix 5. Overview of the RNAseq pipeline used.

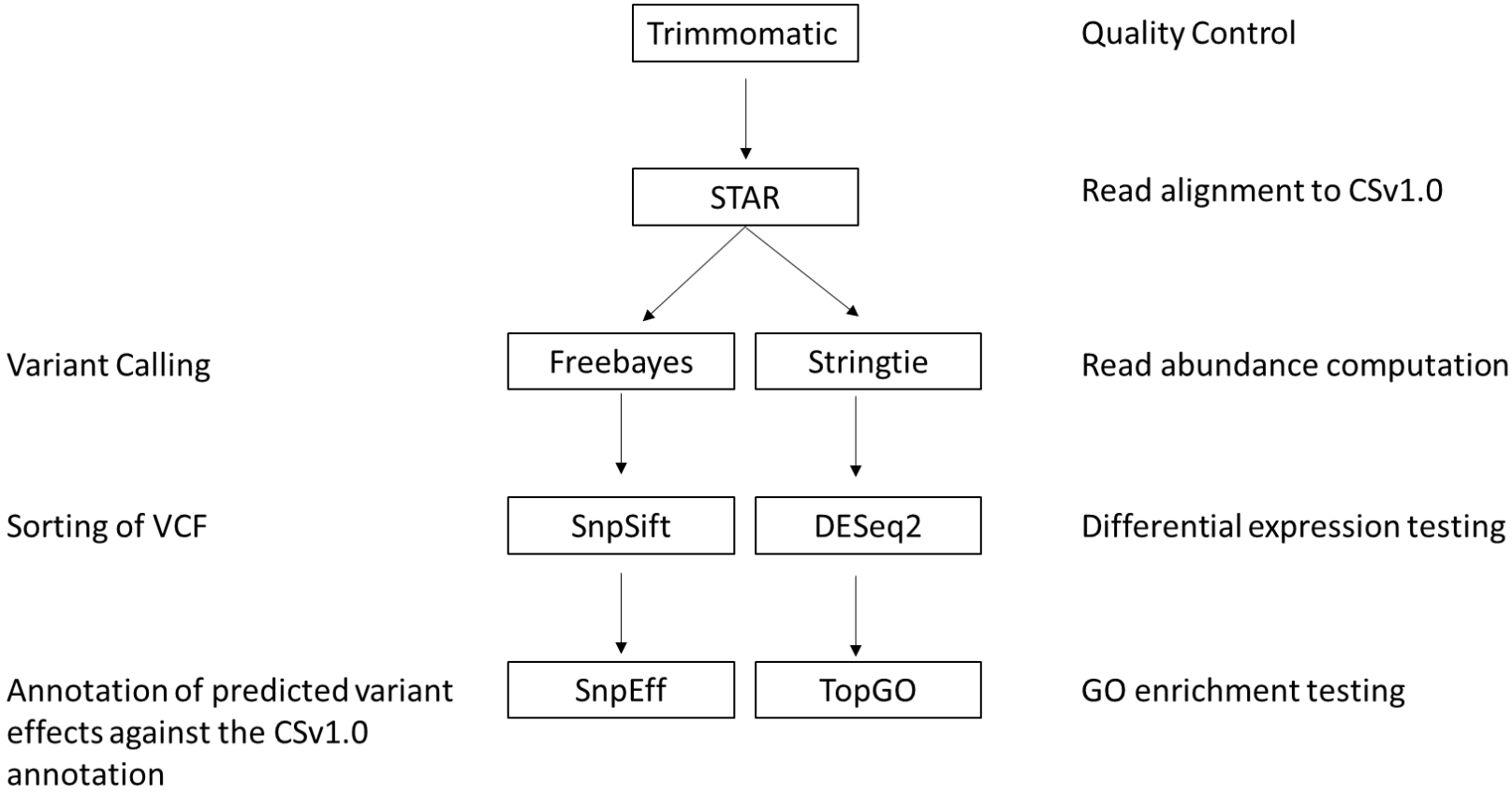

Appendix 6. Scripts used to run RNAseq pipeline.

```
#Written by Kirby Nilsen © 2017

#!/bin/bash

##Step 1, run STAR
#Usage
#runstar.sh 'genome.fasta'

GENOME=$1


SAMPLE=$(ls *_forward_paired.fq.gz | sed 's/_forward_paired.fq.gz//g')

for ITEM in $SAMPLE
do
/storage/users/kirby/source/STAR/bin/Linux_x86_64/STAR --readFilesIn
$ITEM"_forward_paired.fq.gz" $ITEM"_reverse_paired.fq.gz" --runThreadN 8 --
genomeDir /isilon/groups/wheat/star-index/$GENOME".dir" --readFilesCommand zcat --
outReadsUnmapped Fastx --outSAMstrandField intronMotif -runThreadN 8 --
alignIntronMax 10000 --outFilterMismatchNmax 3 --outFilterMatchNminOverLread 0.9 --
outSAMtype BAM SortedByCoordinate --outFileNamePrefix $ITEM

Done

###############################################################################

#!/bin/bash

##Step 2, Count transcript abundance
#note prepde.py is required (Pertea et al., 2016)
# Usage

runstringtie.sh 'annotation.gtf'
ANNOTATION=$1

SAMPLES=$(ls *.bam)
for ITEM in $SAMPLES; do
    /storage/users/kirby/source/stringtie-1.3.0/stringtie -e -B -p 32 -G
$ANNOTATION -o ./ballgown/$ITEM.dir/$ITEM.gtf $ITEM;
done

python /storage/users/kirby/scripts/prepDE.py

###############################################################################

#!/bin/bash

## Step 3. Run differential expression analysis with DESeq2
#note Needs samples.described.txt experimental design file 'CONDITIONA SAMPLE'
#requires the per script run_DE_analysis.pl →
#https://github.com/trinityrnaseq/trinityrnaseq/blob/master/Analysis/DifferentialExpression/run_DE_analysis.pl

# Usage runDE.sh

sed 's|,|\t|g' gene_count_matrix.csv > gene_count_matrix.txt
sed 's|,|\t|g' transcript_count_matrix.csv > transcript_count_matrix.txt

/storage/users/kirby/source/trinityrnaseq-
2.1.0/Analysis/DifferentialExpression/run_DE_analysis.pl --matrix
gene_count_matrix.txt --method DESeq2 --samples_file samples.described.txt

/storage/users/kirby/source/trinityrnaseq-
2.1.0/Analysis/DifferentialExpression/run_DE_analysis.pl --matrix
transcript_count_matrix.txt --method DESeq2 --samples_file samples.described.txt

###############################################################################
#!/bin/bash
## Step 4 run GO enrichment analysis

### BY Kirby 2017.2.10
### Description: Script to filter DESeq2 *results output and run through GO
enrichment VIA topGO
### Usage: Run from working directory containing DEseq2 output files
```

```
### Requires Gene Universe File "gene-universe.txt": Matrix of GO terms extracted
from interproscan database



### Prepare Input Files

### Enter GO Gene Universe
UNIVERSE=$1

SAMPLE=$(ls *results)
for SAMPLE in $SAMPLE
do
awk -F '\t' '{if ($5 >=2 || $5 <= -2) print $1, "1"; else print $1, "0"}f' $SAMPLE
> $SAMPLE.DEGenes.txt
grep -w 1 $SAMPLE.DEGenes.txt | wc -l >> significant-gene-count.txt

done


###Run TOPGO
SAMPLE=$(ls *DEGenes.txt)
for SAMPLE in $SAMPLE
do

echo "#!/usr/bin/env Rscript

library(topGO)

setwd(\".\")
#LOAD MAPPINGS FROM CUSTOM ANNOTATION

geneID2GO <- readMappings(\"$UNIVERSE\")

#CREATE VECTOR
d <- read.table(\"$SAMPLE\") ##2 column file c2=significance (1 means significant),
c1= gene name

e<- factor(d[[2]]) # reads in column1 as a factor
f<- factor(d[[1]]) # reads in column2 as a factor

names(e) <- f      #adds gene names to significant

GOdataBP <- new(\"topGOdata\", ontology = \"BP\", allGenes = e ,annot =
annFUN.gene2GO, gene2GO = geneID2GO)
GOdataBP

GOdataCC <- new(\"topGOdata\", ontology = \"CC\", allGenes = e ,annot =
annFUN.gene2GO, gene2GO = geneID2GO)
GOdataCC

GOdataMF <- new(\"topGOdata\", ontology = \"MF\", allGenes = e ,annot =
annFUN.gene2GO, gene2GO = geneID2GO)
GOdataMF
###########PERform enrichment tests 3 ways
resultFisherBP <- runTest(GOdataBP, algorithm = \"classic\", statistic =
\"fisher\")
resultFisherMF <- runTest(GOdataMF, algorithm = \"classic\", statistic =
\"fisher\")
resultFisherCC <- runTest(GOdataCC, algorithm = \"classic\", statistic =
\"fisher\")


#########just Fischers Exact test
allResBP <- GenTable(GOdataBP, classicFisher = resultFisherBP, topNodes = 100)
allResMF <- GenTable(GOdataMF, classicFisher = resultFisherMF, topNodes = 100)
allResCC <- GenTable(GOdataCC, classicFisher = resultFisherCC, topNodes = 100)
```

Appendix 7. Multiple sequence alignment of *TraesCS3B01G60880* and surrounding sequence in five genomic assemblies. Sequences were aligned using MUSCLE**.**

```
Landmark        AGCAAGCTAGCTAATCAGTACGACATTAATTAATTATTGCAACTGTAGCTAGCAACACTG
Stanley         AGCAAGCTAGCTAATCAGTACGACATTAATTAATTATTGCAACTGTAGCTAGCAACACTG
Svevo           AGCAAGCTAGCTAATCAGTACGACATTAATTAATTATTGCAACTGTAGCTAGCAACACTG
CS              AGCAAGCTAGCTAATCAGTACGACATTAATTAATTATTGCAACTGTAGCTAGCAACACTG
Zavitan         AGAAAGCTAGCTAATCGGTACTACATTAATTAATTATTGCAACTGTAGCTAGCAACACTG
                ** ************** **** ************************************

Landmark        CATGCATCAGCAAGGTAGCATGGGTAGCCGTCTCAGCCCCATCAGCACTCACCATGGAAA
Stanley         CATGCATCAGCAAGGTAGCATGGGTAGCCGTCTCAGCCCCATCAGCACTCACCATGGAAA
Svevo           CATGCATCAGCAAGGTAGCATGGGTAGCCGTCTCAGCCCCATCAGCACTCACCATGGAAA
CS              CATGCATCAGCAAGGTAGCATGGGT---------AGCCCCATCAGCACTCACCATGGAAA
Zavitan         CATGCATCAGCAAGGTAGCATGGGTAGCCGTCTCAGCCCCATCAGCACTCACCATGGAAA
                ************************         *************************

Landmark        AAGCAAAAGTGTGTAAATAAAGGAAAACAACAACAAGATGATGTCCTCTCCCTCCTCCAA
Stanley         AAGCAAAAGTGTGTAAATAAAGGAAAACAACAACAAGATGATGTCCTCTCCCTCCTCCAA
Svevo           AAGCAAAAGTGTGTAAATAAAGGAAAACAACAACAAGATGATGTCCTCTCCCTCCTCCAA
CS              AAGCAAAAGTGTGTAAATAAAGGAAAACAACAACAAGATGATGTCCTCTCCCTCCTCCAA
Zavitan         AAGCAAAAGTGTGTAAATAAAGGAAAACAACAACAAGATGATGTCCTCTCCCTCCTCCAA
                ************************************************************

Landmark        ATCGCCACAAGCT--------AGAGAGAGAGAGAGAGAGAGAGAGAGAGCCTTCTCTC
Stanley         ATCGCCACAAGCTAGAGAGAGAGAGAGAGAGAGAGAGAGAGAGAGAGCCTTCTCTC
Svevo           ATCGCCACAAGCT--AGAGAGAGAGAGAGAGAGAGAGAGAGAGAGAGCCTTCTCTC
CS              ATCGCCACAAGCT------------------AGAGAGAGAGAGAGAGAGAGCCTTCTCTC
Zavitan         ATCGCCACAAGCT--------------AGAGAGAGAGAGAGAGAGAGGCCCTTCTCTC
                *************                  ******************  *********

Landmark        TCATCTCTTGGTTGTGCTGCTACCTGGCGCTCTCTCCTTTTTCTCTCTCCTCTTGGGTAG
Stanley         TCATCTCTTGGTTGTGCTGCTACCTGGCGCTCTCTCCTTTTTCTCTCTCCTCTTGGGTAG
Svevo           TCATCTCTTGGTTGTGCTGCTACCTGGCGCTCTCTCCTTTTTCTCTCTCCTCTTGGGTAG
CS              TCATCTCTTGGTTGTGCTGCTACCTGGCGCTCTCTCCTTTTTCTCTCTCCTCTTGGGTAG
Zavitan         TCATCTCTTGGTTGTGCTGCTACCTGGCGCTCTCTCCTTTTTCTCTCTCCTCTTGGGTAG
                ************************************************************

Landmark        CTCTCGCTCCCTCTCAAAGCAGTCAAGAGCTAGACCCTCCTGTCTCCTCTAGCTTCCATT
Stanley         CTCTCGCTCCCTCTCAAAGCAGTCAAGAGCTAGACCCTCCTGTCTCCTCTAGCTTCCATT
Svevo           CTCTCGCTCCCTCTCAAAGCAGTCAAGAGCTAGACCCTCCTGTCTCCTCTAGCTTCCATT
CS              CTCTCGCTCCCTCTCAAAGCAGTCAAGAGCTAGACCCTCCTGTCTCCTCTAGCTTCCATT
Zavitan         CTCTCGCTCCCTCTCAAAGCAGTCAAGAGCTAGACCCTCCTGTCTCCTCTAGCTTCCATT
                ************************************************************

Landmark        CCATTCCTTTCCTTGGTACTAGTACTCTGATTCCCTTTGATTT-CCCCAGCTGCCGCAGC
Stanley         CCATTCCTTTCCTTGGTACTAGTACTCTGATTCCCTTTGATTT-CCCCAGCTGCCGCAGC
Svevo           CCATTCCTTTCCTTGGTACTAGTACTCTGATTCCCTTTGATTT-CCCCAGCTGCCGCAGC
CS              CCATTCCTTTCCTTGGTACTAGTACTCTGATTCCCTTTGATTT-CCCCAGCTGCCGCAGC
Zavitan         CCATTCCTTTCCTTGGTACTAGTACTCTGATTCCCTTTGATTTCCCCCAGCTGCCGCAGC
                ****************************************** ****************

Landmark        TGCCAAGTCTCTTCCTCCCACTATCTCTTCTCTCCAACCTCCAGCCCTGCCAGCCGCCCA
Stanley         TGCCAAGTCTCTTCCTCCCACTATCTCTTCTCTCCAACCTCCAGCCCTGCCAGCCGCCCA
Svevo           TGCCAAGTCTCTTCCTCCCACTATCTCTTCTCTCCAACCTCCAGCCCTGCCAGCCGCCCA
CS              TGCCAAGTCTCTTCCCCCCACTATCTCTTCTCTCCAACCTCCAGCCCAGCCAGCCGCCCA
Zavitan         TGCCAAGTCTCTTCCCCCCACTATCTCTTCTCTCCAACCTCCAGCCCAGCCAGCCGCCCA
                ************** ****************************** ************

Landmark        AACACCTCTCTCCTCTCCCAACAACTCTCTCTGGAAGTCTAGATCGCCGGCCATGATCTT
Stanley         AACACCTCTCTCCTCTCCCAACAACTCTCTCTGGAAGTCTAGATCGCCGGCCATGATCTT
Svevo           AACACCTCTCTCCTCTCCCAACAACTCTCTCTGGAAGTCTAGATCGCCGGCCATGATCTT
CS              AACACCTCTCTCCTCTCCCAACAACTCTCTCTGGAAGTCTAGATCGCCGGCCATGATCTT
```

```
Zavitan         AACACCTCTCTCCTCTCCCAACAACTCTCTCTGGAAGTCTAGATCGCCGGCCATGATCTT
                ************************************************************

Landmark        CCCTCCTGCCTTCCTCGACTCATCAAGCTGCTGGAACACCAACCACAACCAGCTTCAGGT
Stanley         CCCTCCTGCCTTCCTCGACTCATCAAGCTGCTGGAACACCAACCACAACCAGCTTCAGGT
Svevo           CCCTCCTGCCTTCCTCGACTCATCAAGCTGCTGGAACACCAACCACAACCAGCTTCAGGT
CS              CCCTCCCGCCTTCCTCGACTCATCAAGCTGCTGGAACACCAACCACAACCAGCTTCAGGT
Zavitan         CCCTCCTGCCTTCCTCGACTCATCAAGCTGCTGGAACACCAACCACAACCAGCTTCAGGT
                ****** ***************************************************

Landmark        ATGCATCCTTGCGGTCAATTAATTCTTCTCGCAAGATTTTGTTCACGCAAGAAAA--AGA
Stanley         ATGCATCCTTGCGGTCAATTAATTCTTCTCGCAAGATTTTGTTCACGCAAGAAAAAGAGA
Svevo           ATGCATCCTTGCGGTCAATTAATTCTTCTCGCAAGATTTTGTTCACGCAAGAAAAAGAGA
CS              ATGCATCCTTGCGGTCAATTAATTCTTCTCTCAAGATTTTGTTCACGCAAGAAAA-----
Zavitan         ATGCATCCTTGCGGTCAATTAATTCTTCTCGCAAGATTTTGTTCACGCAAGAAAA----A
                ***************************** ************************

Landmark        GAGAGAGAGAGAGAGAGAATATGTTCTAGCTAAGCTAGGGTTTGCTGATGGCAGATATAC
Stanley         GAGAGAGAGAGAGAGAGAATATGTTCTAGCTAAGCTAGGGTTTGCTGATGGCAGATATAC
Svevo           GAGAGAGAGAGAGAGAGAATATGTTCTAGCTAAGCTAGGGTTTGCTGATGGCAGATATAC
CS              ---AGAGAGAGAGAGAGAATATGTTCTAGCTAAGCTAGGGTTTGCTGATGGCAGATATAC
Zavitan         AAGAGAGAGAGAGAGAGAATATGTTCTAGCTAAGCTAGGGTTTGCTGATGGCAGATATAC
                   ************************************************************

Landmark        ATCCTCTGCTGATTGCTGCACTATGTATCTTGGAATATACTCCATATACACATCTTGGCT
Stanley         ATCCTCTGCTGATTGCTGCACTATGTATCTTGGAATATACTCCATATACACATCTTGGCT
Svevo           ATCCTCTGCTGATTGCTGCACTATGTATCTTGGAATATACTCCATATACACATCTTGGCT
CS              ATCCTCTGCTGATTGCTGCACTATGTATCTTGGAATATACTCAATATACACATCTTGGCT
Zavitan         ATCCTCTGCTGATTGCTGCACTATGTATCTTGGAATATACTCCATATACACATCTTGGCT
                ****************************************** ******************

Landmark        GACGCTTAATTCCTGACCACTTAATTTGCAGCTGCAGCAAATCGGCAGTAACACTCATAT
Stanley         GACGCTTAATTCCTGACCACTTAATTTGCAGCTGCAGCAAATCGGCAGTAACACTCATAT
Svevo           GACGCTTAATTCCTGACCACTTAATTTGCAGCTGCAGCAAATCGGCAGTAACACTCATAT
CS              GACGCTTAATTCCTGACCACTTAATTTGCAGCTGCAGCAAATCGGCAGCAACAGTCATAT
Zavitan         GACGCTTAATTCCTGACCACTTAATTTGCAGCTGCAGCAAATCGGCACCAACAGTCATAT
                ********************************************  **** ******

Landmark        CACTACTACTCCTTCACCTGCTGGCCATGGTCCTGGAGACGGAGGAGGCGGAAACAACAA
Stanley         CACTACTACTCCTTCACCTGCTGGCCATGGTCCTGGAGACGGAGGAGGCGGAAACAACAA
Svevo           CACTACTACTCCTTCACCTGCTGGCCATGGTCCTGGAGACGGAGGAGGCGGAAACAACAA
CS              CACTACTACTCCTTCGCCTGCTGGCCATGGTCCTGGAGACGGAGGAGGCGGAAACAACAA
Zavitan         CACTACTACTCCTTCGCCTGCTGGCCATGGTCCTGGAGACGGAGGAGGCGGAAACAACAA
                *************** ********************************************

Landmark        CAATCATGGTCAGCAGGAAGGATTAATGGCCACGGCCGGGGCGGGAGGAGGTGGTGGTGA
Stanley         CAATCATGGTCAGCAGGAAGGATTAATGGCCACGGCCGGGGCGGGAGGAGGTGGTGGTGA
Svevo           CAATCATGGTCAGCAGGAAGGATTAATGGCCACGGCCGGGGCGGGAGGAGGTGGTGGTGA
CS              CAATCATGGTCAGCAGGAAGGATTAATGGCCACGGCCGGGGCGGGAGGAGGTGGTGGTGA
Zavitan         TAATCATGGTCAGCAGGAAGGATTAATGGCCACGGCCGGGGCGGGAGGAGGTGGTGGTGA
                 ************************************************************

Landmark        TGGTGGTGGCGGCGGCGGTGGGGATGGTGACAGCGCCAGCGGCGGGAACAACAAGCCGAT
Stanley         TGGTGGTGGCGGCGGCGGTGGGGATGGTGACAGCGCCAGCGGCGGGAACAACAAGCCGAT
Svevo           TGGTGGTGGCGGCGGCGGTGGGGATGGTGACAGCGCCAGCGGCGGGAACAACAAGCCGAT
CS              TGGTGGCGGCGGCGGCGGTGGGGATGGTGACAGCGCTGGCGGCGGGAACAACAAGCCGAT
Zavitan         TGGTGGCGGCGGCGGCGGTGGGGATGGTGACAGCGCCGGCGGCGGGAACAACAAGCCGAT
                ****** ***************************  ***********************

Landmark        GTCGATGTCGGAGCGGGCGCGGCTGGCGCGGGTGCCACAGCCGGAGCCGGGGCTCAACTG
Stanley         GTCGATGTCGGAGCGGGCGCGGCTGGCGCGGGTGCCACAGCCGGAGCCGGGGCTCAACTG
Svevo           GTCGATGTCGGAGCGGGCGCGGCTGGCGCGGGTGCCACAGCCGGAGCCGGGGCTCAACTG
CS              GTCGATGTCGGAGCGAGCGCGGCTGGCTCGGGTGCCGCAGCCGGAGCCGGGGCTCAACTG
Zavitan         GTCGATGTCGGAGCGGGCGCGGCTGGCTCGGGTGCCGCAGCCAGAGCCGGGGCTCAACTG
                *************** *********** ******** ***** ****************
```

```
Landmark        CCCGCGCTGCGATTCCACCAACACCAAGTTCTGCTACTTCAACAACTACTCCCTCACCCA
Stanley         CCCGCGCTGCGATTCCACCAACACCAAGTTCTGCTACTTCAACAACTACTCCCTCACCCA
Svevo           CCCGCGCTGCGATTCCACCAACACCAAGTTCTGCTACTTCAACAACTACTCCCTCACCCA
CS              CCCGCGCTGCGACTCCACCAACACCAAGTTCTGCTACTTCAACAACTACTCCCTCACCCA
Zavitan         CCCGCGCTGCGACTCCACCAACACCAAGTTCTGCTACTTCAACAATTACTCCCTCACCCA
                ************ ******************************** **************

Landmark        GCCCCGCCACTTCTGCCGGGCCTGCCGCCGCTACTGGACCCGCGGCGGCGCGCTCCGCAA
Stanley         GCCCCGCCACTTCTGCCGGGCCTGCCGCCGCTACTGGACCCGCGGCGGCGCGCTCCGCAA
Svevo           GCCCCGCCACTTCTGCCGGGCCTGCCGCCGCTACTGGACCCGCGGCGGCGCGCTCCGCAA
CS              GCCCCGCCACTTCTGCCGGGCCTGCCGCCGCTACTGGACCCGCGGCGGCGCGCTCCGCAA
Zavitan         GCCCCGCCACTTCTGCCGCGCCTGCCGCCGCTACTGGACCCGCGGCGGCGCGCTCCGCAA
                ****************** ****************************************

Landmark        CGTCCCCGTCGGCGGAGGGTACCGTCGCCACGCCAAGCGCAGCACCAAGCCCAAGGCCGG
Stanley         CGTCCCCGTCGGCGGAGGGTACCGTCGCCACGCCAAGCGCAGCACCAAGCCCAAGGCCGG
Svevo           CGTCCCCGTCGGCGGAGGGTACCGTCGCCACGCCAAGCGCAGCACCAAGCCCAAGGCCGG
CS              CGTCCCCGTCGGCGGCGGGTACCGTCGCCACGCCAAGCGCAGCACCAAGCCCAAGGCCGG
Zavitan         CGTCCCCGTCGGCGGCGGGTACCGTCGCCACGCCAAGCGCAGCGCCAAGCCCAAGGCCGG
                *************** ************************** ****************

Landmark        GTCGGCTGGATCCGGAACTGCCGCGGCAGGGACGTCGTCTGCGACGTCGACGACGCCCAG
Stanley         GTCGGCTGGATCCGGAACTGCCGCGGCAGGGACGTCGTCTGCGACGTCGACGACGCCCAG
Svevo           GTCGGCTGGATCCGGAACTGCCGCGGCAGGGACGTCGTCTGCGACGTCGACGACGCCCAG
CS              GTCGGCTGGATCCGGAACCGCCGCGGCAGGGACATCGTCTGCGACGTCGACGACGCCCAG
Zavitan         GTCGGCTGGATCCGGAACCGCCGCGGCAGGGACGTCTTCTGCGACGTCGACTACGCCCAG
                ****************** ************** ** ************** ********

Landmark        CACCACTGCTTGCACCACCGGCACAGCTGCCACTGCGCCGCCCGCTCTGCAGTACTCCAT
Stanley         CACCACTGCTTGCACCACCGGCACAGCTGCCACTGCGCCGCCCGCTCTGCAGTACTCCAT
Svevo           CACCACTGCTTGCACCACCGGCACAGCTGCCACTGCGCCGCCCGCTCTGCAGTACTCCAT
CS              CACCACTGCTTGCACCACCGGCA---CTGCCACTGCGCCGCCTGCTCTGCAGTACTCCAT
Zavitan         CACCACTGCTTGCACCACCGGCA---CTGCCACTGCGCCGCCCGCTCTGCAGTACTCCAT
                ************************   ***************** ******************

Landmark        GTTCGGCAGCGCGCCGCCGCACAGCAGCCGGTTCGCCGATAGCTTCGACCCCGCGAGCCT
Stanley         GTTCGGCAGCGCGCCGCCGCACAGCAGCCGGTTCGCCGATAGCTTCGACCCCGCGAGCCT
Svevo           GTTCGGCAGCGCGCCGCCGCACAGCAGCCGGTTCGCCGATAGCTTCGACCCCGCGAGCCT
CS              GTTCGGCAGCGCGCCGCCGCACGGCAGCCGGTTCGCCGATAGCTTCGACCCGGCGAGCCT
Zavitan         GTTCGGCAGCGCGCCGCCGCACGGCAGCCGGTTCGCCGATAGCTTCGACCCCGCGAGCCT
                ********************** **************************** ********

Landmark        CGGCCTCAGCTTCCCCGCCAGGCTGCTCTTCCCCGACAATGGCGCCTACGCTGCCGACGG
Stanley         CGGCCTCAGCTTCCCCGCCAGGCTGCTCTTCCCCGACAATGGCGCCTACGCTGCCGACGG
Svevo           CGGCCTCAGCTTCCCCGCCAGGCTGCTCTTCCCCGACAATGGCGCCTACGCTGCCGACGG
CS              CGGCCTCAGCTTCCCCGCCAGGCTGCTCTTCCCCGACAATGGCGCCTATGCGGCCGACGG
Zavitan         CGGCCTCAGCTTCCCCGCCAGGCTGCTCTTCCCCGACAATGGCGCCTACGCTGCCGACGG
                ************************************************ ** ********

Landmark        TGGCGCGCAGCAGCACCACCACCACCAGGGGAACGGGAACGGCATGGAGCAGTGGGCGGC
Stanley         TGGCGCGCAGCAGCACCACCACCACCAGGGGAACGGGAACGGCATGGAGCAGTGGGCGGC
Svevo           TGGCGCGCAGCAGCACCACCACCACCAGGGGAACGGGAACGGCATGGAGCAGTGGGCGGC
CS              TGGCGCGCAGCAGCACCACCACCACCAGGGGAACGGGAACGGCATGGAGCAGTGGGCGGC
Zavitan         TGGCGCGCAGCAGCACCACCACCACCAGGGGAGCGGGAACGGCATGGAGCAGTGGGCGGC
                ******************************** **************************

Landmark        TGCGCACATGCAGAGCTTCCCGTTCCTGCACGCCATGGACCACCAGATGTCCGGGAATCC
Stanley         TGCGCACATGCAGAGCTTCCCGTTCCTGCACGCCATGGACCACCAGATGTCCGGGAATCC
Svevo           TGCGCACATGCAGAGCTTCCCGTTCCTGCACGCCATGGACCACCAGATGTCCGGGAATCC
CS              TGCGCACATGCAGAGCTTCCCGTTCCTGCACGCCATGGACCACCAGATGTCCGGGAATCC
Zavitan         TGCGCACATGCAGAGCTTCCCGTTCGTGCACGCCATGGACCACCAGATGTCCGGGAATCC
                ************************* **********************************

Landmark        TCAATCAGCTTCGGCAATGCCAACCACAATGGCGGCGATGCAGGGCATGTTCCACCTCGG
```

```
Stanley         TCAATCAGCTTCGGCAATGCCAACCACAATGGCGGCGATGCAGGGCATGTTCCACCTCGG
Svevo           TCAATCAGCTTCGGCAATGCCAACCACAATGGCGGCGATGCAGGGCATGTTCCACCTCGG
CS              TCAATCAGCTTCGGCAATGCCAACCACAATGGCGGCGATGCAGGGCATGTTCCACCTAGG
Zavitan         TCAATCAGCTTCGGCAATGCCCACCACAATGGCGGCGATGCAGGGCATGTTCCACCTAGG
                ********************* ********************************** **

Landmark        GCTACAGAGCGGCGGCGGCGGCGGTAATGGCGACGATGGGGGAAACCACCAGTTCCACCA
Stanley         GCTACAGAGCGGCGGCGGCGGCGGTAATGGCGACGATGGGGGAAACCACCAGTTCCACCA
Svevo           GCTACAGAGCGGCGGCGGCGGCGGTAATGGCGACGATGGGGGAAACCACCAGTTCCACCA
CS              GCTACAGAGCGGCGGCGGCGGCGGTAATGGCGACGATGGGGGAAACCACCAGTTCCACCA
Zavitan         GCTACAGAGCGGCGGCGGCGGCGGCAATGGCGACGATGGGGGAAACCACCAGTTCCACCA
                ************************ ***********************************

Landmark        CCAGCCGGCCAAGAGGGACTAC---AACCAGCAGCAGCAGCAGGATTACCCAAGCAGCAG
Stanley         CCAGCCGGCCAAGAGGGACTAC---AACCAGCAGCAGCAGCAGGATTACCCAAGCAGCAG
Svevo           CCAGCCGGCCAAGAGGGACTAC---AACCAGCAGCAGCAGCAGGATTACCCAAGCAGCAG
CS              CCAGCCGGCCAAGAGGGACTAC---AACCAGCAGCAGCAGCAGGATTACCCAAGCAGCAG
Zavitan         CCAGCCGGCCAAGAGGGACTACCAGCAGCAGCAGCAGCAGCAGGATTACCCAAGCAACAG
                *********************    * **************************** ***

Landmark        GGGCATGTACGGGGACGTGGTCAATGGCAATGGCGGCGGCTTCAATTTCTATTCCAGCAC
Stanley         GGGCATGTACGGGGACGTGGTCAATGGCAATGGCGGCGGCTTCAATTTCTATTCCAGCAC
Svevo           GGGCATGTACGGGGACGTGGTCAATGGCAATGGCGGCGGCTTCAATTTCTATTCCAGCAC
CS              GGGCATGTACGGGGACGTGGTCAATGGCAATGGCGGCGGCTTCAATTTCTATTCCAGCAC
Zavitan         GGGCATGTACGGGGACGTGGTCAATGGCAATGGCGGCGGCTTCAATTTCTATTCCAGCAC
                ************************************************************

Landmark        TAGCAATGCAGCTGGTAATTAGCTAGCTAGATCTAGCTAGCTTTGTTCTTGCAAACCTAG
Stanley         TAGCAATGCAGCTGGTAATTAGCTAGCTAGATCTAGCTAGCTTTGTTCTTGCAAACCTAG
Svevo           TAGCAATGCAGCTGGTAATTAGCTAGCTAGATCTAGCTAGCTTTGTTCTTGCAAACCTAG
CS              TAGCAATGCAGCTGGTAATTAGCTAGCTAGATCTAGCTAGCTTTGTTCTTGCAAACCTAG
Zavitan         TAGCAATGCAGCTGGTAATTAGCTAGCTAGATCTAGCTAGCTTTGTTCTTGCAAACCTAG
                ************************************************************
```

Appendix 8. CNV qPCR primer-sets.

SW_MYB_F1: CTCAACGAACGACAACGAT7
SW_MYB_F2: AGATCACCAGCTGCTCTACACCT

SW_MYB_R1: ATGCGTAGGAGTCCATGAG
SW_MYB_R2: GGCACTATCATAGACGGCG

SW_dof_F1: GTTCCTGCACGCCATGGAC
SW_dof_F2: GATGTCCGGGAATCCTCAAT

SW_dof_R1: TCCCCCATCGTCGCCATTA
SW_dof_R2: TAGTCCCTCTTGGCCGGCT

SW_AAOx_F: CACAGCAGGATTTAAGCTCTGG
SW_AAOx_R:GGGATGGACTAATTTCACAGGC

SW_Aox_F: GACTTGTCATGGTAGATGCCTG
SW_Aox_R: CAGGACGAGCATAACCATTCTC

SW_hnRQ_F: TCACCTTCGCCAAGCTCAGAACTA
SW_hnRQ_R: AGTTGAACTTGCCCGAAACATGCC

Appendix 9. DOF gene family phylogeny in the Refseq v.1.0 annotation. Gene expression (log2Fold change) is shown as a heatmap for hollow vs solid pairwise comparisons. Highlighted in yellow are *TraesCS3B01G60880* and its corresponding A and D genome homoeologues.

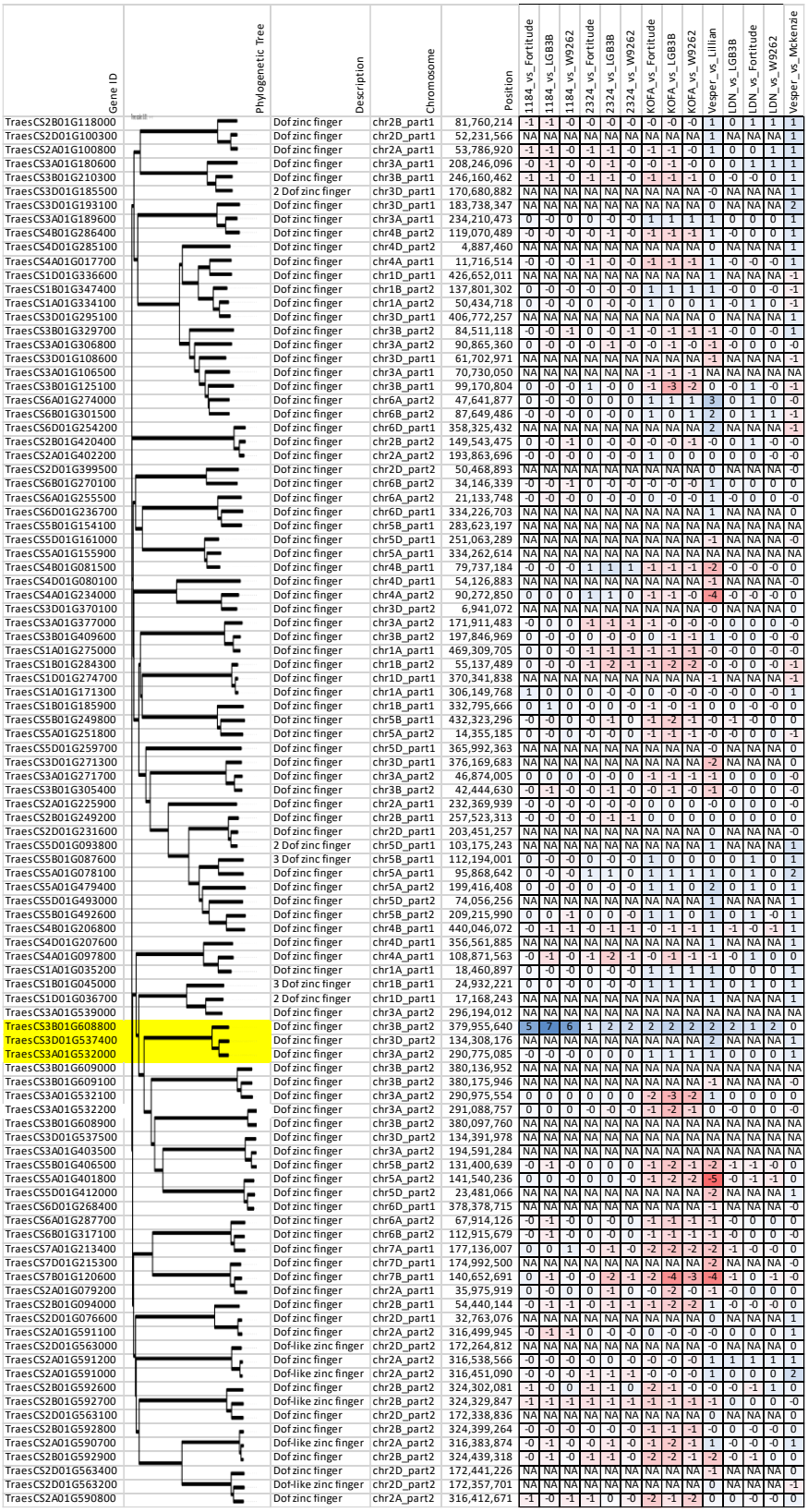

Gene ID	Phylogenetic Tree	Description	Chromosome	Position	1184_vs_Fortitude	1184_vs_LGB3B	1184_vs_W9262	2324_vs_Fortitude	2324_vs_LGB3B	2324_vs_W9262	KOFA_vs_Fortitude	KOFA_vs_LGB3B	KOFA_vs_W9262	Vesper_vs_Lillian	LDN_vs_LGB3B	LDN_vs_Fortitude	LDN_vs_W9262	Vesper_vs_Mckenzie
TraesCS2B01G118000		Dof zinc finger	chr2B_part1	81,760,214	-1	-1	-0	-0	-0	-0	-0	-0	-0	1	0	1	1	1
TraesCS2D01G100300		Dof zinc finger	chr2D_part1	52,231,566	NA	NA	NA	NA	NA	NA	NA	NA	NA	NA	1	NA	NA	NA	1
TraesCS2A01G100800		Dof zinc finger	chr2A_part1	53,786,920	-1	-1	-0	-1	-1	-0	-1	-1	-0	1	0	0	1	1
TraesCS3A01G180600		Dof zinc finger	chr3A_part1	208,246,096	-0	-1	-0	-0	-1	-0	-0	-1	-0	0	0	1	1	1
TraesCS3B01G210300		Dof zinc finger	chr3B_part1	246,160,462	-1	-1	-0	-1	-1	-0	-1	-1	-1	0	-0	-0	0	1
TraesCS3D01G185500		2 Dof zinc finger	chr3D_part1	170,680,882	NA	NA	NA	NA	NA	NA	NA	NA	NA	-0	NA	NA	NA	1
TraesCS3D01G193100		Dof zinc finger	chr3D_part1	183,738,347	NA	NA	NA	NA	NA	NA	NA	NA	NA	0	NA	NA	NA	2
TraesCS3A01G189600		Dof zinc finger	chr3A_part1	234,210,473	0	-0	0	0	-0	-0	1	1	1	1	0	0	0	1
TraesCS4B01G286400		Dof zinc finger	chr4B_part2	119,070,489	-0	-0	-0	-0	-1	-0	-1	-1	-1	1	-0	0	0	1
TraesCS4D01G285100		Dof zinc finger	chr4D_part2	4,887,460	NA	NA	NA	NA	NA	NA	NA	NA	NA	0	NA	NA	NA	1
TraesCS4A01G017700		Dof zinc finger	chr4A_part1	11,716,514	-0	-0	-0	-1	-0	-0	-1	-1	-1	1	-0	-0	-0	1
TraesCS1D01G336600		Dof zinc finger	chr1D_part1	426,652,011	NA	NA	NA	NA	NA	NA	NA	NA	NA	1	NA	NA	NA	-1
TraesCS1B01G347400		Dof zinc finger	chr1B_part2	137,801,302	0	-0	-0	-0	-0	-0	1	1	1	-0	0	-0	-0	-1
TraesCS1A01G334100		Dof zinc finger	chr1A_part2	50,434,718	0	-0	-0	0	-0	-0	1	0	0	1	-0	1	0	-1
TraesCS3D01G295100		Dof zinc finger	chr3D_part1	406,772,257	NA	NA	NA	NA	NA	NA	NA	NA	NA	0	NA	NA	NA	1
TraesCS3B01G329700		Dof zinc finger	chr3B_part2	84,511,118	-0	-0	-1	0	-0	-1	-0	-1	-1	-1	-0	0	-0	1
TraesCS3A01G306800		Dof zinc finger	chr3A_part2	90,865,360	0	-0	-0	-0	-1	-0	-0	-1	-0	-1	-0	0	0	-0
TraesCS3D01G108600		Dof zinc finger	chr3D_part1	61,702,971	NA	NA	NA	NA	NA	NA	NA	NA	NA	-1	NA	NA	NA	-1
TraesCS3A01G106500		Dof zinc finger	chr3A_part1	70,730,050	NA	NA	NA	NA	NA	NA	-1	-1	-1	NA	NA	NA	NA	NA
TraesCS3B01G125100		Dof zinc finger	chr3B_part1	99,170,804	0	-0	-0	1	-0	0	-1	-3	-2	0	-0	1	-0	-1
TraesCS6A01G274000		Dof zinc finger	chr6A_part2	47,641,877	0	-0	-0	0	0	0	1	1	1	3	0	1	0	-0
TraesCS6B01G301500		Dof zinc finger	chr6B_part2	87,649,486	-0	-0	-0	0	-0	0	1	0	1	2	0	1	1	-1
TraesCS6D01G254200		Dof zinc finger	chr6D_part1	358,325,432	NA	NA	NA	NA	NA	NA	NA	NA	NA	2	NA	NA	NA	-1
TraesCS2B01G420400		Dof zinc finger	chr2B_part2	149,543,475	0	-0	-1	0	-0	-0	-0	-0	-1	-0	0	1	-0	-0
TraesCS2A01G402200		Dof zinc finger	chr2A_part2	193,863,696	-0	-0	-0	0	-0	-0	1	0	0	0	0	0	-0	-0
TraesCS2D01G399500		Dof zinc finger	chr2D_part2	50,468,893	NA	NA	NA	NA	NA	NA	NA	NA	NA	0	NA	NA	NA	-0
TraesCS6B01G270100		Dof zinc finger	chr6B_part2	34,146,339	-0	-0	-1	0	-0	-0	-0	-0	-0	1	0	0	0	0
TraesCS6A01G255500		Dof zinc finger	chr6A_part2	21,133,748	-0	-0	-0	0	-0	-0	0	-0	-0	1	-0	0	0	-0
TraesCS6D01G236700		Dof zinc finger	chr6D_part1	334,226,703	NA	NA	NA	NA	NA	NA	NA	NA	NA	1	NA	NA	NA	0
TraesCS5B01G154100		Dof zinc finger	chr5B_part1	283,623,197	NA	NA	NA	NA	NA	NA	NA	NA	NA	NA	NA	NA	NA	NA
TraesCS5D01G161000		Dof zinc finger	chr5D_part1	251,063,289	NA	NA	NA	NA	NA	NA	NA	NA	NA	-1	NA	NA	NA	-0
TraesCS5A01G155900		Dof zinc finger	chr5A_part1	334,262,614	NA	NA	NA	NA	NA	NA	NA	NA	NA	NA	NA	NA	NA	NA
TraesCS4B01G081500		Dof zinc finger	chr4B_part1	79,737,184	-0	-0	-0	1	1	1	-1	-1	-1	-2	-0	-0	-0	0
TraesCS4D01G080100		Dof zinc finger	chr4D_part1	54,126,883	NA	NA	NA	NA	NA	NA	NA	NA	NA	-1	NA	NA	NA	-0
TraesCS4A01G234000		Dof zinc finger	chr4A_part2	90,272,850	0	0	0	1	1	0	-1	-1	-0	-4	-0	-0	-0	0
TraesCS3D01G370100		Dof zinc finger	chr3D_part2	6,941,072	NA	NA	NA	NA	NA	NA	NA	NA	NA	-0	NA	NA	NA	0
TraesCS3A01G377000		Dof zinc finger	chr3A_part2	171,911,483	-0	0	0	-1	-1	-1	-1	-0	-0	-0	0	0	0	-0
TraesCS3B01G409600		Dof zinc finger	chr3B_part2	197,846,969	0	-0	-0	0	-0	-0	0	-1	-1	1	-0	0	-0	-0
TraesCS1A01G275000		Dof zinc finger	chr1A_part1	469,309,705	0	0	-0	-1	-1	-1	-1	-1	-1	-0	-0	0	-0	-0
TraesCS1B01G284300		Dof zinc finger	chr1B_part2	55,137,489	0	-0	-0	-1	-2	-1	-1	-2	-2	-0	-0	0	-0	-1
TraesCS1D01G274700		Dof zinc finger	chr1D_part1	370,341,838	NA	NA	NA	NA	NA	NA	NA	NA	NA	-1	NA	NA	NA	-1
TraesCS1A01G171300		Dof zinc finger	chr1A_part1	306,149,768	1	0	0	0	-0	-0	0	-0	-0	-0	-0	0	-0	1
TraesCS1B01G185900		Dof zinc finger	chr1B_part1	332,795,666	0	1	0	-0	0	-0	-1	-0	-1	0	0	-0	-0	0
TraesCS5B01G249800		Dof zinc finger	chr5B_part1	432,323,296	-0	-0	0	-0	-1	0	-1	-2	-1	-0	-1	-0	0	0
TraesCS5A01G251800		Dof zinc finger	chr5A_part2	14,355,185	0	-0	0	-0	-0	0	-1	-1	-1	-0	-0	0	0	-1
TraesCS5D01G259700		Dof zinc finger	chr5D_part1	365,992,363	NA	NA	NA	NA	NA	NA	NA	NA	NA	-0	NA	NA	NA	0
TraesCS3D01G271300		Dof zinc finger	chr3D_part1	376,169,683	NA	NA	NA	NA	NA	NA	NA	NA	NA	-2	NA	NA	NA	0
TraesCS3A01G271700		Dof zinc finger	chr3A_part2	46,874,005	0	0	0	-0	-0	0	-1	-1	-1	-1	0	0	0	-0
TraesCS3B01G305400		Dof zinc finger	chr3B_part2	42,444,630	-0	-1	-0	-0	-1	-0	-0	-1	-0	-1	-0	0	0	-0
TraesCS2A01G225900		Dof zinc finger	chr2A_part1	232,369,939	-0	-0	-0	-0	-0	-0	0	0	0	-0	0	0	0	-0
TraesCS2B01G249200		Dof zinc finger	chr2B_part1	257,523,313	-0	-0	-0	-0	-1	-1	0	0	0	0	0	0	0	0
TraesCS2D01G231600		Dof zinc finger	chr2D_part1	203,451,257	NA	NA	NA	NA	NA	NA	NA	NA	NA	0	NA	NA	NA	-0
TraesCS5D01G093800		2 Dof zinc finger	chr5D_part1	103,175,243	NA	NA	NA	NA	NA	NA	NA	NA	NA	1	NA	NA	NA	1
TraesCS5B01G087600		3 Dof zinc finger	chr5B_part1	112,194,001	0	-0	-0	0	-0	-0	1	0	0	0	0	1	0	1
TraesCS5A01G078100		Dof zinc finger	chr5A_part1	95,868,642	0	-0	-0	1	1	0	1	1	1	1	0	1	0	2
TraesCS5A01G479400		Dof zinc finger	chr5A_part2	199,416,408	0	-0	-0	0	-0	-0	1	1	0	2	0	1	0	1
TraesCS5D01G493000		Dof zinc finger	chr5D_part2	74,056,256	NA	NA	NA	NA	NA	NA	NA	NA	NA	1	NA	NA	NA	1
TraesCS5B01G492600		Dof zinc finger	chr5B_part2	209,215,990	0	0	-1	0	0	-0	1	1	0	1	0	1	-0	1
TraesCS4B01G206800		Dof zinc finger	chr4B_part1	440,046,072	-0	-1	-1	-0	-1	-1	-0	-1	-1	1	-1	-0	-1	1
TraesCS4D01G207600		Dof zinc finger	chr4D_part1	356,561,885	NA	NA	NA	NA	NA	NA	NA	NA	NA	1	NA	NA	NA	1
TraesCS4A01G097800		Dof zinc finger	chr4A_part1	108,871,563	-0	-1	-0	-1	-2	-1	-0	-1	-1	-1	-0	1	0	0
TraesCS1A01G035200		Dof zinc finger	chr1A_part1	18,460,897	0	-0	-0	0	-0	-0	1	1	1	1	0	0	0	1
TraesCS1B01G045000		3 Dof zinc finger	chr1B_part1	24,932,221	0	0	-0	0	-0	-0	1	1	1	1	0	1	0	1
TraesCS1D01G036700		2 Dof zinc finger	chr1D_part1	17,168,243	NA	NA	NA	NA	NA	NA	NA	NA	NA	1	NA	NA	NA	1
TraesCS3A01G539000		Dof zinc finger	chr3A_part2	296,194,012	NA	NA	NA	NA	NA	NA	NA	NA	NA	NA	NA	NA	NA	NA
TraesCS3B01G608800		Dof zinc finger	chr3B_part2	379,955,640	5	7	6	1	2	2	2	2	2	2	2	1	2	0
TraesCS3D01G537400		Dof zinc finger	chr3D_part2	134,308,176	NA	NA	NA	NA	NA	NA	NA	NA	NA	2	NA	NA	NA	1
TraesCS3A01G532000		Dof zinc finger	chr3A_part2	290,775,085	-0	-0	-0	0	0	0	1	1	1	1	0	0	0	1
TraesCS3B01G609000		Dof zinc finger	chr3B_part2	380,136,952	NA	NA	NA	NA	NA	NA	NA	NA	NA	NA	NA	NA	NA	NA
TraesCS3B01G609100		Dof zinc finger	chr3B_part2	380,175,946	NA	NA	NA	NA	NA	NA	NA	NA	NA	-1	NA	NA	NA	-0
TraesCS3A01G532100		Dof zinc finger	chr3A_part2	290,975,554	0	0	0	0	0	0	-2	-3	-2	1	0	0	0	0
TraesCS3A01G532200		Dof zinc finger	chr3A_part2	291,088,757	0	0	0	-0	-0	-0	-1	-2	-1	0	-0	0	0	-0
TraesCS3B01G608900		Dof zinc finger	chr3B_part2	380,097,760	NA	NA	NA	NA	NA	NA	NA	NA	NA	NA	NA	NA	NA	NA
TraesCS3D01G537500		Dof zinc finger	chr3D_part2	134,391,978	NA	NA	NA	NA	NA	NA	NA	NA	NA	NA	NA	NA	NA	NA
TraesCS3A01G403500		Dof zinc finger	chr3A_part2	194,591,284	NA	NA	NA	NA	NA	NA	NA	NA	NA	NA	NA	NA	NA	NA
TraesCS5B01G406500		Dof zinc finger	chr5B_part2	131,400,639	-0	-1	-0	0	0	0	-1	-2	-1	-2	-1	-1	-0	0
TraesCS5A01G401800		Dof zinc finger	chr5A_part2	141,540,236	0	0	-0	0	0	-0	-1	-2	-2	-5	-0	-1	-1	0
TraesCS5D01G412000		Dof zinc finger	chr5D_part2	23,481,066	NA	NA	NA	NA	NA	NA	NA	NA	NA	-2	NA	NA	NA	1
TraesCS6D01G268400		Dof zinc finger	chr6D_part1	378,378,715	NA	NA	NA	NA	NA	NA	NA	NA	NA	-1	NA	NA	NA	-0
TraesCS6A01G287700		Dof zinc finger	chr6A_part2	67,914,126	-0	-1	-0	0	-0	0	-1	-1	-1	-1	-0	0	0	0
TraesCS6B01G317100		Dof zinc finger	chr6B_part2	112,915,679	-0	-1	-0	0	-0	0	-1	-1	-1	-1	-0	0	0	-0
TraesCS7A01G213400		Dof zinc finger	chr7A_part1	177,136,007	0	0	1	-0	-1	-0	-2	-2	-2	-2	-1	-0	-0	0
TraesCS7D01G215300		Dof zinc finger	chr7D_part1	174,992,500	NA	NA	NA	NA	NA	NA	NA	NA	NA	-2	NA	NA	NA	-0
TraesCS7B01G120600		Dof zinc finger	chr7B_part1	140,652,691	0	-1	-0	-0	-2	-1	-2	-4	-3	-4	-1	0	-1	-0
TraesCS2A01G079200		Dof zinc finger	chr2A_part1	35,975,919	0	-0	0	0	-1	0	-0	-2	-0	-1	-0	0	0	0
TraesCS2B01G094000		Dof zinc finger	chr2B_part1	54,440,144	-0	-1	-1	-0	-1	-1	-1	-2	-2	1	-0	-0	-0	0
TraesCS2D01G076600		Dof zinc finger	chr2D_part1	32,763,076	NA	NA	NA	NA	NA	NA	NA	NA	NA	0	NA	NA	NA	1
TraesCS2A01G591100		Dof zinc finger	chr2A_part2	316,499,945	-0	-1	-1	0	-0	-0	0	-0	-0	-0	0	0	0	1
TraesCS2D01G563000		Dof-like zinc finger	chr2D_part2	172,264,812	NA	NA	NA	NA	NA	NA	NA	NA	NA	-0	NA	NA	NA	0
TraesCS2A01G591200		Dof zinc finger	chr2A_part2	316,538,566	-0	-0	-0	-0	0	-0	-0	-0	-0	1	1	1	1	1
TraesCS2A01G591000		Dof-like zinc finger	chr2A_part2	316,451,090	-0	-0	-0	-1	-1	-1	-0	-0	-0	1	0	0	0	2
TraesCS2B01G592600		Dof zinc finger	chr2B_part2	324,302,081	-1	-0	0	-1	-1	0	-2	-1	-0	-0	-0	-1	1	0
TraesCS2B01G592700		Dof-like zinc finger	chr2B_part2	324,329,847	-1	-1	-1	-1	-1	-1	-1	-1	-1	-1	0	0	0	-0
TraesCS2D01G563100		Dof zinc finger	chr2D_part2	172,338,836	NA	NA	NA	NA	NA	NA	NA	NA	NA	0	NA	NA	NA	0
TraesCS2B01G592800		Dof zinc finger	chr2B_part2	324,399,264	-0	-0	-0	-0	-0	-0	-1	-1	-1	-0	0	-0	-0	0
TraesCS2A01G590700		Dof-like zinc finger	chr2A_part2	316,383,874	-0	-1	-0	-0	-1	-0	-1	-2	-1	1	-0	-0	-0	1
TraesCS2B01G592900		Dof zinc finger	chr2B_part2	324,439,318	-0	-1	-0	-1	-1	-0	-2	-2	-1	-2	-0	-1	0	0
TraesCS2D01G563400		Dof zinc finger	chr2D_part2	172,441,226	NA	NA	NA	NA	NA	NA	NA	NA	NA	-1	NA	NA	NA	0
TraesCS2D01G563200		Dof-like zinc finger	chr2D_part2	172,357,701	NA	NA	NA	NA	NA	NA	NA	NA	NA	0	NA	NA	NA	-1
TraesCS2A01G590800		Dof zinc finger	chr2A_part2	316,412,671	-1	-0	-1	-1	0	-0	-2	-1	-2	0	0	-0	-0	0

Appendix 10. MUMMER alignments of chromosome 3B of Svevo vs: a) Zavitan, b) CDC Landmark, c) CDC Stanley, d) Refseq v.1.0. Red dots represent an alignment that matches in the same direction, whereas blue lines denote an alignment that matches in the opposite direction between the two assemblies. Svevo is plotted along the X-axis in each image

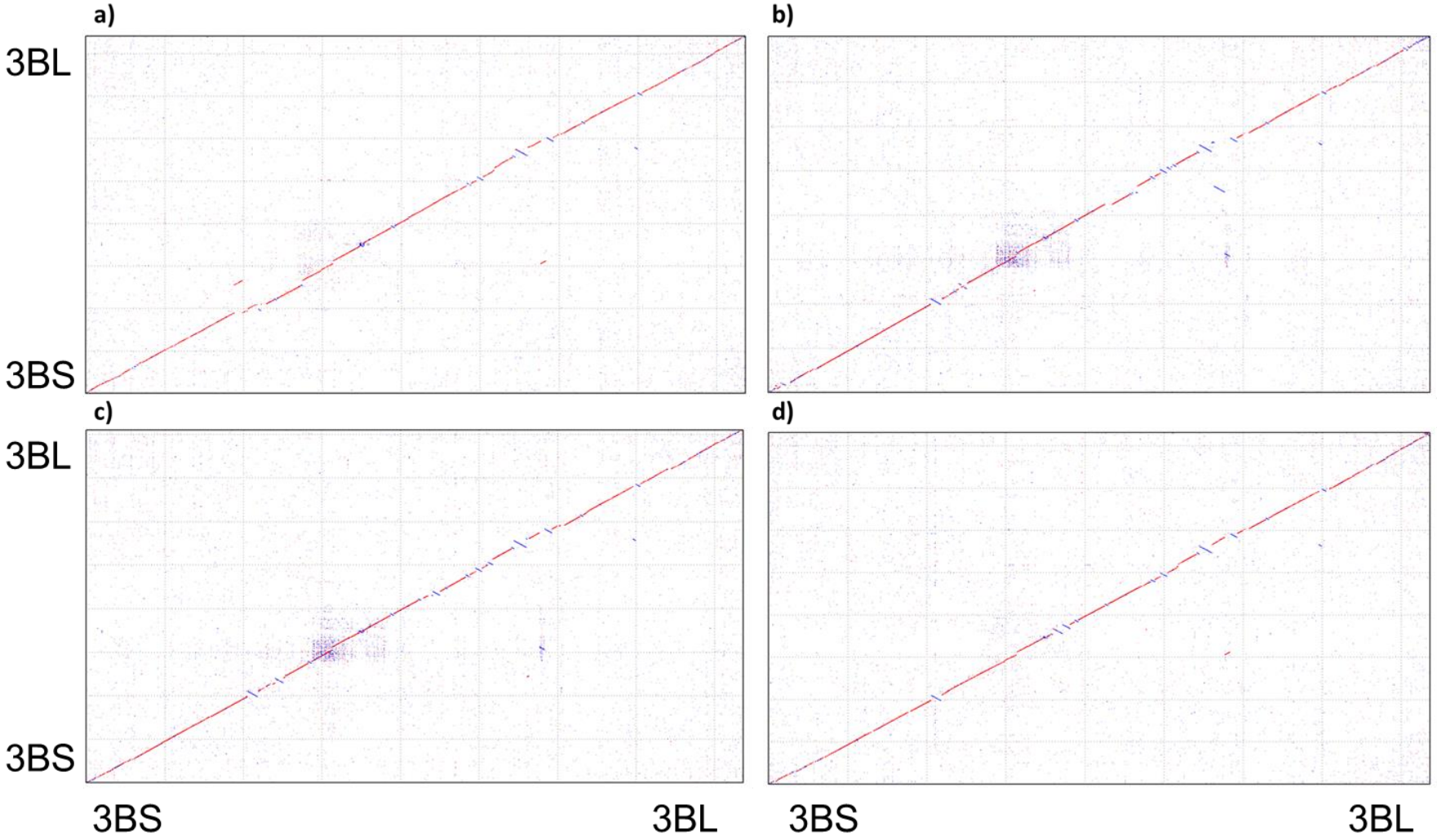

Appendix 11. Comparative genomic analysis of 90K probes source sequences and Refseq v1.0 gene models between Svevo and Zavitan assemblies

Appendix 12. Comparative genomic analysis of 90K probes source sequences and Refseq v1.0 gene models between Svevo and Refseq v.1.0 assemblies

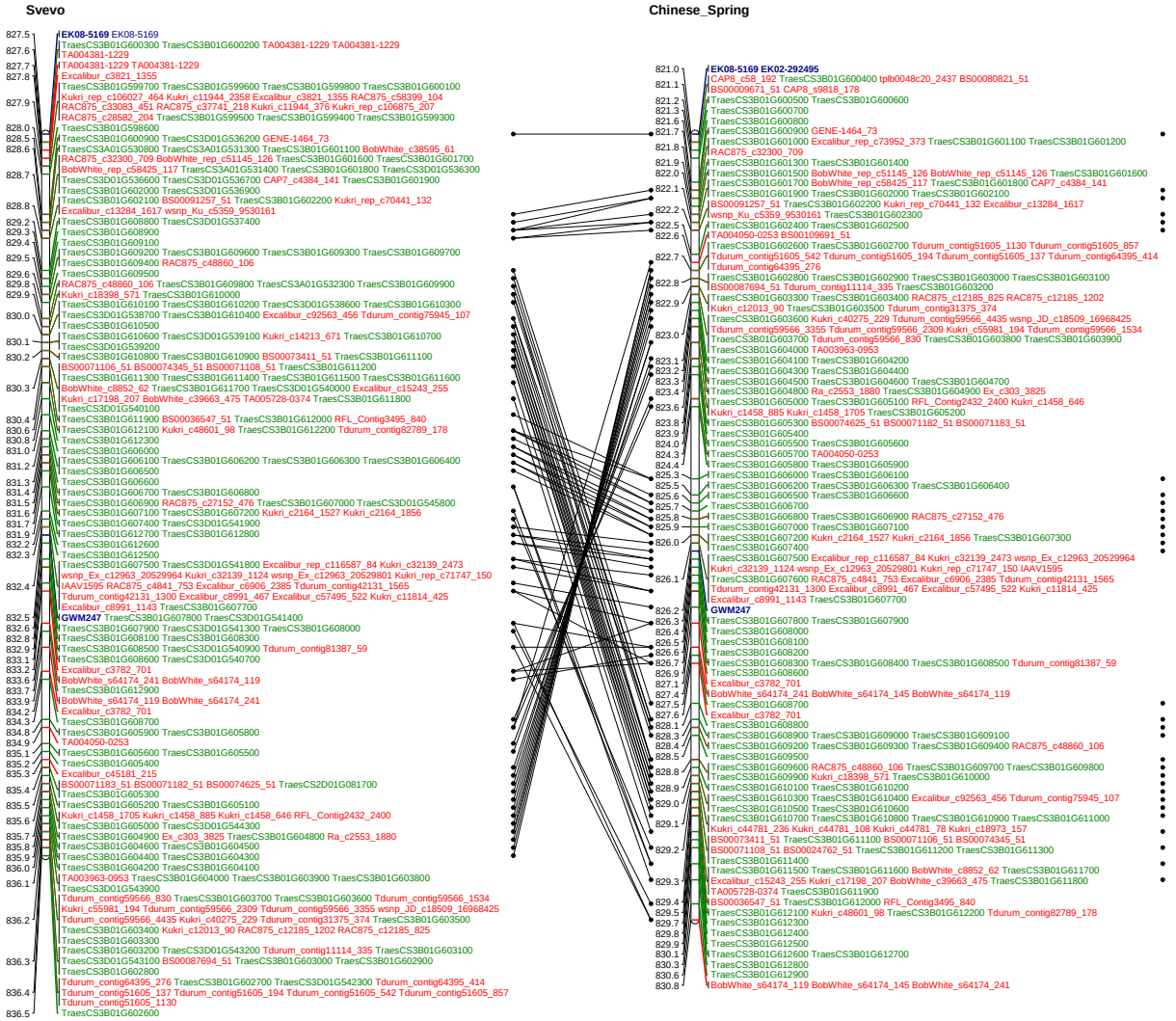

Appendix 13. Comparative genomic analysis of 90K probes source sequences and Refseq v1.0 gene models between Svevo and CDC Landmark assemblies.

Appendix 14. Comparative genomic analysis of 90K probes source sequences and Refseq v1.0 gene models between Svevo and CDC Stanley assemblies

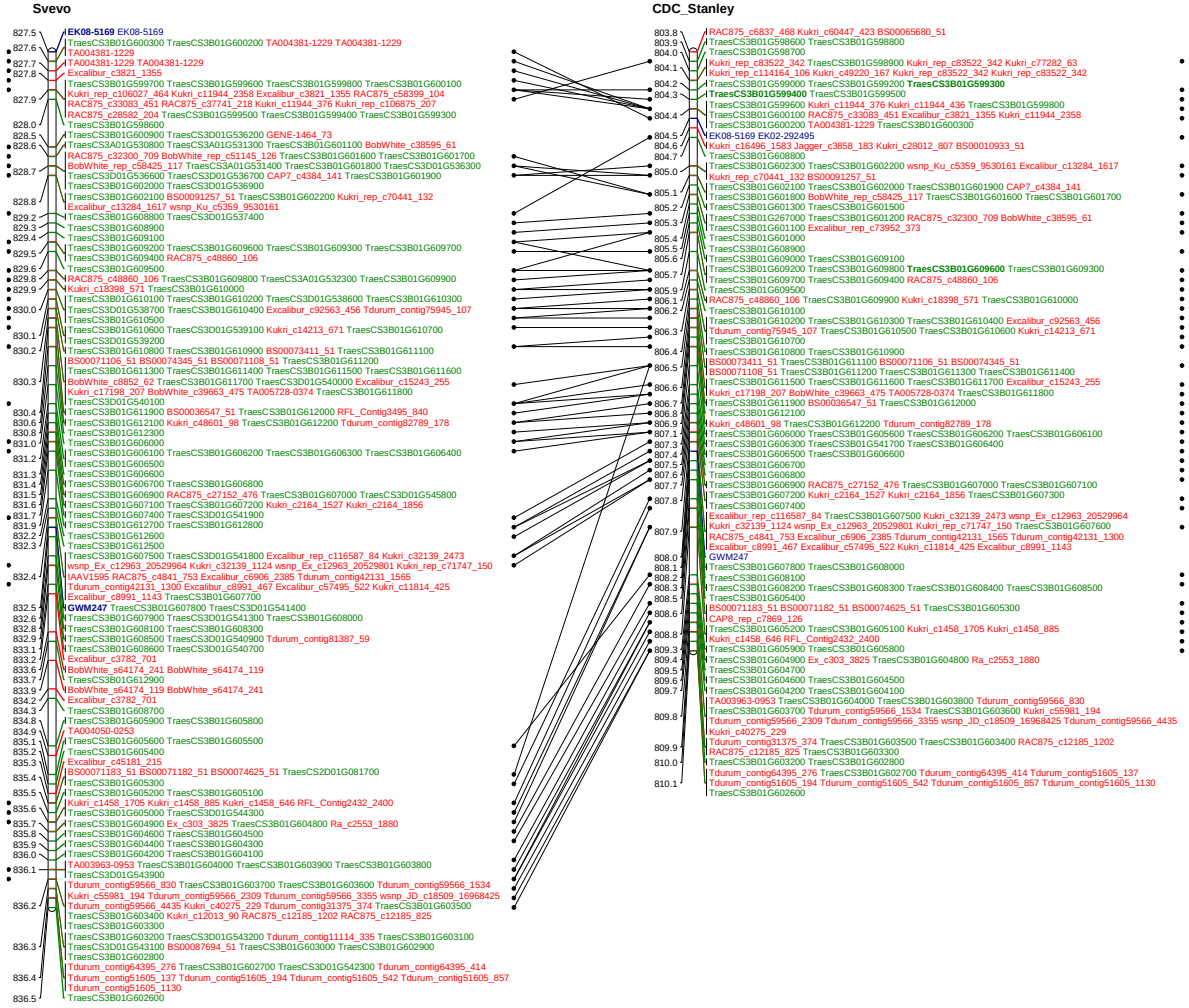

Appendix 15. Functionally enriched GO terms associated with DEGs occurring in >75% of hollow solid comparisons. Select terms with a potential role in stem-solidness are in red text.

Biological Process	
GO:0006950	response to stress
GO:0009056	catabolic process
GO:0071554	cell wall organization or biogenesis
GO:0019748	secondary metabolic process
GO:0042546	cell wall biogenesis
GO:0006468	protein phosphorylation
GO:0009698	phenylpropanoid metabolic process
GO:1902221	erythrose 4-phosphate/phosphoenolpyruvate family amino acid metabolic process
GO:1901361	organic cyclic compound catabolic process
GO:0006558	L-phenylalanine metabolic process
GO:0006979	response to oxidative stress
GO:0009072	aromatic amino acid family metabolic process

Cellular Component	
GO:0005576	extracellular region
GO:0030312	external encapsulating structure
GO:0048046	apoplast
GO:0071944	cell periphery
GO:0005618	cell wall

Molecular Function	
GO:0008171	O-methyltransferase activity
GO:0009055	electron carrier activity
GO:0020037	heme binding
GO:0016679	oxidoreductase activity, acting on diphenols and related substances as donors
GO:0016491	oxidoreductase activity
GO:0097367	carbohydrate derivative binding
GO:0043531	ADP binding
GO:0046906	tetrapyrrole binding
GO:0036094	small molecule binding
GO:1901265	nucleoside phosphate binding
GO:0043168	anion binding
GO:0043167	ion binding
GO:0016682	oxidoreductase activity, acting on diphenols and related substances as donors, oxygen as acceptor
GO:0016746	transferase activity, transferring acyl groups
GO:1901363	heterocyclic compound binding
GO:0097159	organic cyclic compound binding
GO:0016705	oxidoreductase activity, acting on paired donors, with incorporation or reduction of molecular oxygen
GO:0032559	adenyl ribonucleotide binding

Appendix 16. Summary of *TraesCS3B01G60880* gene prediction using FGENESH.

```
      FGENESH 2.6 Prediction of potential genes in Triticum genomic DNA
      Length of sequence: 1356
      Number of predicted genes 1: in +chain 1, in -chain 0.
      Number of predicted exons 2: in +chain 2, in -chain 0.
      Positions of predicted genes and exons: Variant   1 from   1,
Score:290.976587
         G Str   Feature   Start        End    Score           ORF           Len

         1 +    1 CDSf         4 -        69   12.83         4 -        69     66
         1 +    2 CDSl       281 -      1348  295.25       281 -      1348   1068

      Predicted protein(s):
      >FGENESH:[mRNA]   1   2 exon (s)      4  -   1348  1134 bp, chain +
      ATGATCTTCCCTCCTGCCTTCCTCGACTCATCAAGCTGCTGGAACACCAACCACAACCAG
      CTTCAGCTGCAGCAAATCGGCAGTAACACTCATATCACTACTACTCCTTCACCTGCTGGC
      CATGGTCCTGGAGACGGAGGAGGCGGAAACAACAACAATCATGGTCAGCAGGAAGGATTA
      ATGGCCACGGCCGGGGCGGGAGGAGGTGGTGGTGATGGTGGTGGCGGCGGCGGTGGGGAT
      GGTGACAGCGCCAGCGGCGGGAACAACAAGCCGATGTCGATGTCGGAGCGGGCGCGGCTG
      GCGCGGGTGCCACAGCCGGAGCCGGGGCTCAACTGCCCGCGCTGCGATTCCACCAACACC
      AAGTTCTGCTACTTCAACAACTACTCCCTCACCCAGCCCCGCCACTTCTGCCGGGCCTGC
      CGCCGCTACTGGACCCGCGGCGGCGCGCTCCGCAACGTCCCCGTCGGCGGAGGGTACCGT
      CGCCACGCCAAGCGCAGCACCAAGCCCAAGGCCGGGTCGGCTGGATCCGGAACTGCCGCG
      GCAGGGACGTCGTCTGCGACGTCGACGACGCCCAGCACCACTGCTTGCACCACCGGCACA
      GCTGCCACTGCGCCGCCCGCTCTGCAGTACTCCATGTTCGGCAGCGCGCCGCCGCACAGC
      AGCCGGTTCGCCGATAGCTTCGACCCCGCGAGCCTCGGCCTCAGCTTCCCCGCCAGGCTG
      CTCTTCCCCGACAATGGCGCCTACGCTGCCGACGGTGGCGCGCAGCAGCACCACCACCAC
      CAGGGGAACGGGAACGGCATGGAGCAGTGGGCGGCTGCGCACATGCAGAGCTTCCCGTTC
      CTGCACGCCATGGACCACCAGATGTCCGGGAATCCTCAATCAGCTTCGGCAATGCCAACC
      ACAATGGCGGCGATGCAGGGCATGTTCCACCTCGGGCTACAGAGCGGCGGCGGCGGCGGT
      AATGGCGACGATGGGGGAAACCACCAGTTCCACCACCAGCCGGCCAAGAGGGACTACAAC
      CAGCAGCAGCAGCAGGATTACCCAAGCAGCAGGGGCATGTACGGGGACGTGGTCAATGGC
      AATGGCGGCGGCTTCAATTTCTATTCCAGCACTAGCAATGCAGCTGGTAATTAG
      >FGENESH:   1   2 exon (s)      4  -   1348   377 aa, chain +
      MIFPPAFLDSSSCWNTNHNQLQLQQIGSNTHITTTPSPAGHGPGDGGGGNNNNHGQQEGL
      MATAGAGGGGGDGGGGGGGDGDSASGGNNKPMSMSERARLARVPQPEPGLNCPRCDSTNT
      KFCYFNNYSLTQPRHFCRACRRYWTRGGALRNVPVGGGYRRHAKRSTKPKAGSAGSGTAA
      AGTSSATSTTPSTTACTTGTAATAPPALQYSMFGSAPPHSSRFADSFDPASLGLSFPARL
      LFPDNGAYAADGGAQQHHHHQGNGNGMEQWAAAHMQSFPFLHAMDHQMSGNPQSASAMPT
      TMAAMQGMFHLGLQSGGGGGNGDDGGNHQFHHQPAKRDYNQQQQQDYPSSRGMYGDVVNG
      NGGGFNFYSSTSNAAGN
```

Appendix 17. *TraesCS3B01G60880* SSR/CNV markers screened on the common wheat diversity panel. Stem-solidness ratings (average from whole stem rated at maturity) for each line grown in replicated field trials (Nilsen et al., 2017) are presented in column 2.

		TraesCS3B01G608800		DOF-3B-SSR-907MF-1310R - Band Sizes							
Sample	**Solidness**	**Copy Number**	**SEM**	**395**	**407**	**409**	**411**	**415**	**417**	**419**	**421**
Choteau	4.3	9.9	0.5			409.6			417.7		421.7
Fortuna	3	10.4	0.2			409.6			417.6		421.8
Lancer	3	10.3	0.4			409.5			417.6		421.7
AAC Bailey	2.5	9.6	0.9			409.6			417.6		421.8
AC Eatonia	2.5	8.5	0.5			409.5			417.6		421.7
Frontana	2.5	2.3	0.3						415.8	417.8	
G9608B1-L12J11BF02	2.5	6.0	0.2								
Janz	2.5	1.4	0.1	395.6				415.6			
Leader	2.5	3.7	0.2						417.5		
Lillian	2.5	10.1	0.7			409.5			417.5		421.7
LJP1091P	2.5	7.7	0.4	395.6	407.5				417.6		421.7
Mott	2.5	10.3	1.1	395.7		409.6			417.7		421.7
Rescue	2.5	6.2	0.1			409.7			417.7		421.8
S-615	2.5	10.8	0.3			409.5			417.6		421.7
AC Abbey	1.9	6.4	0.4			409.5			417.7		421.7
CDC Landmark	1.9	7.7	0.4			409.4			417.5		421.5
Glencross	1.8	5.9	0.4							419.6	421.7
McKenzie	1.8	8.9	0.4								
CDC Rama	1.7	3.5	0.2							419.7	421.7
Unity	1.7	11.1	0.7			409.5			417.6		421.8
Glenlea	1.5	3.8	0.2							419.6	421.7
CDC Teal	1.3	2.7	0.1						417.6		
AC Crystal	1.2	2.9	0.2								421.7
AC Vista	1.2	3.1	0.2								421.7
Alvena	1.2	4.4	0.2								421.8
Burnside	1.2	6.0	0.2							419.6	421.7

AC Andrew	1.1	2.4	0.1	415.6	417.7		
AC Splendor	1.1	3.3	0.1		417.7		
AC Taber	1.1	2.6	0.1				421.7
CDC Bison	1.1	5.1	0.2			419.5	421.6
CDC Stanley	1.1	1.8	0.1				
CDC Walrus	1.1	2.4	0.0	415.5	417.6		
Kane	1.1	4.6	0.2		417.7		
Katepwa	1.1	2.8	0.1		417.7		
Laser	1.1	4.1	0.1		417.6	419.7	
5500HR	1	2.8	0.1			419.7	
5600HR	1	3.0	0.4		417.6		
5601HR	1	3.0	0.1		417.7		
5602HR	1	3.7	0.1	415.5	417.6	419.7	
5603HR	1	3.4	0.2	415.6		419.6	
5700PR	1	2.4	0.2				421.7
5701PR	1	2.7	0.1		417.7		
5702PR	1	2.1	0.2	415.6			
AC Barrie	1	2.9	0.1				
AC Cadillac	1	3.5	0.3				
AC Domain	1	3.1	0.2		417.7		
AC Elsa	1	3.0	0.2				421.7
AC Foremost	1	2.5	0.1				421.7
AC Intrepid	1	3.2	0.2				
AC Karma	1	2.5	0.2				421.7
Alikat	1	2.2	0.2		417.7		
Carberry	1	3.2	0.1		417.6		
CDC Abound	1	3.9	0.3		417.8		
CDC Alsask	1	2.8	0.2		417.7		
CDC Bounty	1	3.0	0.2		417.7		
CDC Go	1	3.1	0.1		417.6		
CDC Imagine	1	4.1	0.5				

CDC Kernen	1	2.1	0.2			417.8		
CDC Merlin	1	2.8	0.1			417.5		
CDC Osler	1	3.0	0.2			417.7		
CDC Thrive	1	2.5	0.1			417.8		
CDC Utmost	1	2.0	0.3			417.6	419.7	
Chinese Spring	1	1.4	0.0					
Cutler	1	4.1	0.3					421.7
Glenn	1	4.0	0.4		415.6	417.6		
Goodeve VB	1	4.2	0.2			417.6		
GP069	1	2.7	0.1					421.6
Harvest	1	4.6	1.0					
Helios	1	4.8	0.3			417.7		
Infinity	1	3.8	0.2		415.7	417.7		
Journey	1	3.0	0.1			417.7		
Laura	1	3.2	0.2			417.6		
Lovitt	1	3.2	0.1			417.7		
Minnedosa	1	3.4	0.3					421.8
Muchmore	1	3.8	0.3			417.7		
Neepawa	1	4.2	0.3			417.6		
Park	1	2.4	0.2				419.7	
Peace	1	4.6	0.6				419.6	
Prodigy	1	4.1	0.3					
PT559	1	2.7	0.1			417.8		
Red Fife	1	2.6	0.1		415.6			
RL4137	1	0.8	0.1			417.6		
Roblin	1	3.1	0.1			417.7		
Sadash	1	3.2	0.1		415.6	417.6		
Selkirk	1	3.6	0.3				419.7	
Snowbird	1	2.4	0.2			417.6		
Snowstar	1	3.7	0.2			417.6		
Somerset	1	4.5	0.3			417.5		

Stanley	1	3.6	0.3			417.7		
Stettler	1	3.7	0.2			417.8		
Sumai 3	1	3.2	0.1		415.6		419.6	
Superb	1	3.1	0.1			417.7		
SY985	1	2.9	0.2					421.7
Vesper	1	2.9	0.2			417.6	419.7	
Waskada	1	3.3	0.3			417.7		

Appendix 18. *TraesCS3B01G60880* SSR/CNV markers screened on the durum wheat diversity panel. Stem-solidness ratings (average from whole stem rated at maturity) for each line grown in replicated field trials (Nilsen et al., 2017) are presented in column 2.

		TraesCS3B01G608800		DOF-3B-SSR-907MF-1310R - Band Sizes				
Sample	**Solidness**	**Copy Number**	**SEM**	**415**	**417**	**419**	**421**	**424**
Green27	.	1.1	0.5	415.7				
DT838	5	2.9	0.7	415.7			421.7	
DT726	5	4.2	0.2	415.5			421.6	
DT732	5	3.9	0.2	415.5			421.7	
DT795	5	4	0.2	415.6			421.7	
DT751	5	2.3	0.1	415.5			421.7	
DT777	5	3.8	0.2		417.7		421.7	
DT817	5	3.4	0.1	415.6			421.7	
AAC Raymore	5	4.4	0.3	415.6			421.7	
DT824	5	4.3	0.2	415.7			421.8	
DT837	5	3.8	0.1	415.6			421.7	
DT840	5	4.4	0.2	415.5			421.7	
DT845	5	3.4	0.1	415.5			421.6	
CDC Fortitude	5	3	0.6	415.6			421.6	
9661-AF1D	4.7	4.6	0.3	415.7			421.7	
Camacho	4.7	2.1	0.1			419.7	421.8	
Lesina	4.6	4.8	0.1		417.7		421.8	
Mongibello	4.1	3.1	0.1		417.6		421.8	
Colosseo	4.1	2.3	0.2					423.6
Fortore	3.6	2.6	0.1	397.4				
Ciccio	2.7	1.1	0.0		417.6			
Mexa	2.6	1.2	0.2	415.8				
Nedda	2.4	.	.					
940955	2.4	2.5	0.1			419.8		
Gianna	2.4	0.8	0.0	415.7				
Parsifal	2.4	0.6	1.3	415.7				
Wollaroi	2.2	3.9	0.0			419.7		
RABD 93.40	2.1	1.1	0.1	415.6				
Vitron	2.1	0.8	0.1					
D-73-15	2.1	0.8	0.0	415.7				

Gidara 17a	2	1	0.0	415.7			
D940098	2	0.6	0.1	415.6			
Buck Ambar	2	1.1	0.1		417.7		
940030	1.9	1.9	0.1			419.7	
Bonaerance Inta Cumenay	1.9	1.5	0.1		417.7		
Kronos	1.9	1.1	0.0	415.7			
Demetra	1.9	1.1	0.1	415.7			
Svevo	1.9	0.8	0.1	415.5			
44616	1.9	0.7	0.1		417.7		
920334	1.8	1.9	0.1			419.8	
Varano	1.8	1.4	0.0				
Buck Topacio	1.8	1	0.1		417.7		
44721	1.7	0.8	0.1	415.6			
Langdon	1.7	0.8	0.0	415.6			
Durafit	1.7	1.1	0.1	415.6			
Arcobelano	1.7	1.6	0.0		417.8		
Grazia	1.7	1.2	0.1	415.7			
CRDW17	1.7	1.4	0.1				
Commander	1.7	0.8	0.1	415.6			
950844	1.7	3.5	0.1			419.6	
Ocotillo	1.7	1.1	0.0	415.7			
Arrivato	1.7	0.9	0.1	415.8			
950329	1.7	2.7	0.0			419.8	
Marjak	1.7	1.1	0.0	415.5			
Altar-Aos	1.7	1.5	0.1		417.1		
Duilio	1.7	1.2	0.0		417.7		
AC Pathfinder	1.7	1	0.1				
Bonaerance Valverde	1.7	1.2	0.1		417.7		
Tamaroi	1.7	0.8	0.1	415.7			
Bonaerance Quilaco	1.7	1.3	0.1	415.8			
Carioca	1.7	1.1	0.1	415.7			
Bronte	1.6	0.8	0.0	415.6			
Durex	1.6	3.1	0.1				421.8
Borli	1.6	0.9	0.1		417.8		
CFR5001	1.6	0.6	0.0		417.8		

Green 34	1.6	0.9	0.0	415.7	
Ariesol	1.6	0.6	0.1	415.7	
D940027	1.6	0.7	0.1		
940435	1.6	0.9	0.2	415.8	
Agridur	1.5	0.9	0.0	415.6	
DHTON 1	1.5	0.8	0.1	415.7	
DT705	1.5	0.7	0.1	415.7	
Simeto	1.5	0.7	0.1		417.7
Iride	1.5	1	0.0		417.7
Gallareta	1.5	1.3	0.0		
Kofa	1.5	1.4	0.1	415.6	
DT695	1.4	1.2	0.0	415.8	
DT536	1.4	1.2	0.0	415.7	
Strongfield	1.4	0.9	0.1	415.7	
DT711	1.4	1	0.0	415.6	
DT710	1.4	1.2	0.0	415.6	
Tresor	1.4	1.1	0.0		
DT707	1.4	0.9	0.0	415.7	
DT704	1.4	1.1	0.1	415.7	
AC Avonlea	1.4	1.3	0.1	415.7	
Nacori 97	1.4	1.2	0.1	415.6	
AC Morse	1.4	0.9	0.1	415.6	
Kyle	1.4	1.1	0.1	415.7	
DT540	1.4	0.8	0.1	415.7	
DT709	1.4	0.7	0.0	415.7	
Westbred881	1.3	0.8	0.1	415.6	
9661-CA5E	1.3	1.1	0.1	415.6	
AC Navigator	1.3	1	0.0	415.8	
Durabon	1.3	0.8	0.2	415.7	
DT691	1.3	1.2	0.1	415.7	
Plaza	1.3	0.4	0.1	415.7	
AC Napoleon	1.3	1.1	0.1		
Tetradur	1.3	1.2	0.1	415.7	
D95580	1.3	0.6	0.0	415.6	
D24-1773	1.2	0.8	0.0	415.8	

AC Melita	1.2	1.1	0.0	415.7
D941038	1.2	0.4	0.1	415.7
DT696	1.2	1.1	0.1	415.7
DT513	1.2	0.8	0.1	415.5
K-39099	1.1	0.8	0.0	415.7